DISSERTATION

THREE ESSAYS ON THE USE OF SPATIAL DATA TO INFORM ENVIRONMENTAL AND RESOURCE MANAGEMENT

Submitted by

Di Sheng

Department of Agricultural and Resource Economics

In partial fulfillment of the requirements

For the Degree of Doctor of Philosophy

Colorado State University

Fort Collins, Colorado

Fall 2022

Doctoral Committee:

Advisor: Jordan F. Suter

Dale T. Manning
Christopher G. Goemans
Ryan T. Bailey

ABSTRACT

THREE ESSAYS ON THE USE OF SPATIAL DATA TO INFORM ENVIRONMENTAL AND RESOURCE MANAGEMENT

This dissertation consists of three essays that use of spatial data to inform trade-offs related to environmental and resource management. The first essay explores how a spatially targeted differentiated payment design can reduce the social cost of achieving a given level of ecosystem service (ES) provisions. Performance comparisons between uniform payments and differentiated payments for ecosystem services help to identify the context under which differentiated payments offer the largest advantage relative to a uniform payment. A mathematical programming model is developed to explore the performance of different payment schemes and to derive generalized lessons from simulations. Then generalized lessons are evaluated with two case studies related to water quality management. It is found that the simulations and case studies align with each other in terms of the total cost reductions, but they diverge in the payment rate choice due to the underlying distributional differences. The findings suggest that a higher payment rate for parcels that systematically provide higher levels of ES can reduce the social cost of providing the ES of interest, particularly for cases where the mean ES provision benefits across land types are different and ES provision targets are relatively low. In the second essay, I examine whether China's pilot carbon emission trading system (ETS) has the co-benefit of reducing local PM2.5 levels. Two ETS pilot provinces are selected to be the treated group, while the control group is constructed with institutional knowledge. Static and dynamic difference-in-differences designs are adopted and compared to reveal the ETS treatment effect. The spatial and temporal variation in the ETS pilot areas allows me to adopt a dynamic two-way fixed effects model to estimate heterogeneous treatment effects on the treated areas. I find that the ETS improves the local air quality in Hubei but not in Guangdong. A further analysis suggests that a sector-standards based allowance allocation mechanism

can cause local air quality to deteriorate. The third essay revisits the groundwater resource value question in the Ogallala aquifer through estimation of an econometric model of agricultural land prices that includes fixed effects, with the repeated transactions from the ZTRAX data product. Saturated thickness is used to present the groundwater availability and the study includes irrigated parcels only. Heterogeneous responses in land values to groundwater stock changes are found across Colorado and Nebraska. The marginal value of groundwater stock is highest at low levels of groundwater availability, which implies that additional groundwater depletion in Colorado is more costly than depletion in Nebraska.

ACKNOWLEDGEMENTS

I would like to express my deepest gratitude to my advisor Dr. Jordan Suter for his invaluable patient guidance and supportive mentorship. I am also very grateful for my defense committee members Dr. Dale Manning, Dr. Chris Goemans and Dr. Ryan Bailey, who generously provided knowledge and expertise. And special thanks to Prof. Tim Quine from University of Exeter who offers me great support and mentorship during the last year of my PhD journey.

I also could not have undertaken this journey without many teachers, students and staffs from the Department of Agricultural and Resource Economics at Colorado State University.

Lastly, I would be remiss in not mentioning my parents and my best friend Lingyan Liu. Thank you for always believing in me. I would also like to thank my idols Satoshi Ohno and Tsuyoshi Domoto for entertainment and emotional support.

DEDICATION

For my mother, Cuihua Liu

TABLE OF CONTENTS

LIST OF TABLES

LIST OF FIGURES

Chapter 1

Differentiated Payments for the Provision of Ecosystem Services

1.1 Introduction

Payment for ecosystem service (PES) programs provide incentives for voluntary participation in ecosystem service (ES) supply and have been widely used for environmental management. To achieve cost-effective ES provision, it is necessary to enroll ES providers with the highest environmental benefits and lowest provision costs. However, lack of disaggregated cost and benefit information leads to information rent and efficiency loss. For example, a uniform payment scheme will tend to enroll providers with the lowest provision costs, without regard to the heterogeneity in benefits that are provided. More complex PES designs such as procurement auctions and screening contracts could alleviate information asymmetry and reduce information rents [8]. However, the greater implementation costs and administrative efforts of a complex PES design can also reduce a PES program's participation rate and cost-effectiveness [61]. Therefore, an appropriate PES design requires a careful balance between the effectiveness of the PES program and the complexity of implementation.

A cost-effective PES would ideally pay for the outcome rather the action. A spatial targeting PES design incorporates the correlation between parcel attributes and ES provision outcome, and therefore can help the program pay more for the outcome. Ezzine-de Blas et al. [28] studied 55 PES programs worldwide and found that design factors such as spatial targeting and payment differentiation positively contribute to the efficiency of PES.

To balance the program simplicity and efficiency, we propose a simple differentiated payment[1] scheme for ES provision that offers a higher payment rate to parcels with identifiable spatial at-

[1]It might also be referred as a targeted payment or fixed payment with targeting in other literature.

tributes that are correlated with higher ES provision, and investigate its performance empirically with simulations and case studies. Examples of attributes that could be used for targeting payments include land slope class, management practice and distance to waterways. For land slope, we would expect the land profitability to decrease and environmental impact to increase as the land slope increases. Therefore, it could be cost-effective to conserve land with greater slope. The Grain for Green program in China is a land conservation program targeting on sloping land [80]. Different management practices can affect land profitability as well as environmental impacts from agricultural activities. USDA conservation programs offer financial and technical supports to promote a wide range of management practices, including conservation tillage, terraces, and nutrient management plans. Riparian buffers are conservation practices addressing water quality that involves distance to waterways, where land located immediately adjacent to and parallel to a water body and/or seasonal stream and wetland are eligible for higher compensations. Currently, the USDA Conservation Reserve Enhancement Program provides additional 20% rental rate incentives for riparian buffer zones compared with average fields [82]. In these three examples of observable attribute choices, the slope and the distance to waterways are exogenous attributes, while management practices are endogenous attributes. It should be noted, however, that if the cost of management practice adoption is smaller than payment differences, payment differentiation on endogenous attributes might stimulate behavior changes that deteriorates a conservation program's cost-effectivess.

The objective of this paper is twofold: (1) to identify scenarios when a differentiated payment scheme offers the greatest advantages relative to a uniform payment scheme, and (2) to identify optimal differentiated payments for ES provision. We combine optimizations and hypothetical simulations to develop generalized lessons and then use results from a Soil and Water Assessment Tool (SWAT) model to conduct water quality management case studies of two watersheds in the states of Colorado and Iowa.

Both hypothetical simulations and case studies suggest that cost-effectiveness of a PES program can be significantly increased by a differentiated payment design when the difference in

mean ES provision benefits across land types is large and a low ES provision is desired. Further, the case study in Iowa reveals that when the benefit-cost ratio and ES provision cost have a positive correlation, payment differentiation can yield a desired ES outcome at a lower social cost compared with a uniform payment rate.

1.2 Literature Review

Over three decades of development has yielded numerous PES programs designed for the provision of different ESs, implemented across the world. Engel [27] and Wunder et al. [90] provide comprehensive reviews of PES designs to generate guidance for PES effectiveness. Both papers conclude that PES design should be based on a careful understanding of specific ecologic-economic context.

It is well recognized that asymmetric information causes efficiency loss in PES programs, and solutions have been proposed for various ES objectives. Mason and Plantinga [55] focused on additionality under asymmetric information, and they proposed a contract design to mitigate the impact of asymmetric information. Despite the fact that auction schemes and screening contracts are theoretically appealing, empirical evidence of these mechanisms in practice is limited. Currently, the Conservation Reserve Program (CRP) is the largest scale governmental program that applies an auction mechanism to conserve ES [51]. Ferraro [30] also pointed out that screening contracts are difficult to implement in the field as it requires adequate knowledge of land distribution and sophisticated calculations of incentive compatibility by the conservation practitioners.

Wunder et al. [90] reviewed 70 worldwide PES programs and found that administrative burden is one reason why many sophisticated and theoretically informed schemes are practically unpopular. However, policy simplification can lead to efficiency loss. Armsworth et al. [2] calculated the cost of policy simplification and found that common policy simplification can result in significant biodiversity loss due to the lack of consideration of biodiversity provision cost variation. Lundberg et al. [51] demonstrated that context matters for PES design. They compared the performance of a uniform payment scheme to a procurement auction under various scenarios to identify the im-

pact of baseline compliance, correlation between benefit and cost distribution, and budget sizes on the effectiveness of different payment designs. It is shown that uniform payments are more effective with a high baseline compliance (voluntary ES provision without payment) and positive correlation between benefit and cost. Therefore, an effective PES design requires balancing the implementation complexity and effectiveness and accounting for the context.

Engel [27] summarized conditions when alternative payment schemes are favorable. According to Engel, a differentiated payment scheme is favorable when there are (1) significant heterogeneity in provision cost and/or ES provision across sites and (2) available estimates of differentiating criterion. For example, differentiating criterion could be observed parcel attributes like distance to surface water and/or soil type. In addition, benefit targeting is preferred to a uniform payment scheme when ES benefit varies significantly across sites and data on ES benefit is available. Armsworth et al. [2], Wunder and Albán [89] and Ezzine-de Blas et al. [28] have demonstrated that targeting sites with higher expected ES benefit or lower expected provision cost can significantly increase the ES outcome with a given budget. Palm-Forster et al. [61] applied a farmer behavioral model with SWAT outputs to simulate and compare phosphorous reductions under a reverse auction, as well as targeted and un-targeted uniform payment programs. The results revealed that when the transaction cost of applying a reverse auction is twice the cost of the uniform payment program, the uniform payment is more cost-effective. Wünscher et al. [92] examined eight spatial targeting PES schemes and found efficiency improvements in all of them compared to a uniform payment scheme. It is recognized in the paper that spatially targeted PES based on attributes can boost the PES efficiency. In most cases, it is costly to estimate the site-level provision cost or ES benefit data. Therefore, Wünscher et al. [92], Wünscher and Engel [91] and Engel [27] suggested the use of observable site characteristics as a proxy for the cost or benefit as a low cost approach to spatial targeting.

This study, while similar to Lundberg et al. [51] in examining the performances of alternative PES payment designs under various contexts, differs in two aspects: (1) we investigate how different underlying distributions of provision cost and benefit affect the PES performance with different

payment schemes, while Lundberg et al. [51] only tests on one set of normal distributions of ES provision cost and benefit; (2) our conceptual PES has an ES provision target while Lundberg et al. [51] set a budget target for their conceptual PES program; Particularly, we are able to identify the impacts of (1) the first moments of cost and benefit distributions, (2) correlation between ES benefit and provision cost, and (3) provision targets on the PES performance and optimal payment rate choices. In addition, we incorporate SWAT models calibrated with observational data to construct water quality management cases, to which we apply our generalized lesson from the simulations.

1.3 Methods

To evaluate the performance of alternative PES schemes under various contexts, we adopt simulations to generalize policy insights. This section describes the model development and simulation procedures. We adopt mathematical programming to search for the minimum social cost of achieving specific ES targets under three payment programs: efficient, uniform and differentiated payment. It is assumed that there are two observable parcel types A and B, and type B parcels have some observable attributes that leads to higher ES supply on average. Policy makers are assumed to be aware of the distributions of the costs and benefits for the two types of parcels, but don't know specific parcel-level cost and benefit values. We compare the performance of three types of PES payment schemes: uniform payment, differentiated payment and the efficient payment. Table A.1 summarizes the comparisons among three PES payment schemes. In practice, some PES programs are publicly funded, while others are privately funded. According to Ezzine-de Blas et al. [28], 35% of PES programs in Latin America and 85% of PES in Africa are privately funded. While in Asia, Europe and North America, about 70% of PES are publicly funded. With a publicly funded PES, the policy makers may be more likely to seek to minimize the social cost of achieving an ES outcome. In this paper, we focus on the total social cost. In future research, we can also include the analysis where policy makers seek to minimize expenditures[2], or rather to maximize benefits subject to a budget constraint.

[2]Min $Expenditure = \lambda \int_0^{\lambda} f_c(c)dc = \lambda F_c(\lambda)$, where $f_c(c)$ is the PDF of opportunity cost c.

A uniform payment program offers one payment rate for enrolled parcels, regardless of the parcel type. It is assumed that the owner of a given parcel will participate (enroll) as long as the payment rate is greater than or equal to their opportunity cost. In this setting, the social planner chooses a minimum uniform payment rate that would enroll enough parcels to provide a given level of ecosystem services.

When costs and benefits are continuously distributed, the expected total social cost given a uniform payment rate λ can be expressed as equation 1.1:

$$E(TC) = \int_0^{\lambda} c f_c^A(c) dc + \int_0^{\lambda} c f_c^B(c) dc \tag{1.1}$$

Define $f_c^A(c)$ and $f_c^B(c)$ as the probability density functions of opportunity costs (c) for type A and B parcels, respectively.

Given a uniform payment λ, the expected ES provision is defined in equation 1.2:

$$E(ES) = \int_0^{\lambda} \int_V v f_{cv}^A(c, v) dv dc + \int_0^{\lambda} \int_V v f_{cv}^B(c, v) dv dc \tag{1.2}$$

Define $f_{cv}(c, v)$ as the joint pdf of cost (c) and benefit (v) variables, with superscripts denoting parcel types. V denotes the domain of the parcel-level benefit variable.

A cost-minimizing social planner chooses a uniform payment rate to achieve an ES provision target:

$$\underset{\lambda}{\text{Min}} \quad \int_0^{\lambda} c f_c^A(c) dc + \int_0^{\lambda} c f_c^B(c) dc \tag{1.3}$$

$$\text{s.t.} \quad \int_0^{\lambda} \int_V v f_{cv}^A(c, v) dv dc + \int_0^{\lambda} \int_V v f_{cv}^B(c, v) dv dc \geq \tau M \tag{1.4}$$

where M is the maximum possible ES provision level, e.g., when every parcel is enrolled; τ, the ES provision target, which ranges from 0% to 100%. The left-hand side of equation 1.4 represents expected ES provision[3] greater than the desired level τM.

[3] $\int_V v f_{cv}(\lambda, v) dv = E(v|\lambda)$, which is the conditional mean of benefit given the payment rate λ.

A differentiated payment program offers different payment rates for different types of parcels. Within a specific parcel type, the payment rate is uniform across parcels. The social planner is assumed to choose the differentiated payment rates to minimize the total cost of ES provision to achieve a desired ES target, while the enrollment decision at the parcel level is determined by the magnitude of the payment rate and the opportunity cost. With continuously distributed costs and benefits, the problem of choosing the differentiated payment program that minimizes the expected social cost, subject to meeting an ecosystem service target, is presented below:

$$\underset{\lambda_A,\lambda_B}{\text{Min}} \quad \int_0^{\lambda_A} c f_c^A(c)dc + \int_0^{\lambda_B} c f_c^B(c)dc \tag{1.5}$$

$$\text{subject to} \quad \int_0^{\lambda_A}\int_V v f_{cv}^A(c,v)dvdc + \int_0^{\lambda_B}\int_V v f_{cv}^B(c,v)dvdc \geq \tau M \tag{1.6}$$

where all notation is similarly and separately defined as above for type A and B parcels, indicated by the subscripts. The decision variables, λ_A and λ_B here are the payment rates for type A and type B parcels.

The efficient payment scheme selects the parcels with the highest benefit-cost ratio and offers a payment higher than the enrolled parcel's opportunity cost. Under this scheme, parcels with the highest ES benefit-cost ratio are enrolled until the ES provision target is achieved. The efficient payment scheme serves as a theoretical optima, while it's unlikely to be achieved in practice, it provides an important comparison that illustrates the upper bound of what a PES program could achieve with perfect information.

To develop a general understanding of the variation in optimal differentiated payments, and the potential cost savings associated with a differentiated payment compared to a uniform payment program, we carry out simulations as described below.

Hypothetical Simulations

To execute the simulations, we first draw random samples from cost and benefit coefficient distributions for type A and type B parcels, respectively. Meanwhile, the correlation between cost and benefit variables is kept to be ρ for both types. c and v denote the cost and benefit variables,

with $c_A \sim \mathcal{N}(\mu, \sigma^2)$, and $c_B \sim \mathcal{N}(\mu + k\sigma, \sigma^2)$; $v_A \sim \mathcal{N}(\eta, \xi^2)$ and $v_B \sim \mathcal{N}(\eta + m\xi, \xi^2)$. In the simulation, we assume the variance of each variable is the same across the two types of parcels. We specify the differences in mean cost and mean benefit between the two types of parcels by k and m times of the standard deviation, respectively. Positive m implies that type B parcels are associated with a higher mean ES benefit. Due to the discrete nature of the simulation setting, the optimization results with extreme ES provision targets might not provide much policy insights, we therefore constrain the results to ES provision targets between 20% and 80%. Due to the discrete nature of the simulation, the continuous problems are transformed to discrete optimizations, and $N = 10$ randomly selected coefficient realizations are used for each scenario.

Parameters used for simulations are summarized as below. We randomly draw 500 type A and 500 type B parcels for each scenario. All parcels are assumed to be the same geographic area. Type A parcels have a mean cost and standard deviation of $\mu = 150$ and $\sigma = 30$, respectively; type A parcels have a mean benefit and standard deviation of $\eta = 150$, and $\xi = 10$, respectively. $m \in \{0, 1, 2, 3, 4\}$ and various m values allow different mean benefits between type A and B parcels. Also, $k \in \{-1, 0, 1\}$ permits lower, same and higher mean cost of type B parcels. To reduce the probability of getting negative cost coefficient values from random draws, we set $\sigma = 30$ to make sure three standard deviations from the mean is non-negative for all k values. With $\xi = 10$, we model a case where the variance in benefit is smaller than the variance in the cost. Positive m and k gives higher mean benefit and cost of B parcels, respectively. When m and k are 0, the mean benefit and mean cost of the two types of parcels are the same. Table 1.1 summarizes the cost and benefit means of type B parcels under all scenarios. The simulations assume that parcel owners are rational and enroll parcels when the payment rate is at least as high as their opportunity costs.

The correlation between the cost and benefit coefficients are taken from the set $\rho \in \{-0.5, 0, 0.5\}$. In total, the simulations consider 45 sets of distribution parameters for each P_0, Figure 1.1a plots out 45 sets of ES provision benefits and costs of hypothetical parcels used in the simulations. The joint distributions of benefit and cost of type A and type B parcels overlap less as the absolute value of m and k increases. Figure 1.1b plots the benefit-cost ratio of 45 scenarios across type A and B

Table 1.1: Summary of Benefit and Cost Parameter Scenarios

		Mean Cost of Type B		
		k = 1	k = 0	k = -1
Mean Benefit of Type B	m = 0	150, 180	150, 150	150, 120
	m = 1	160, 180	160, 150	160, 120
	m = 2	170, 180	170, 150	170, 120
	m = 3	180, 180	180, 150	180, 120
	m = 4	190, 180	190, 150	190, 120

Note: Type A mean benefit and mean cost is (150, 150) in all scenarios.

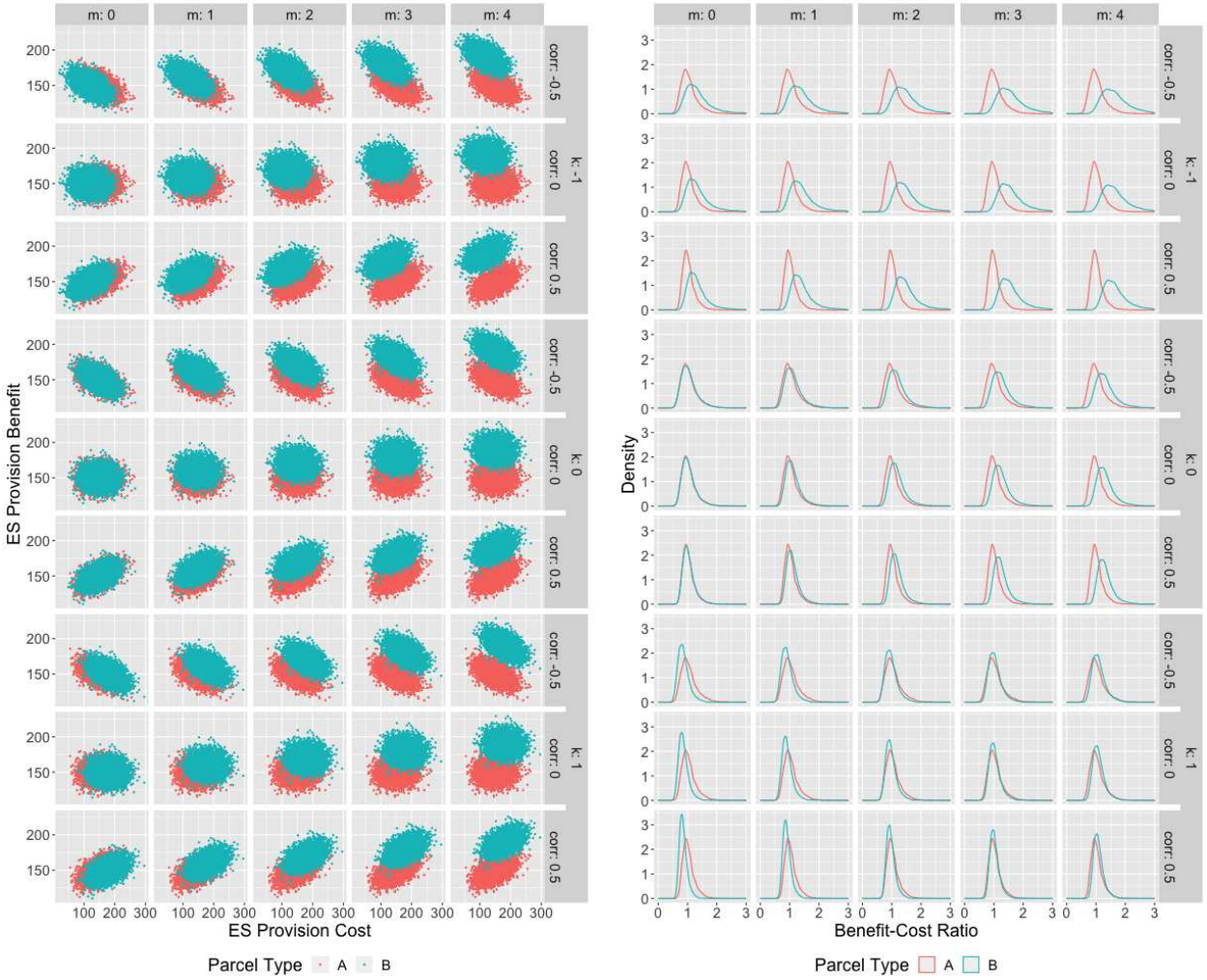

(a) Benefit and Cost

(b) Benefit-Cost Ratio Density

Figure 1.1: Plots Coefficients under Various Scenarios

parcels. Define the relative mean benefit difference and the relative mean cost difference between A and B as $\frac{m\xi}{\eta}$ and $\frac{k\sigma}{\mu}$, respectively. We observe that the more $\frac{m\xi}{\eta}$ deviates from $\frac{k\sigma}{\mu}$, the more the benefit-cost ratio distributions of A and B deviate from each other. When $\frac{m\xi}{\eta}$ is greater than $\frac{k\sigma}{\mu}$, the mean ratio of type A is smaller than the mean ratio of type B, and vice versa. The variance of ratio distributions decreases as the benefit-cost correlation ρ increases.

1.4 Results and Discussion

We first run simulations under parameters listed above to better understand the performance of differentiated payments in a variety of contexts. Then we evaluate case studies in which SWAT model outputs help to define the case.

1.4.1 Results of Hypothetical Simulations

The benefit-cost ratio is a key factor that determines optimal enrollment, since it is more cost-effective to enroll parcels with a higher benefit-cost ratio. When type A and B parcels have similar benefit-cost ratio distributions, we would expect the enrollment rate of both types of parcels to be close to 50%; when the ratio of distributions diverge from each other, the optimal enrollment should consist of more parcels of one type than the other. Our hypothesis is that a significant departure between the ratio distributions of the two types of parcels underscores the value of differentiated payments.

In practice, the social planner may be aware of the first two moments of the benefit and cost distributions, but is unlikely to know the parcel-level benefit and cost coefficients. Therefore, we randomly draw $N = 10$ realizations of cost and benefits coefficients for each scenario, and identify the optimal solution that minimizes the expected total cost of providing an expected ES no less than the target across the 10 realizations.

To investigate the main research question of this paper, we define the following outcome variables: Payment Difference Rate (PDR), Total Cost (TC) and Total Cost-effectiveness Improvement (%) (TCI):

$$PDR(\%) = 100 * \frac{\lambda_B - \lambda_A}{\lambda_A} \tag{1.7}$$

$$TCI(\%) = 100 * \frac{TC_{unif} - TC_{diff}}{TC_{eff}} \tag{1.8}$$

where the λ_A and λ_B denote payment rates for type A and B parcels, respectively; TC_{unif} and TC_{diff} are the total cost of achieving specific ES provision targets with a uniform payment and differentiated payments, respectively. TC_{eff} denotes the total cost with the efficient payment scheme.

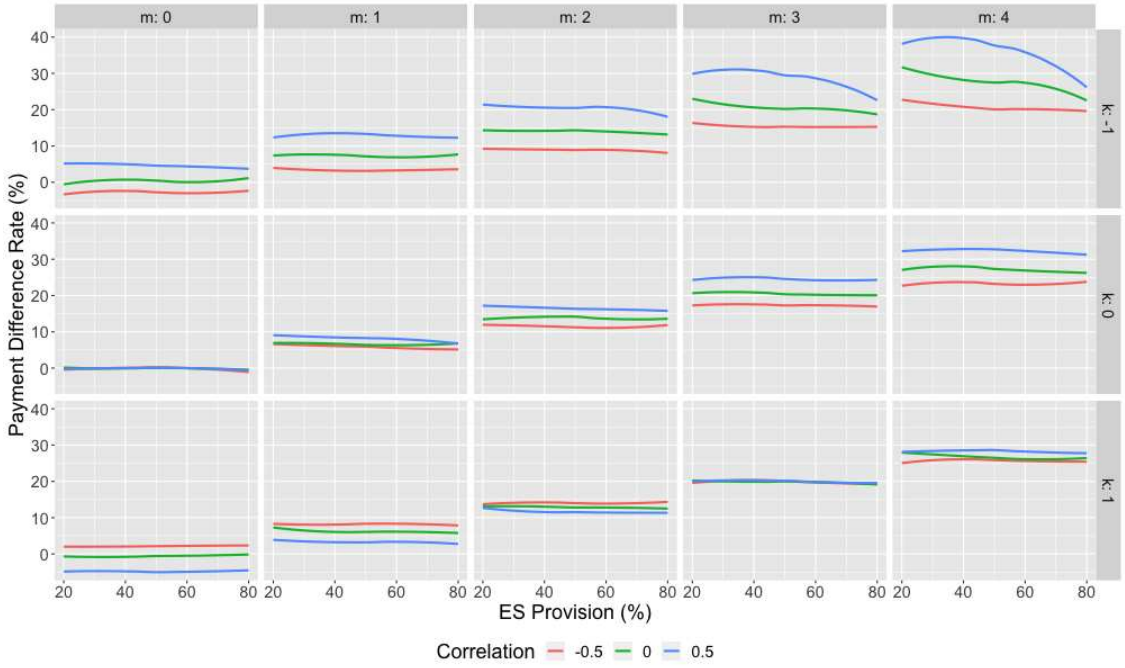

Figure 1.2: Payment Difference Rate under Various Scenarios

Figure 1.2 plots the PDR against the ES provision target τ for various mean benefit difference (m), mean cost difference (k) and benefit-cost correlation (ρ) settings. From Figure 1.2 we observe that PDR increases as m increases, while PDR is not sensitive to K in general; since conservation program should pay for ES benefit, when m increases, more type B parcels should be conserved, and larger PDR helps to conserve more type B parcels. When combining Figures 1.2 and 1.1b,

we conclude that (1) the impact of ρ on PDR is positive when the relative mean benefit difference is greater than the relative mean cost difference, and vice versa. Based on 1.1b we know that when relative mean benefit difference is greater than relative mean cost difference, the mean ratio of type B is greater than type A, which suggests positive PDR. When ρ increases, the variance of the ratio distribution decreases, and the ratio distributions overlap less between A and B, which underpins larger PDR. So in this case, as ρ increases, PDR increases. On the other hand, when the relative mean benefit difference is smaller than the relative mean cost difference, it's a flipped case where the mean ratio of type B is smaller than type A, which suggests negative PDR, and as ρ increases, PDR decreases. For example, subfigures (m:0, k:1) and (m:0, k:-1)[4], subfigures (m:1, k:0) and (m:2, k:1)[5] present vertical mirroring pattern. We also conclude that (2) the average PDR of each scenario equals to the relative mean benefit difference: $PDR \approx 100 * \frac{m\xi}{\eta}$, which aligns with the previous finding that PDR increases as m increases. Generally, the PDR results suggest that in practice PDR should target the relative mean benefit difference between type A and B parcels.

The efficient payment scheme reveals a theoretical cost-effective program that achieves a given ES provision target with the lowest social cost. We compare the total social cost from a uniform payment program and a differentiated program with the efficient payment program to evaluate how much cost-effectiveness improvement can be achieved by adopting payment differentiation compared with a uniform payment.

Figure 1.3 plots the TC difference rate between the efficient payment and the uniform payment[6] and shows that the social cost of a uniform payment can be as much as 8% higher than the efficient payment in general, and the total cost differences are larger when ES provision target τ is lower and when Type B parcels have higher mean benefits compared to Type A parcels.

The simulations present a case where a uniform payment rate can have relatively high cost-effectiveness. In practice, it is unlikely that the uniform payment rate will be chosen optimally, as

[4]when $m = 0, k = 1$, $\frac{m\xi}{\eta} - \frac{k\sigma}{\mu} = -30$; when when $m = 0, k = -1$, $\frac{m\xi}{\eta} - \frac{k\sigma}{\mu} = 30$;

[5]when $m = 1, k = 0$, $\frac{m\xi}{\eta} - \frac{k\sigma}{\mu} = 10$; when when $m = 2, k = 1$, $\frac{m\xi}{\eta} - \frac{k\sigma}{\mu} = -10$;

[6]TC difference rate = $100 * \frac{TC_{unif} - TC_{eff}}{TC_{eff}}$

it is in the simulations. We plot the benefit-cost ratio (ES provision ratio) against the ES provision cost in Figure 1.4[7] to further explore the results. As the benefit-cost ratios (ES provision ratios) are negatively correlated with the ES provision cost in the simulations as shown in Figure 1.4, parcels with lower cost have higher benefit-cost ratios, in which case a uniform payment rate can achieve a similar result as the efficient payment rate.

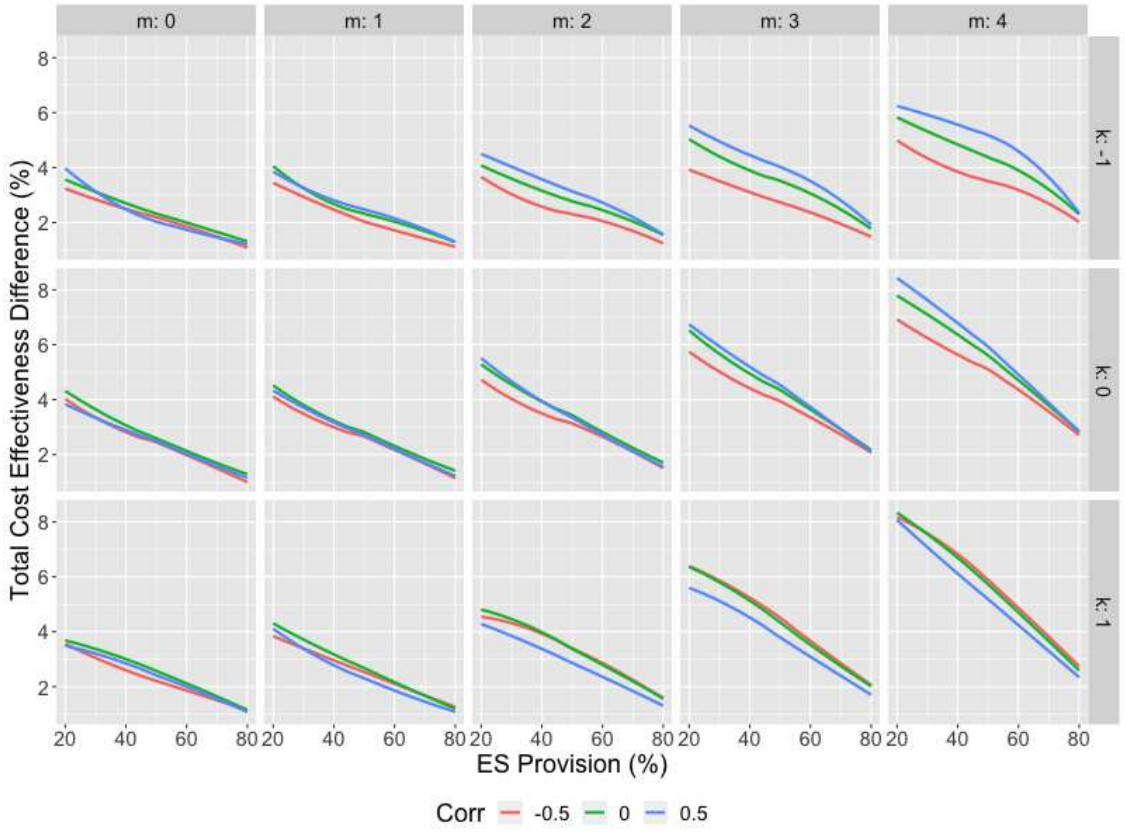

Figure 1.3: Total Cost Difference Between Efficient Payment and Uniform Payment

Next, we evaluate the TCI of the simulation. Figure 1.5 presents a clear positive impact of m on TCI with a negative impact of ES provision target τ on TCI. As m increases, when holding k and ρ the same, the benefit-cost ratio between A and B increases, which leads to higher TCI. As τ increases, the number of enrolled parcels increases, and it is inevitable that most parcels from both A and B need to be enrolled to achieve an ES provision target at 80% level or above. An

[7]Locally weighted smoothing across parcels is presented in the Figure

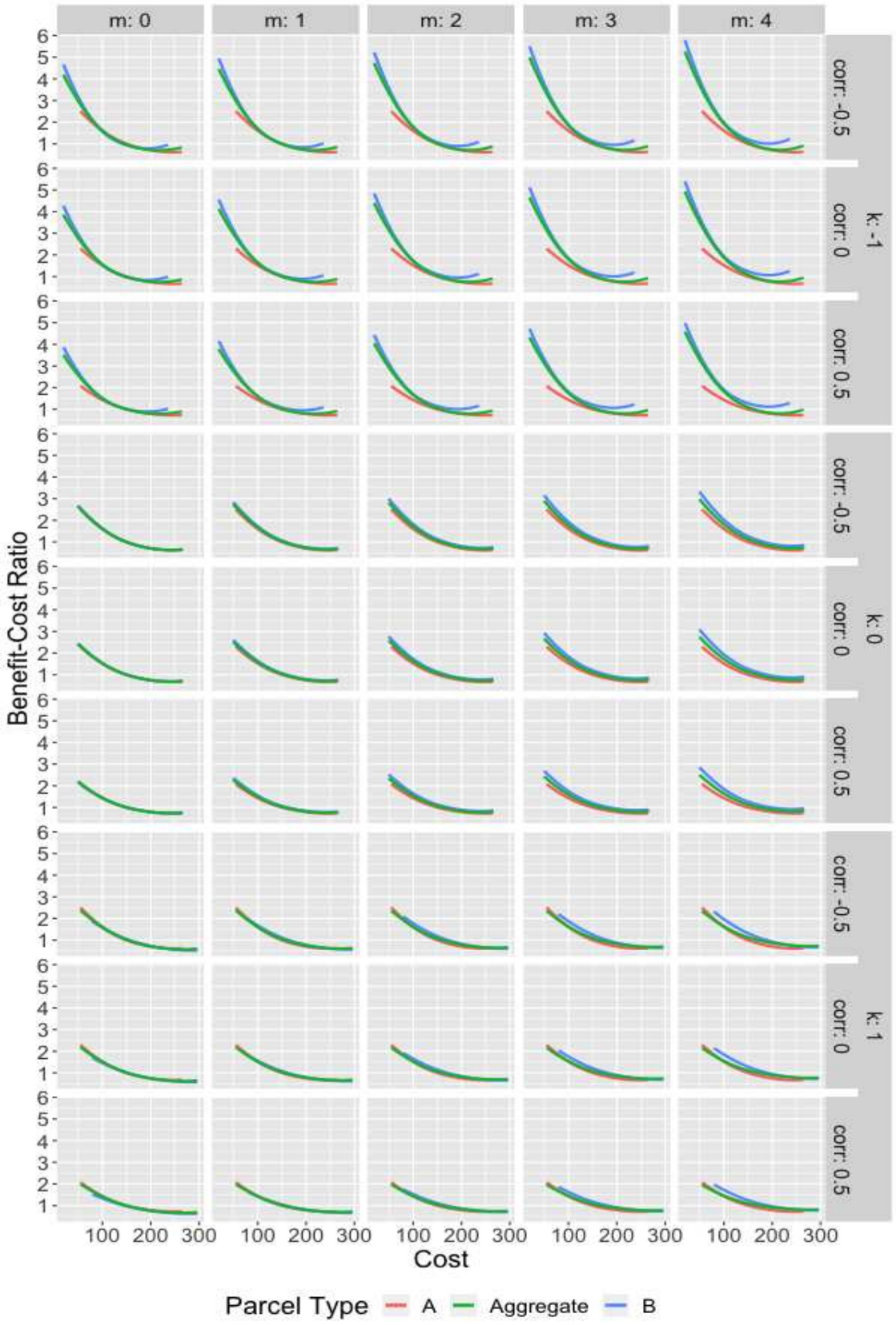

Figure 1.4: Benefit-Cost Ratio against Cost

extreme case is where all parcels need to be enrolled to achieve 100% ES provision target, and in this case, all three payment schemes exhibit the same social cost. Therefore, the higher τ is, the larger number of enrolled parcels across land types which implies lower TCI. The results suggest that in a case where the mean ES benefit difference between land types is high and the ES provision target is low, payment differentiation generates a larger advantage in terms of reducing the social cost in percentage compared with a uniform payment program. The comparisons of absolute value of social costs can be found in Figures A.1, A.2 and A.3. In absolute value terms, the social cost reduction of the differentiated payment relative to a uniform payment tends to be highest for the mid-range targets (around 60%).While TCI in the presented simulations ranges from 1% to 7%, which is relatively small, we should focus on the direction rather than the actual magnitude of the impact.

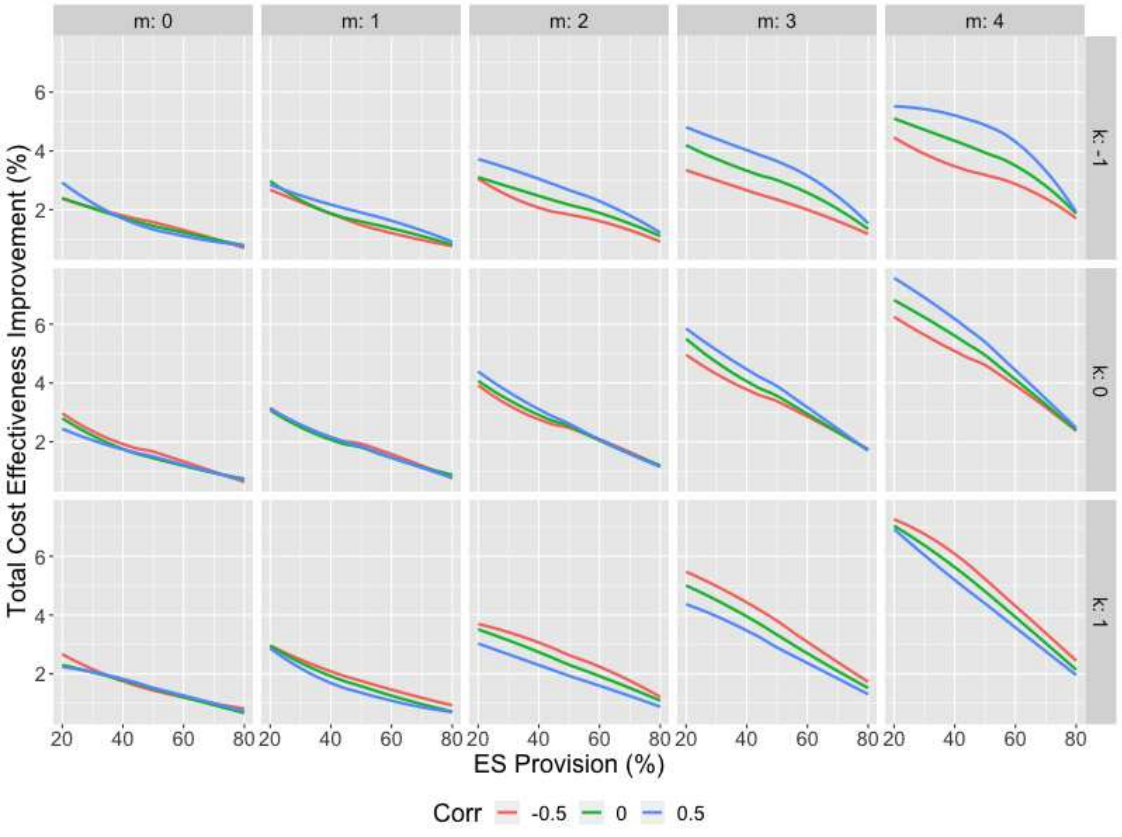

Figure 1.5: Total Cost-effectiveness Improvement under Various Scenarios

The response of TCI to k can be explained by Figure 1.4. Under the efficient payments, parcels with highest benefit-cost ratio are enrolled first. If the relationships between benefit-cost ratio and cost are quite different from the aggregate distribution versus the individual land type distribution, the payment differentiation could increase TCI. From Figure 1.4, we observe that (1) when m is small, the ratio-cost curves are highly overlapped, and therefore TCI curves show a similar pattern; and (2) the aggregate ratio-cost curves for the k:0 group from both A and B group deviate more than that in the k:1 group, and therefore TCI with $k = 0$ is generally higher than TCI with $k = 1$. As to $k = -1$, there are type B parcels providing high ES outcomes with very low cost. Therefore, a very low uniform payment rate can achieve a similar result as payment differentiation when k = -1 and the ES provision target is low. This is why we observe the lowest TCI with $k = -1$ in most scenarios.

1.4.2 Analysis with SWAT-based Case Studies

To illustrate specific applications of our findings, we consider a PES program that seeks to improve water quality. The spatial attribute we propose to use to differentiate the payments to participation is the presence of agricultural tile-drainage. Agricultural tile-drainage systems, pervasively installed in the U.S. Midwest, serve to transport excess water from the soil. Literature has revealed that tile-drainage systems have significant impacts on the underground transportation of nutrients, and tiled-fields tend to have higher nutrient run-off for a given time period [74, 35, 7]. We have a Soil and Water Assessment Tool (SWAT) model calibrated for the Lower Arkansas River Basin in southeast Colorado and the South Fork Watershed in central Iowa. While only the 66th sub-basin of the Lower Arkansas River basin contains tiled parcels, the South Fork Watershed overall is heavily tiled. Case studies for these two watersheds provide an opportunity to evaluate how a differentiated payment program would work under very different underlying tile-drain installment cases.

SWAT is a model that incorporates agricultural activities[8], soil characteristics, weather and groundwater information to simulate the environmental impact of land management practices and climate change. SWAT is widely used in assessing soil erosion, non-point source pollution and watershed management. A watershed is first divided into several subbasins and each subbasin possesses one reach segment. A subbasin is then divided into Hydrological Response Units (HRUs) which are portions of a subbasin that possess unique land use and soil attributes. An HRU is the basic analysis unit of SWAT, and HRUs are assumed to be independent in terms of nutrient loadings, which means a given HRU's nutrient loading is not impacted by its neighbor HRUs' activities Arnold et al. [3]. SWAT provides HRU-level crop yield (ton/ha) and nutrient loading of nitrate and phosphorus for a given realization of weather outcomes over a year.

We conduct case studies on the fields in each study area with major economic crops. The ES provision in the case study is nitrate loading reductions, and land owners are assumed to reduce nitrate loading by switching from planting commodity crops to pasture. We run SWAT simulations under crop and pasture land uses to obtain corresponding annual nitrate loading (kg/ha) at HRU level, then combined with HRU-level area, total annual nitrate loading mass (kg) are calculated. The HRU-level nitrate loading mass difference between crop and pasture land uses serves as HRU-level ES provision benefit estimate. The ES provision cost is the opportunity cost of switching a commodity crop to pasture. SWAT simulated crop yields, crop budgets in Colorado[9] [Colorado State University] and Iowa[10] [Iowa State University] along with crop price from USDA NASS [83] are used to calculate parcel level ES provision costs, measured in US dollar.

Colorado: Lower Arkansas River Basin (LARB)

The LARB SWAT model is calibrated with observational streamflow data from 2015, and the HRU boundaries account for homogeneous soil attributes as well as actual field boundaries in the LARB SWAT. Therefore, in the LARB case study, the HRU boundaries are identical to field

[8]For example, crop planting, irrigation, fertilization, tillage and harvesting.

[9]https://abm.extension.colostate.edu/enterprise-budgets-crop/

[10]https://www.extension.iastate.edu/agdm/cdcostsreturns.html#summaries

Table 1.2: Summary Statistics of LARB Case Study

Grid-level	Non-tiled (A)	Tiled (B)
Number	1002	822
Correlation	0.31	0.43
Mean ES Provision Benefit (g)	61.60	1718.41
Standard Deviation of Beneift	97.60	2354.63
Mean ES Provision Cost ($/acre)	255.20	323.03
Standard Deviation of Cost	171.42	207.66
Mean ES Provision Ratio	0.26	4.87
Standard Deviation of Ratio	0.31	6.20

boundaries, and we use field as the unit of analysis. The calibrated SWAT for sub-basin 66 has been found to provide satisfactory simulation for streamflow with Percent bias[11] (PBIAS) smaller than 10% and Nash Sutcliffe Efficiency[12] (NSE) greater than 0.6 for both scheduled and automatic irrigation scenarios [88].

In sub-basin 66, there are 160 fields in total. We focus on the fields that planted corn, alfalfa, winter wheat and sorghum in 2015 and had positive crop yield, and we are left with 91 fields, consisting of 29 tiled fields (type B) with total area of 1110 hectares and 62 non-tiled fields (type A) with total area of 1238 hectares. As the field area is different, we transform a given field to multiple homogeneous 1-acre grids, and all 1-acre grids in a field share the same field-level cost and benefit coefficients, which inevitably results in clusters in grid-level coefficients. To avoid outliers' contamination on the outcomes, we further trim the data by excluding grids with benefit-cost ratio larger than the 90% percentile value or smaller than the 10% percentile value by parcel type, and we end up with 822 tiled grids (type B) and 1002 non-tiled fields (type A). Table 1.2 summarizes statistics of the LARB case study, and Figure 1.6 provides the geographical context.

By switching the actual crop planted in 2015 to pasture in the SWAT model for each field, we obtain the nutrient reduction with a conservation action (land fallowing) for each field. The

[11]Percent bias (PBIAS) measures the average tendency of the simulated values to be larger or smaller than their observed ones. Absolute value of PBIAS $< 10\%$ indicates very good simulation performance.

[12]The Nash-Sutcliffe efficiency (NSE) measures the relative magnitude of the residual variance compared to the measured data variance. NSE ranges from 0 to 1, and a larger NSE indicates better model goodness-of-fit.

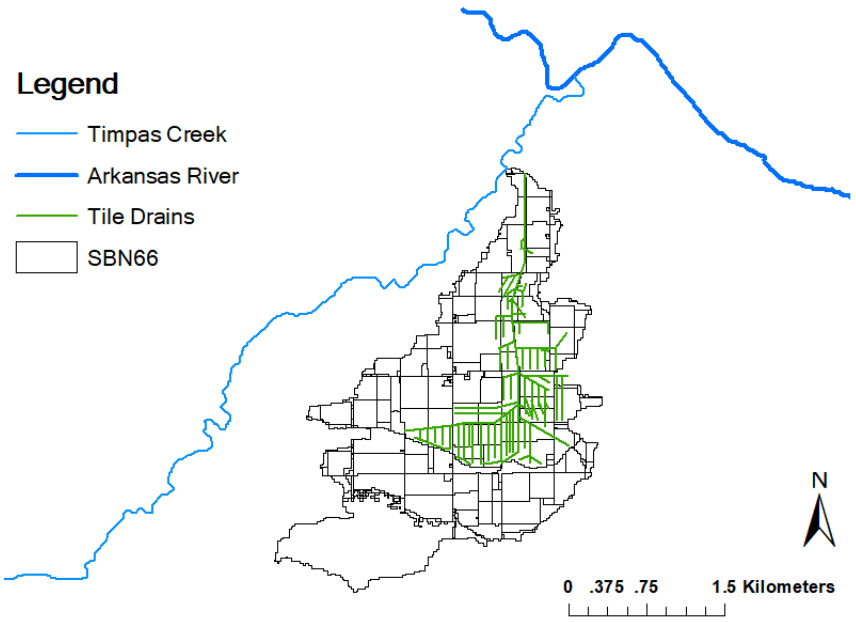

Figure 1.6: Study Area of LARB case: Sub-basin 66

822 tiled grids in total reduce a maximum of 1.41 ton of nitrates, while the 1002 non-tiled fields in total only reduce 0.06 ton of nitrates. The mean benefit of tiled parcels is more than 27 times that of the non-tiled parcels, while the cost of tiled parcels is not significantly different from the non-tiled parcels. In other words, there is a huge difference in nutrient loading between the tiled and non-tiled fields.

Figure 1.7 summarizes the TCI, TC and PDR of the LARB case. We observe in Figure 1.7a that TCI decreases as ES provision target increases, which aligns with the findings from the simulations presented in the previous section. Due to the large difference in the mean benefits across tiled and non-tiled grids, payment differentiation offers significant social cost saving ranging from 100% to 900%. From Figure **??**, we observe that TC of a uniform payment program is always greater than that of a differentiated payment program. The TC difference between the uniform payment program and the differentiated payment program does not change significantly. This is mainly due to the discrete and clustering nature in the coefficient. An increase in payment rate could result in large increase in enrollment and therefore overshoot for the ES provision target. PDR curves in Figure 1.7b look different from the simulation-derived pattern. This is mainly

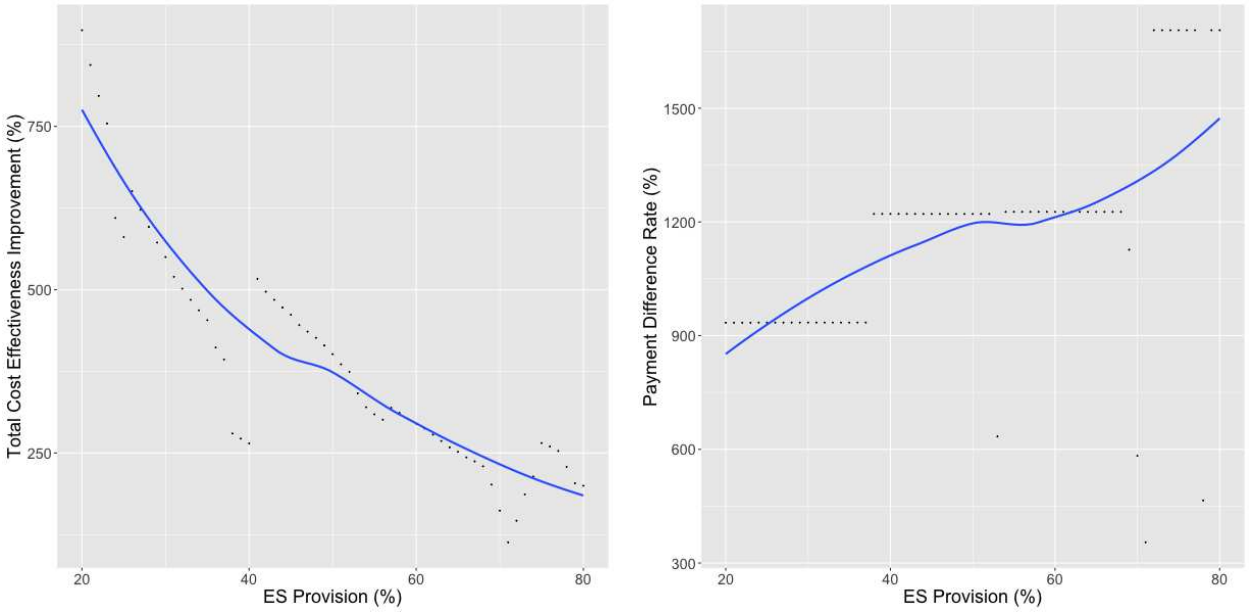

(a) Benefit and Cost

(b) Benefit-Cost Ratio Density

Figure 1.7: Colorado Case Study Results

due to the significant difference in the mean benefits across parcel types. When non-tiled grid's standard deviation of ES benefit is used, m is about 17. Such a large m means that most nitrate loading reduction are provided by tiled grids, and therefore, the tiled-grids enrollment rate is 97% on average across ES provision targets. Therefore, non-tiled grids enrollment remains low while tiled-grids enrollment grows to achieve increasing ES provision target, which leads to increasing PDR as ES provision target increases. In addition, the clustered nature of the grid-level benefit and cost coefficients results in a large number of grids to be enrolled with an increase in payment rate, which leads to the stair-step pattern in realized PDR outcomes. For example, offering \$35 per acre for non-tiled grids and \$358 per acre for tiled grids would enroll 10 grids of non-tiled grids and 453 tiled grids, and collectively provide 37% of the nitrate reduction capacity. Therefore, we observe the same realized PDR when τ ranges from 20% to 37%. If we keep the payment rate for non-tiled grids the same, and increase the payment rate for tiled grids to \$459 per acre, then 579 tiled grids in total would enroll to the program and jointly provide 68% of nitrate reduction capacity. This is why we observe that the PDR remains around 1200 for most τ between 38% and 68%.

The LARB case study suggests that the conclusion about the TCI from the simulation holds in general, while the PDR patterns are affected by the ES provision shares across land types which is not considered in the previous simulations.

Iowa: South Fork Watershed

SWAT+, a revised version of SWAT, is used for the case study of the South Fork Watershed (SFW) in Iowa. SWAT+ was released on Apr 15th 2021, and the HRUs have not been transformed based on the field boundaries. Differences in the data preparation between Iowa and Colorado case studies are described below.

Unlike the LARB, tile-drainage systems were extensively installed in the SFW, and therefore the actual locations of tile-drainage in this area are not available. The tile-drainage information is provided at the grid level in SWAT+. If the grid's soil permeability is poor, the grid is assumed to be tiled[13]. Figure 1.8 provides the distribution of grid-level tile-drainage.

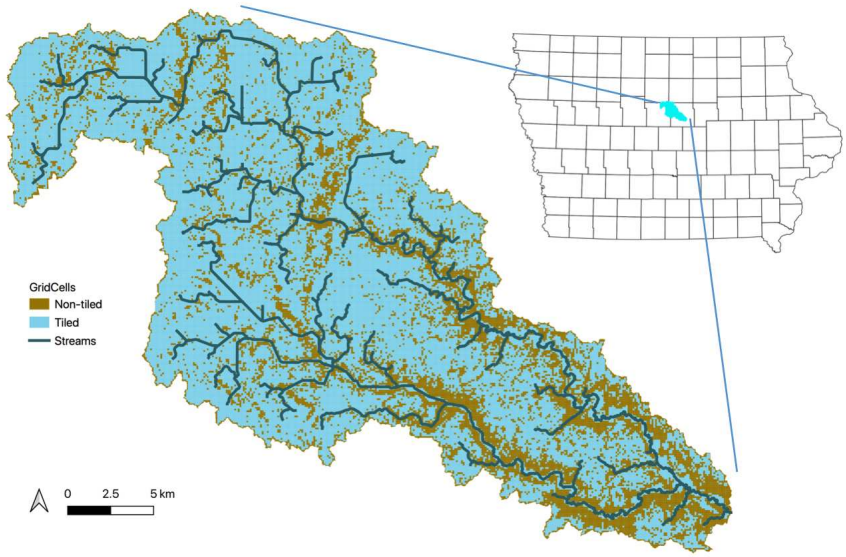

Figure 1.8: Distribution of Grid-Level Tile Flag in the South Fork Watershed

[13]Tile Flag $= 1$ if tiled, otherwise, 0

SWAT+ provides HRU-level crop yield (ton/ha) and nitrate loadings (kg/ha) which contribute to calculate HRU-level ES provision cost and benefit. Fields are the desired units of economic analysis, so the next step is to obtain field-level ES provision cost and benefit. We first obtain grid-level data based on the connection between HRU and grid[14], and then aggregate grid-level data to the field level with the field boundaries from the land use shapefile[15]. Last, we keep only fields planting corn or soybeans in the case study. Figure 1.9 shows the locations of agricultural use fields. The percentage of area with tile-drainage system is calculated for each field, and a field is defined as tiled if the it has over 75% of its area is tiled. Since area varies across fields, we investigate the cost, benefit and ratio coefficients at a 1-hectare grid level rather than the field level. We trim the decision units to fields with over 80% of their area planted in either corn or soybeans. After excluding fields with extreme ratio values larger than the 90% percentile value or smaller than 10% percentile value, we end up with 514 non-tiled fields with total area of 15,468 hectares and 709 tiled-fields with total area of 26,598 hectares. Correlations between cost and benefit are both positive for tiled and non-tiled fields. Figure 1.10 summarizes the density plots of the SFW case.

Table 1.3: Summary Statistics of SFW Case Study

Grid-level	A	B
Number	15476	26598
Correlation	0.49	0.52
Mean ES Provision Benefit (g)	1470	1639
Standard Devision of Benefit	1139	991
Mean ES Provision Cost ($/acre)	293	294
Standard Devision of Cost	13.3	14.6
Mean ES Provision Ratio	4.94	5.49
Standard Devision of Ratio	3.75	3.19

[14]SWAT+ developer delineates SFW to 59,490 grids where most grids are 1-hectare, except ones on the edge of the SFW boundary. Then HRUs are created based on hydrological characteristics and soil properties. We obtain the grid-HRU connection information from SWAT+ developer and identify what grids fall into each HRU. Grids fall into a given HRU share the HRU-level coefficients.

[15]SWAT+ developer share HRU-level land use shapefile with us, which help us to generate grid-level land use data.

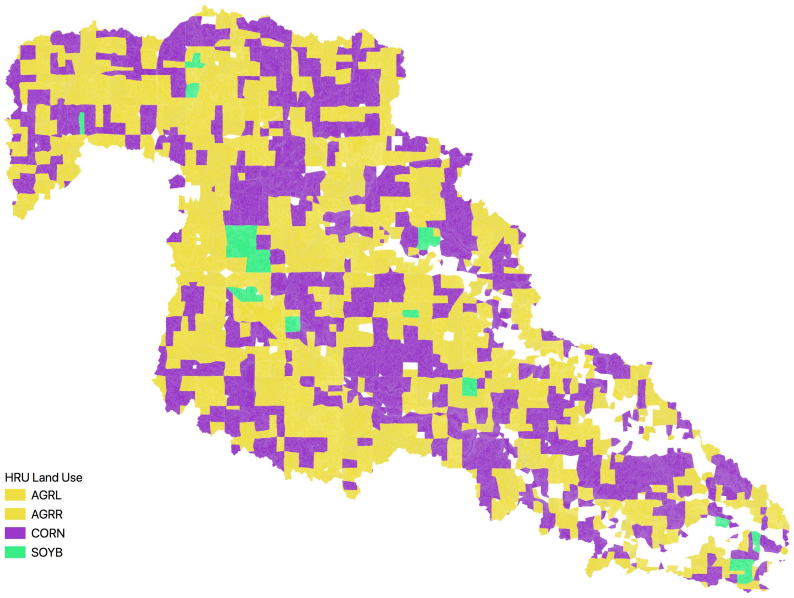

Figure 1.9: Fields with Corn or Soybeans in the South Fork Watershed

Note: AGRL: corn-soybeans rotation; AGRR: soybean-corn rotation

Figure 1.11 summarizes the TCI, TC and PDR in the SFW case, where m and k are not significantly different from 0. The SFW case results show that (1) the TCI shows a decreasing trend against the ES provision target, as suggested by the simulations, (2) the total cost difference between a differentiated payment program and a uniform payment program decreases as the ES provision target increases, and (3) PDR varies across ES provision target, which is different from what is suggested by the simulations.

Though the TCI trend against the ES provision target aligns with the simulation results, the TCI level is significantly larger than what we find in the simulation results when $m = 0$. To investigate this divergence, we plot the benefit-cost ratios (ES provision ratios) against the ES provision costs in the SFW case (Figure 1.12) and compare them with Figure 1.4. We find the following differences: (1) there are three groups of parcels with different cost rangesCost groups in SFW case are due to different crop choices and rotations in the SFW case in 1.12a, and (2) there is a clear negative correlation between benefit-cost ratio and cost in Figure 1.4 for both types of parcels while in Figure 1.12b the correlation is positive.

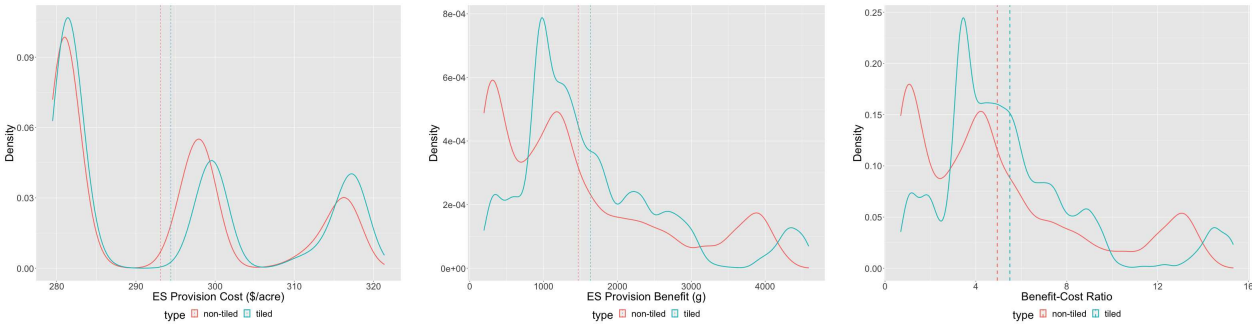

(a) Cost **(b)** Benefit **(c)** B-C Ratio

Figure 1.10: Density Plots of Coefficients: South Fork Watershed

Note: Dashed lines represent mean values of the variable across two types of fields

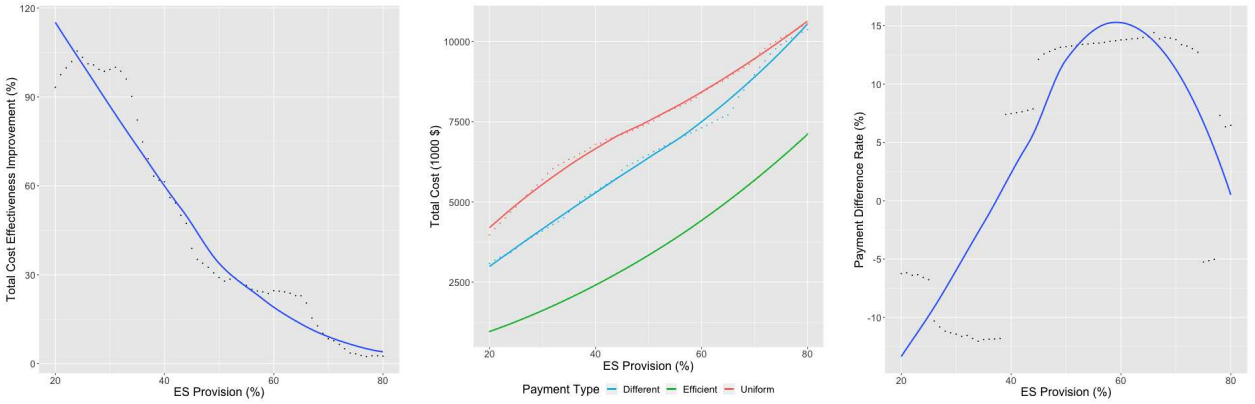

(a) TCI **(b)** Total Cost **(c)** PDR

Figure 1.11: Iowa Case Study Results

To test whether the cost range groups lead to the high TCI levels in the SFW case, we assign grids to three groups based on cost ranges . Grids with ES provision cost less than 290 $/acre fall into low cost group, and grids with ES provision cost greater than 305$/acre fall into high cost group, and the rest are considered as medium cost group. Results for individual subgroups are summarized in Figure 1.13, in which all TCI in subgroups present a decreasing trend against the ES provision target, while the TCI levels still remain high relative to the simulation results.

Therefore, we conclude that the relationship between benefit-cost ratio (ES provision ratio) and ES provision cost plays the major role in determining TCI levels. In the simulation, benefit-cost ratios decrease as costs increase, where enrolling parcels with lower cost means enrolling parcels

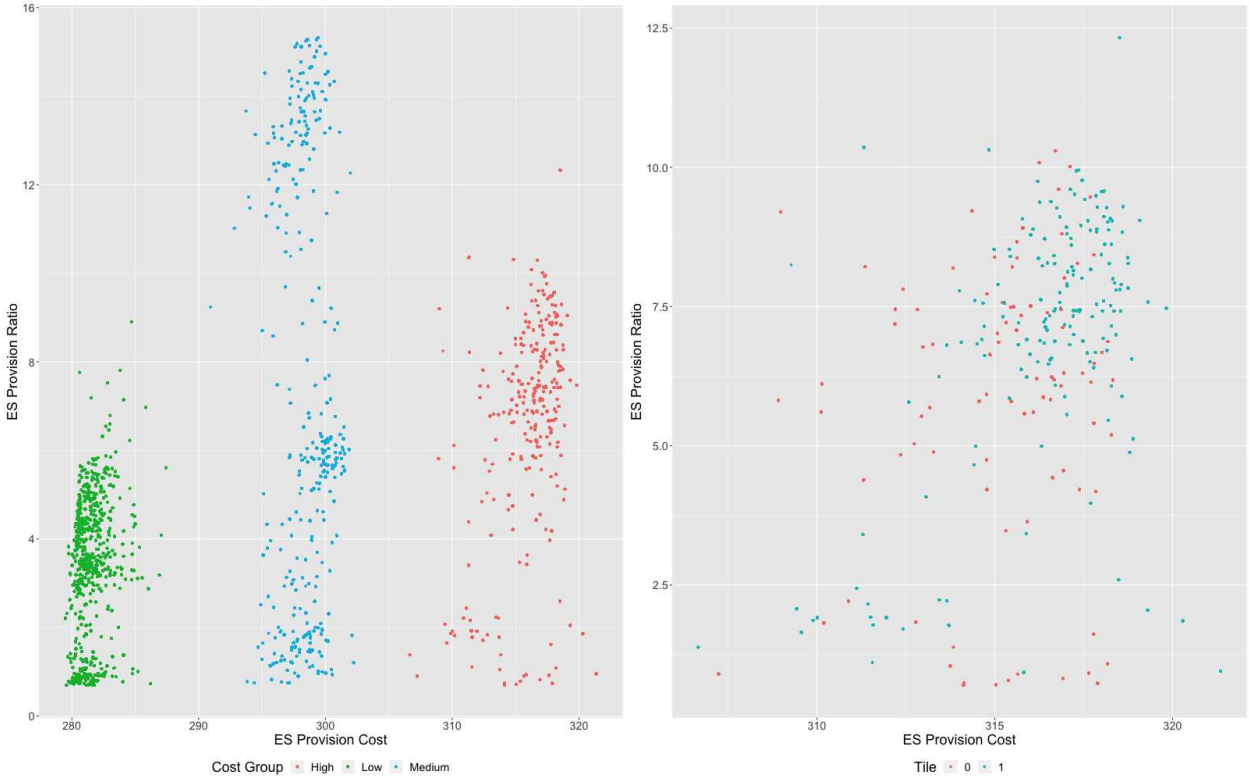

(a) By Cost Range **(b)** By Land Type

Figure 1.12: ES Provision Ratio against ES Provision Cost

with higher ratio, and therefore we observe that the performance of a uniform payment rate is close to that of efficient payment rate (Figure 1.3), and therefore the performance improvement of payment differentiation adoption is trivial and low TCI is observed. In the SFW case, the correlation between ratio and cost is positive in general, while we don't observe a significant difference in ES provision ratio nor in ES provision benefits between tiled and non-tiled grids. Therefore, when the underlying distributions of the ES provision benefit and cost for the area of interest are similar, positive correlations between ratio and cost results in relative high TCI levels.

As to the PDR, PDR levels are sensitive to the ES provision target. Again, we test whether the trimodal distributional form of the ES provision cost leads to this result. Figure 1.14 summarizes the PDR results for different cost subgroups. Though the PDR levels vary across ES provision targets, the PDR levels in all medium cost and high cost subgroups fluctuate around 0, which aligns with what suggested in simulation that average $PDR \approx 100 * \frac{m\xi}{\eta} = 0$.

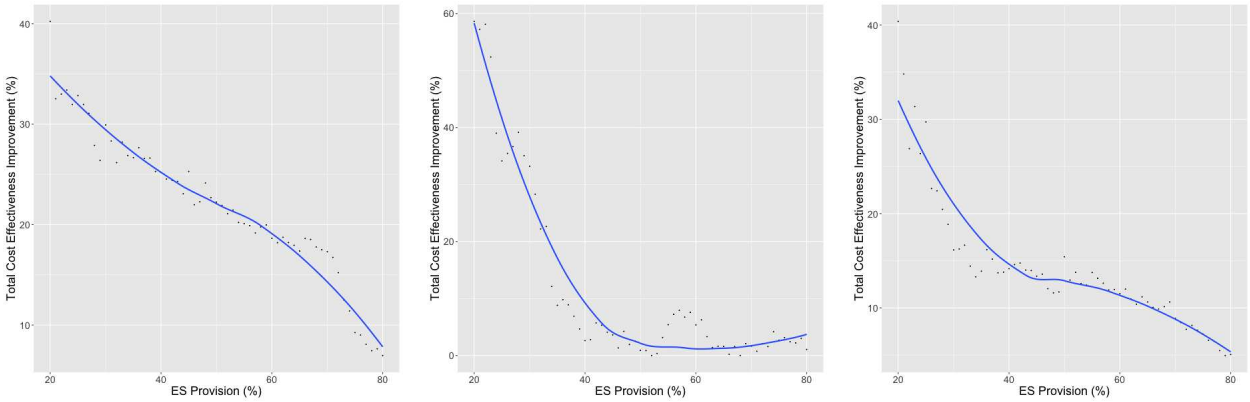

(a) Low Cost **(b)** Medium Cost **(c)** High Cost

Figure 1.13: TCI Results by Subgroup

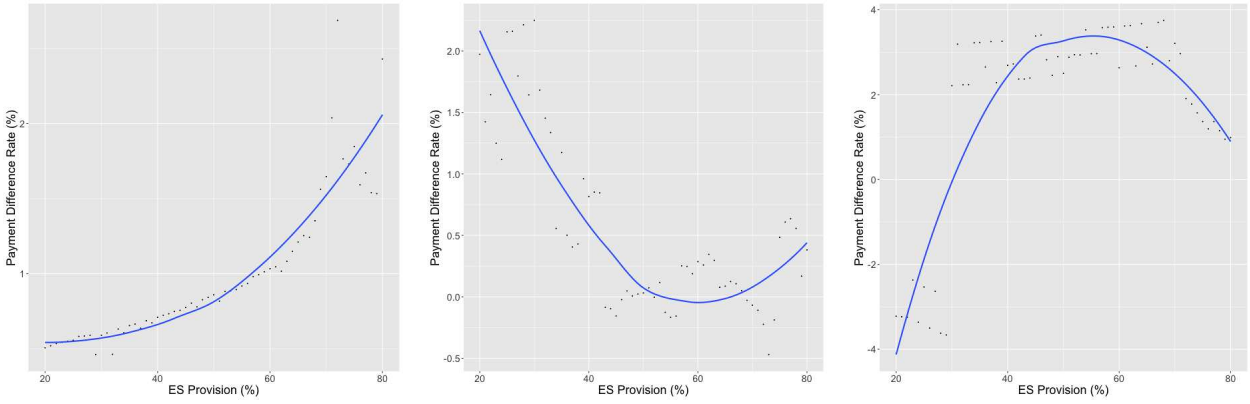

(a) Low Cost **(b)** Medium Cost **(c)** High Cost

Figure 1.14: PDR Results by Subgroup

Collectively, the LARB case and the SWF case provide two examples for the simulation scenarios, where the LARB has a large m and $k = 0$, and the SWF is a case where $m = 0$ and $k = 0$. As suggested from the simulations, when m is large, a higher TCI is achieved, and the TCI decreases as the ES provision target raises. While the findings about the PDR from the case studies diverge from that in the simulations, the divergence can be partially explained by the different functional forms of the cost distributions in the case study.

Generally, the ES provision benefit and cost distributions are quite different from the ones used in the simulations. Therefore, we don't see tight alignment between simulation lessons and the case study performance, which underpin extensions of the simulation settings. In future study, using

copulas to describe the joint distributions of ES provision benefits and costs with other marginal distributions, such as beta and gamma distributions with a wide range of benefit-cost correlations may better describe a scenario similar to the case studies. Comparisons between simulations and case studies reveal that choices of different payment rates across land types would require additional knowledge, besides the benefit-cost correlation, mean and variance of benefit and cost across land types.

1.5 Conclusions

This paper aims to evaluate the performance of a differentiated payment scheme compared with a uniform payment scheme under various contexts, and identify when the differentiated payment scheme creates total cost reductions associated with achieving specific ES provision targets. The contributions of this study is (1) exploring the performance of payment differentiation under various distributions of the ES provision benefits and costs; and (2) then taking advantage of hydrological modeling to conduct case studies on two watersheds with quite different agricultural and watershed characteristics.

Based on the simulation results, we conclude that when the cost and benefit distribution of different types of parcels are normally distributed (1) cost-effectiveness of a PES program increases as the mean benefit difference across land type increases, and (2) the cost-effectiveness improvement of a PES program decreases as the ES provision target increases. These two findings are reiterated by two SWAT-based case studies. Therefore, it is particularly beneficial to adopt a differentiated payment program with low ES provision targets and high mean benefit differences between land types.

While the simulations and case studies agree on the general conclusions, the simulation has limited power to describe PDR in the case studies, and the reasons are: (1) the simulation results are based on normally distributed costs and benefits across parcel types, while the case studies reveal skewed and/or multi-modal distributions for costs and benefits across parcel types; (2) the parcels in the simulations have the same area, while in the case studies, field areas are naturally

different. Though we have transformed the field-level data to uniform grid-level data to maintain identical size across decision units, we cannot avoid clusters in both coefficients and results. This is particularly obvious in the LARB case.

We recognize some limitations of our study, and we suggest future studies to extend this research by introducing other types of distributions, such as beta and gamma distributions which are closer to the distributions revealed in the case studies, and using copula methods to construct the joint distributions of ES provision benefit and cost. In addition, case studies based on other environmental issues can be addressed by applying different payment rates on other land attributes, such as land classification on land slope to address soil erosion issues. Future studies can also include administrative cost and try to explore the cost-effectiveness of adopting more than two payment rates in a PES program. Other transformations of payment differentiation may also be interesting to explore. For example, a PES program in which enrollment eligibility is based on land attributes. All these extensions would provide useful insights on PES practices under different contexts.

Chapter 2

Greenhouse Gas Emissions Trading System and Air Quality: Evidence from China

2.1 Introduction

China committed under the Paris Agreement to reduce carbon intensity (CO_2/GDP) by 60% to 65%, compared to 2005 levels by 2030. One significant move China has made to reduce carbon intensity is to establish the carbon Emission Trading System (ETS). Seven ETS pilot areas were formally announced in October 2011 and later started operation between 2013 and 2014[16]. The seven pilots together cover geographic areas that make up 18% of China's total population and 27% of China's GDP. Figure 2.1 presents a time trend of the proportion of total CO_2 emissions in pilot areas relative to China's total CO_2 emissions [53, 72].

It has been recognized in previous studies that CO_2 reduction activities can help to reduce local air pollution.Cheng et al. [18] adopted a Computable General Equilibrium (CGE) model to simulate the air pollution flow caused by the ETS in Guangdong province of China, and found that the ETS not only reduced carbon emissions, but also helped to reduce the emissions of SO_2 and NO_x. Dong et al. [25] examined the correlation between CO_2 emissions and aggregate PM 2.5 emissions in China with data collected from previous literature and the National Bureau of Statistics of China, and they found that CO_2 reduction activities can reduce PM 2.5 levels. Therefore, the carbon ETS, a system driven by carbon emission control, has the potential co-benefit of reducing local air pollution.

Air pollution has negative impacts on health outcomes [70], life expectancy [26, 37], school attendance [22] and could raise household averting expenditures [93]. Recent studies also reveal air pollution's impact on labor supply. Chang et al. [15] found negative impacts of air pollution on

[16]ETS operation staring time: Shenzhen, June 2013; Beijing and Shanghai, November 2013; Guangdong and Tianjin, December 2013; Hubei, April 2014; Chongqing, June 2014

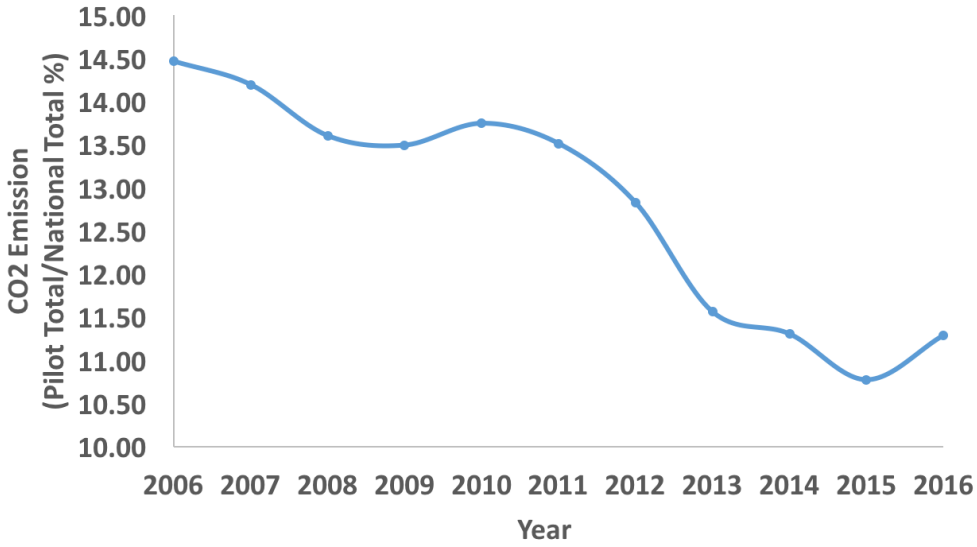

Data Source: Shan et al. [72]

Figure 2.1: Total CO2 Emission Percentage of Pilot Areas

work productivity with China's calling center data. Fan and Grainger [29] focused on the impacts of long-term exposure to PM 2.5 on labor supply and found a negative impact of air pollution on hours worked in China. He et al. [41] investigated short-term air pollution's impact on hours worked and found an insignificant response to concurrent PM 2.5 levels and a modest negative impact on lagged air pollution in China. The synergistic impacts of ETS through air pollution reductions motivate me to evaluate the impact of China's ETS on local air quality.

As a pilot program, each ETS pilot has its own operation timeline and regulations which implies the potential for heterogeneous treatment effects across pilots. Therefore the widely used two-way fixed effect (TWFE) model does not necessary provide meaningful average treatment effect estimates. I follow Steigerwald et al. [75] to estimate the heterogeneous treatment effects with dynamic two-way TWFE model as well as individual TWFE models. The results suggested that ETS does not reduce the PM 2.5 level in Guangdong while it does in Hubei. A further analysis focusing on the allowance allocation mechanism suggested that a sector-standards based mechanism can provide incentive for regulated facilities to expand their output which can lead to increases in overall emissions.

The contributions of this paper are twofold: (1) This paper contributes to an active literature on obtaining robust inference from two-way fixed effects models with multiple treatment timings, by introducing an empirical study for China ETS's impact on local air quality.; (2) I examine how the ETS allowance allocation mechanism affects the treatment effect associated with the ETS.

2.2 Literature Review

Before China's ETS pilot programs, the European Union (EU) launched the first large-scale cap-and-trade program in 2005, and the U.S. implemented the Regional Greenhouse Gas Initiative (RGGI) in 2009. Previous studies have adopted different methods to evaluate both the ex-ante and ex-post impact of programs in the EU and the U.S. Chan and Morrow [14] use a difference-in-differences (DD) approach to estimate the casual effect of RGGI on pollutant emission and the associated damages. Manion et al. [52] and Perera et al. [63] identify public health improvements from RGGI by connecting the health impact from ambient PM2.5 changes due to pollutant emission reductions. In their studies, COBRA[17] and BenMAP[18], impact assessment models developed by EPA, are used to quantify the air quality changes and accompanying health impacts. DD approaches have also been used to estimate the EU ETS's impacts on firm-level employment [13] and patenting behavior [11]. Chan et al. [13] find the EU ETS does not deteriorate firm's competitiveness during the first phase (2005-2007), and Calel and Dechezleprêtre [11] argue that the EU ETS increases low-carbon patenting by 36.2%. Verde [85] collects and summarizes 20 studies addressing the EU ETS's impact on firm competitiveness and carbon leakage. 11 out of 18 studies that evaluate ETS's impact on firm competitiveness use a DD design. While ETS program could have many consequences and co-benefits, our work focuses on the effect of ETS program on local air quality, which is not explicitly targeted by the program.

Due to the lack of random assignment of ETS, quasi-experiment designs often serve as the second best choice to evaluate policy performance. DD is a quasi-experimental design widely

[17]CO-Benefits Risk Assessment Health Impacts Screening and Mapping Tool

[18]BenMAP: Environmental Benefits Mapping and Analysis Program

adopted in the ETS impact assessment literature. A canonical DD design consists of two groups (treated and control) and two periods (before and after treatment). With parallel trends and exogenous treatment, the canonical DD provides consistent estimates of the Average Treatment effect on the Treated group (ATT). Many studies are motivated by the canonical DD and increasing data availability to adopt a two-way fixed effect model to estimate the ATT, in hopes of accounting for unobservable time invariant attributes with unit fixed effects and to account for common nonlinear effects over time with time fixed effects. However, many studies deviate from the canonical DD due to the staggered adoption of policy, where units receive treatment in different time periods. In a staggered adoption case, the traditional two-way fixed effect (TWFE) model implicitly uses the units that receive the treatment earlier as a control group for the units that receive the treatment later, as in the later time period, the treatment status of the earlier unit does not change. The traditional TWFE provides treatment effect estimates equal to a linear combination of heterogeneous treatment effects, and the weights associated with some heterogenous treatment effects could be negative [36, 46, 75]. Since negative weights can generate a misleading summary of the heterogeneous treatment effect, the literature concludes that a traditional TWFE does not provide insightful estimates of interest, and suggests in this case to (1) conduct pair-wise 2 by 2 canonical DD with the same untreated[19] group and calculate a weighted average treatment effect based on institutional knowledge[20], or (2) to adopt a dynamic TWFE model to estimate the heterogeneous treatment effects.

The dynamic specifications also have been used to provide statistical tests on the parallel trends. Though the parallel trend assumption during the treatment periods is not testable, parallel trends in the pre-treatment periods can still provide some support with arguments about why the parallel trends would continue after the policy implementation [48]. The literature also explores violation of the parallel trend assumption. Callaway and Sant'Anna [12] proposed an estimator when parallel

[19] All of or a subset of the untreated units serve as the common control group

[20] The research question itself provides hints on the weight calculation. Sample size, and related variables can be used to calculate the associated weights for each group. In this paper, since the ETS affects local air pollution through economic activities, the pilot-level GDP can be used to calculate the weight associated with the pilot-specific ATT.

trends holds after conditioning on observed covariates, and Rambachan and Roth [65] develop an estimator that imposes restrictions on possible trend differences between treated and control groups.

The other widely adopted quasi-experimental empirical method is Regression Discontinuity (RD). The surge of RD application is due to its relatively milder assumption compared to other quasi-experiment methods, which can make it closer to a randomized trial. While the natural RD is based on a continuous running variable which determines the treatment, such as test score [78] and distance [16], the “Regression Discontinuity in Time" (RDiT) takes time as a running variable, and has been applied to assess the response of air quality to driving restrictions [23, 33], gasoline content regulation [4] and urban rail transit [17]. However, the "Regression Discontinuity in Time" (RDiT) is only appropriate under certain contexts: (1) relatively large sample size within a short time period. The nature of RD design implies a high internal validity around the chosen threshold of the running variable. Including more observations that are far away from the threshold does not benefit the RD design. However due to the concern of the sample size and statistical power, many studies include a long time period when using RDiT. (2) Appropriate control for covariates. In the natural RD, the treatment is as good as a random trial within a narrow bandwidth, therefore few controls are needed. However, since treatment of time is generally not randomly assigned, appropriate controls for covariates are critical when using RDiT to mitigate causal identification concerns. China’s ETS pilots are implemented at the province level, so the cross-sectional dimension is very limited. The ETS allowance quota is assigned annually. As a result, to obtain an adequate sample size, I would have to include a long time period, which goes against the requirements of a valid RD estimate. Therefore, I don’t use RDiT for this analysis.

2.3 Emission Trading System (ETS) in China

The ETS program is proposed to achieve the goal of reducing carbon intensity and the growth rate of total carbon emissions. Seven ETS pilots were announced in 2011 and they started ETS op-

eration at different times between 2013 and 2014. Figure 2.2 summarizes when the ETS operation started in each pilot area.

Figure 2.2: ETS Operation Timeline by Pilot

These seven pilots consist of four municipalities, one sub-provincial city and two provinces (Figure 2.3). Table 2.1 provides a summary of GDP, population and the cap for CO_2 emissions for each pilot in the first year of ETS pilot operation, and Table B.1 (in the Appendix) summarizes each ETS pilot's coverage in terms of regulated sectors and enrollment threshold. Regulated facilities are the major participants of trading within each ETS pilot area, and allowances for a given pilot should be used for the compliance within the pilot. Allowances can be used for compliance across sectors within a pilot, but cannot be traded across pilot areas. The local government of each pilot area has some allowances reserved for market adjustments.

Table 2.1: Statistics of Pilots in Early Stage of ETS Pilot Period

Pilots	Administration	2013 Population (millions)	2014 GDP (trillions US$)	CO_2 under cap (%)	CO_2 under cap (Million Ton)
Shenzhen	sub-provincial city	10.4	0.26	40	33
Beijing	municipality	20.7	0.35	49	57
Shanghai	municipality	23.7	0.38	57	160
Tianjin	municipality	14.7	0.25	60	160
Chongqing	municipality	29.7	0.23	30	125
Guangdong	province	106.4	0.84	54	388
Hubei	province	58	0.45	44	324

Data Source: Margolis et al. [53]

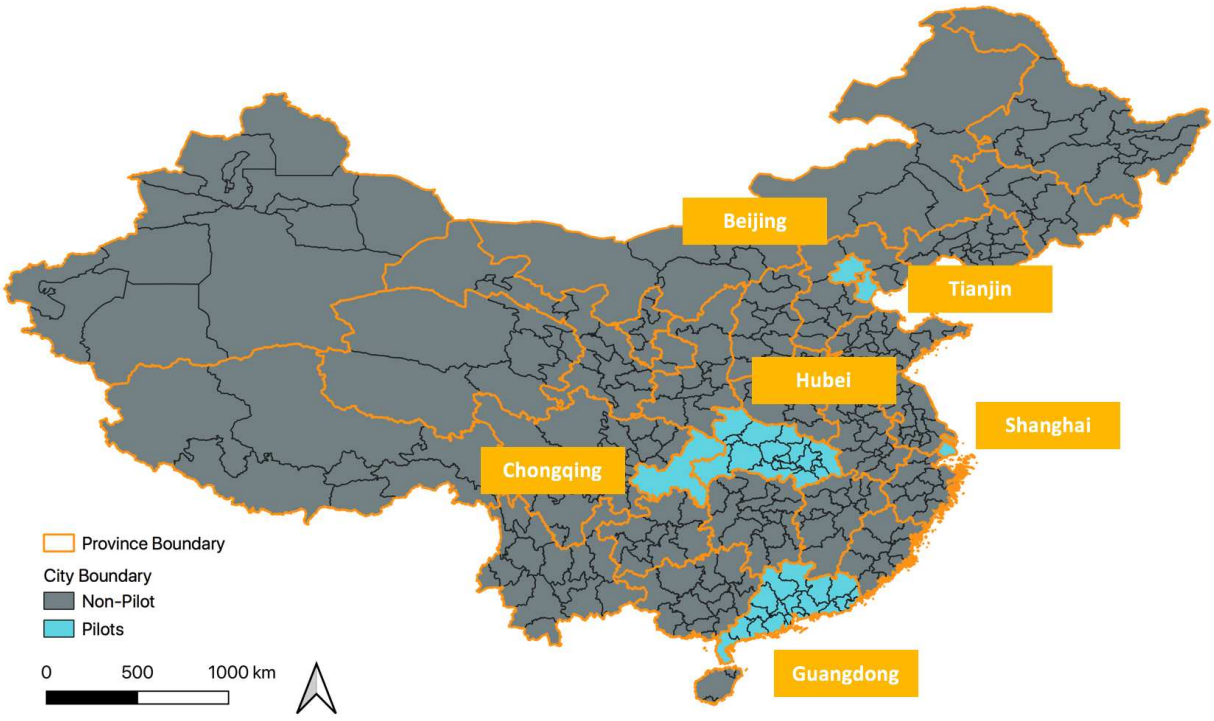

Figure 2.3: Location of China ETS Pilots

The structural hierarchy of the administrative divisions of China, from top to bottom, are provincial level, prefectural level, county level, township level and basic level autonomy. Figure 2.4 briefly presents the first two levels that are involved in this study. The first level is provincial-level, which consists of 23 provinces, 5 autonomous regions, 4 municipalities and 2 special administrative regions. The second level is prefectural level, which consists of 293 prefectural cities[21], 7 prefectures, 30 autonomous prefectures and 3 leagues.

This paper focuses on estimating the ETS treatment effect in the Hubei and Guangdong ETS pilots. Due to the administrative and economic specialty of the municipalities: Beijing, Shanghai, Tianjin, Chongqing are not included in the analysis. Shenzhen, known as the Silicon Valley of China, is a sub-provincial city in Guangdong province. However, Shenzhen has its own ETS regulation and operational timeline, therefore Shenzhen is excluded from Guangdong province in the analysis.

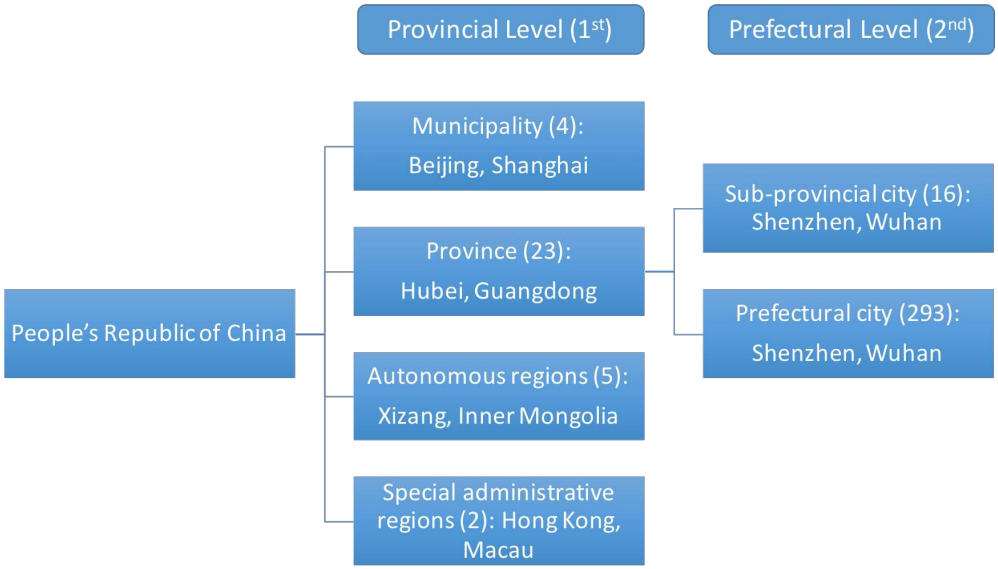

Figure 2.4: The Administrative Divisions of China

[21] 16 out of 293 prefectural are also classified as sub-provincial cities due to their critical economic role and large population

2.3.1 Description of Emission Trading System Pilots

The central government determines the annual total carbon emission allowances for each ETS pilot area based on the national carbon intensity reduction goal and provincial economic growth plans. Then each pilot's annual allowances are further distributed to sectors and sub-regions within the pilot. Finally each regulated facility receives individual emission allowances. Three general allowance allocation schemes are used to determine the facility-level allowance allocation in China's ETS pilot: historical emission level, historical emission intensity and sector standards. Facilities' responses towards alternative allowance mechanisms are assumed to be different, and Figure 2.5 summarizes possible responses.

Regulated facilities that emit more carbon emissions than allowances they receive can purchase allowances through the ETS market within the pilot for the compliance. On the other hand, facilities who receive more allowances than their actual emissions can save the allowance surplus for future compliance or sell them through the ETS market. Compliance failure can result in penalties that are documented in Table B.2 (in the Appendix).

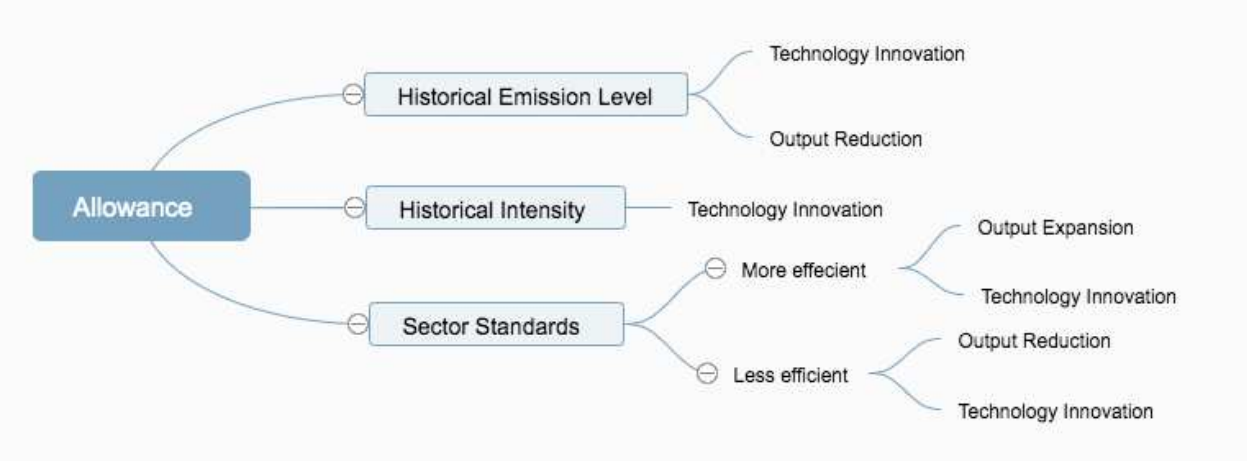

Figure 2.5: Alternative Response of Regulated Facilities to Different Allowance Mechanisms

1. Allowance based on historical emission level (A1)

Each regulated facility i in year t receives emission allowance A_{it} based on the benchmark[22] historical emission,E_{is}, and a carbon emission regulation coefficient f_t:

$$A_{it} = (\frac{1}{3}\sum_{s=t-1}^{t-3} E_{is}) * f_t \tag{2.1}$$

where i denotes facility and t denotes year. Guangdong and Hubei consider emissions in the last three years as historical emissions. The regulation coefficient, $f_t \leq 1$, is non-increasing as t increases. Under this allowance mechanism, the total emission level of regulated facilities would decrease as f_t decreases over time.

2. Allowance based on historical emission intensity[23] (A2)

Each regulated facility i receives emission allowance A_{it} in year t based on the output level P_{it}, the benchmark historical carbon intensity I_{is} and a regulation coefficient f_t:

$$A_{it} = P_{it} * \frac{\sum_{s=t-1}^{t-3} I_{is}P_{is}}{\sum_{s=t-1}^{t-3} P_{is}} * f_t \tag{2.2}$$

where the regulation coefficient $f_t \leq 1$ and is non-increasing as t increases. Under this allowance mechanism, regulated facilities don't have incentives to reduce their output level as the allowance are based on carbon intensity and output level. If a facility has a production function such that marginal carbon emissions do not increase with output, then the facility can achieve the target carbon intensity by expanding its output level. Though this mechanism provides little incentive on output reduction, regulated facilities would achieve cleaner production through technology innovation, in the long term, as f_t continues to decrease.

[22]Usually use the average of CO_2 emissions of previous years. Guangdong and Hubei use a rolling period (last three years). While some pilots use a fixed period to calculate the historical average: Beijing (2009-2012). Since the analysis focuses on Hubei and Guangdong, the formula is based on designs in Hubei and Guangdong

[23]Carbon intensity is calculated as carbon emission divided by the level or market value of output

3. Allowance based on sector standards (A3)

Each regulated facility i in sector k receives emission allowance A_{it}, in year t, based on the output level and a sector-specific carbon intensity in year t, S_{kt}:

$$A_{it} = P_{it} * I_k * f_{kt} = P_{it} * S_{kt} \tag{2.3}$$

where $S_{kt} = I_k * f_{kt}$ [24], and I_k denotes sector-specific time-invariant intensity and sector-specific regulation coefficient $f_{kt} \leq 1$ is non-increasing as t increases. Under this mechanism, regulated facilities have incentives to reduce their carbon intensity to gain an allowance surplus. However, the allowances granted to the sector could be larger than the total emission level of the sector. For example, in Hubei the sector standard of a sector in year t is based on the sector's 50 percentile (median) carbon intensity value in $t-1$. If the sector's median carbon intensity value is higher than the mean carbon intensity, then it is possible that the granted allowance to the sector is more than the total emissions of the sector. In this way, an allowance surplus is granted and ETS is expected to have little effect on the sector's total emission and might also reduce the ETS's effect on other sectors through inter-sector allowance trade.

While A1 impose a conventional cap on carbon emission level directly, A2 and A3 are based on carbon intensity instead. Allocations of allowances under A2 and A3 consist of two steps in both Guangdong and Hubei. First, an initial allowance[25] to a facility in year t is allocated at the beginning of year t's ETS operation; Second, at the end of year t, the final allowance is calculated with the actual facility-level output in year t. Regulated facilities receive (return) additional allowance if the initial allowance is less (more) than the final allowance.

In general, A1 and A2 tend to reduce carbon emission for regulated sectors and could therefore be expected to improve local air quality, while A3 does not necessarily reduce carbon emissions

[24] Some pilots release the S_{kt} while others release I_k and f_{kt}

[25] Initial allowance to facility i in year t = facility i's output level in year $(t-1)$ $\times$ the sector-standard of year t

due to a possibility of creating allowance surplus. Therefore, I empirically investigate how A3 affects the ETS's impact on the local air quality in section 6.1.

ETS Pilot in Guangdong

Guangdong province is a coastal province in South China, with GDP of 10.77 trillion CNY (1.66 trillion USD) and population of 115.21 million in 2019. The first ETS transaction of Guangdong province (Shenzhen excluded) happened on December 2013. The ETS in Guangdong province has covered steel, power, cement and petrochemical since 2014, while paper production as well as civil aviation entered the ETS from 2017. Allowances to facilities in steel and cement sectors are mostly based on sector standards while a small portion are based on historical emission levels. Allowances to facilities in the power sector are mainly based on sector standards. There are a small portion of facilities with allocations based on historical emission levels before 2017 and historical emission intensity after 2017. The paper sector mainly bases allocations on sector standards, while a small portion uses historical intensity. Civil aviation adopted a sector-standards mechanism in 2017, and uses the same system as the paper sector afterwards. Table 2.2 provides a detailed summary of the allowance allocation approach assigned to each ETS regulated sector in Guangdong over time.

ETS Pilot in Hubei

Hubei province is a landlocked province in the central China, with GDP of 4.58 trillion CNY and population of 59.27 million in 2019. The first ETS transaction was launched in April 2014. Hubei adopted the sector-standard approach to allocate allowances for the power and cement sectors from 2015, while the remaining industries were based on the historical emission levels method since 2015. The rolling baseline level used in the historical method is calculated with emission levels from the very last three years. Table 2.3 provides a detailed summary of the allowance allocation approach assigned to each ETS regulated sector in Hubei.

Generally speaking, the pilot ETS in Hubei province covers more sectors than that in Guangdong, while Hubei has a lower A3 adoption share across sectors than Guangdong. Therefore, I

Table 2.2: ETS Coverage and Allowance Allocation Approach in Guangdong

		Approach					
Industry	Subsector	2014	2015	2016	2017	2018	2019
Power	Fossil Fuel Power Station: Gas	A3	A3	A3	A3	A3	A3
	Fossil Fuel Power Station: Coal	A3	A3	A3	A3	A3	A3
	Fossil Fuel Heat Station: Gas	A3	A3	A3	A3	A3	A3
	Fossil Fuel Heat Station: Coal	A3	A3	A3	A3	A3	A3
	Combined Heat and Power	A1	A1	A3	A3	A3	A3
	Others	A1	A1	A1	A2	A2	A2
Cement	Raw material mining	A1	A3	A3	A3	A3	A3
	Kilning	A3	A3	A3	A3	A3	A3
	Clinker grinding	A1	A1	A1	A1	A1	A1
	Others	A1	A1	A1	A1	A1	A2
Iron & Steal	Long-process steel making	A3	A3	A3	A3	A3	A3
	Other steel making	A1	A1	A1	A1	A1	A1
Petrochemical	Petrochemical	A1	A1	A1	A1	A1	A1
Paper	Normal paper products	/	/	/	A3	A3	A3
	Special paper products	/	/	/	A2	A2	A2
Civil aviation	Primary civil aviation	/	/	/	/	/	A3
	Other civil aviation	/	/	/	/	/	A2

Summarized by the author; Source: http://drc.gd.gov.cn/qtwj/content/post_844376.html
A1: Allowance based on historical emission level
A2: Allowance based on historical emission intensity
A3: Allowance based on sector standards

hypothesize that (1) the pilot ETS has a stronger effect on reducing air pollution in Hubei than Guangdong due to larger sector coverage and lower A3 adoption rate, and (2) the pilot ETS in Guangdong might not have significant impact on the local air quality due to high A3 adoption rate across sectors.

2.4 Method

The goal of this study is to identify the extent to which the ETS pilot program affects local air quality in terms of PM 2.5 concentration. Ideally, a random selection of ETS pilots would serve as a natural experiment for ETS impact assessment. However, Chinese government select ETS pilots based on baseline pollution level, economic performance and environmental regulation investment

Table 2.3: ETS Coverage and Allowance Allocation Approach in Hubei

		Approach				
Industry	subsector	2015	2016	2017	2018	2019
Power	Fossil Fuel Power Station: Gas	A3	A3	A3	A3	A3
	Fossil Fuel Power Station: Coal	A3	A3	A3	A3	A3
	Fossil Fuel Heat Station: Gas	A3	A3	A3	A3	A3
	Fossil Fuel Heat Station: Coal	A3	A3	A3	A3	A3
	Combined Heat and Power	A3	A3	A3	A2	A2
Cement	Raw material mining	A3	A3	A3	A3	A3
	Kilning	A3	A3	A3	A3	A3
	Clinker grinding	A3	A3	A3	A3	A3
	Others	A3	A3	A3	A3	A3
Glass	Glass	A1	A2	A2	A2	A2
Ceramics	Ceramics	A1	A2	A2	A1	A1
Paper	Paper	A1	A1	A1	A2	A2
Machinery Manufacuring	Machinery Manufacuring	A1	A1	A1	A1	A2
Others	Others	A1	A1	A1	A1	A2
Water supply	Water supply	/	/	/	A1	A2

Summarized by the author; Source: http://sthjt.hubei.gov.cn/fbjd/zc/zcwj/sthjt/ehf/202008/t20200819_2807965.shtml

Others include iron & steel, vehicle manufacturing, petrochemical, textile, food & drink, medical and non-ferrous metals

A1: Allowance based on historical emission level

A2: Allowance based on historical emission intensity

A3: Allowance based on sector standards

[87, 45] of different provinces and cities. Therefore, carefully constructing the control group in the DD design is critical.

Matching is a common approach to build comparable control group. The goal of matching is to maximize the covariate balance between treated and control groups and the matched sample size. Ferraro and Miranda [31] demonstrate that a DD design with matched data can approximate random control trials and perform better in treatment effect estimates. Commonly used matching approaches are Propensity Score Matching (PSM), Mahalanobis Distance Matching (MDM), Coarsened Exact Matching (CEM). The first two methods fixed the size for matched data and hope to get sufficient covariate balance between treated and control group, while the CEM approaches

fix the level of imbalance and hope the resulted matched sample size is sufficiently large. Wang et al. [87] and Huang et al. [45] suggest a list of factors that contribute to ETS pilot choice in China, including economic development, industrialization, foreign investment, technology, education, pollution and pollution abatement.

Though I managed to obtain city-level economic indicators that can present the level of these factors, the dataset has a significant amount of missing values. It is unlikely to obtain a balanced matched data with sparse city-level economic indicator data. Matching analyses based on time series of different combinations of available economic indicators are conducted for both PSM and CEM. Log transformation and classification of raw economic indicator data have been conducted, yet the matching analyses don't generate balanced covariates between pilot and selected control cities. Also, the parallel pre-trend does not hold with the matched outcome. Therefore, I choose to utilize institutional knowledge to carefully build the control group. Due to the diversity in geology, economy, climate and resource endowments across provinces of China, it is not appropriate to treat all the non-pilot areas as the control group. I choose cities from three provinces[26] around and between Guangdong and Hubei as a control groups. Figure 2.6 shows the location of the control cities.

Due to the flexibility of ETS regulation designs across ETS pilot areas, I expect heterogeneous treatment effects across locations. I also expect the treatment effect vary over time as (1) sector coverage changes over time and (2) carbon-efficient technology are likely to evolve over time. The empirical analysis begins with a static two-way fixed effect (TWFE) model, assuming time-invariant treatment effects, for each pilot province. Next, I adopt the dynamic TWFE method to allow heterogeneous treatment effects across time and locations. Results from both methods are compared to see if the treatment effect estimates are robust across different specifications.

[26] Adjacent provinces of Guangdong and Hubei include Shaanxi, Henan, Anhui, Hunan, Guangxi, Jiangxi and Fujian. Shaanxi, Henan and Anhui provinces are excluded as they are in the north of China and have different heating policy. Almond et al. [1] discussed the impact of China's Huai River policy on local air pollution. Guangxi is excluded as it is an autonomous region whose economy relies heavily on agriculture and tourism.

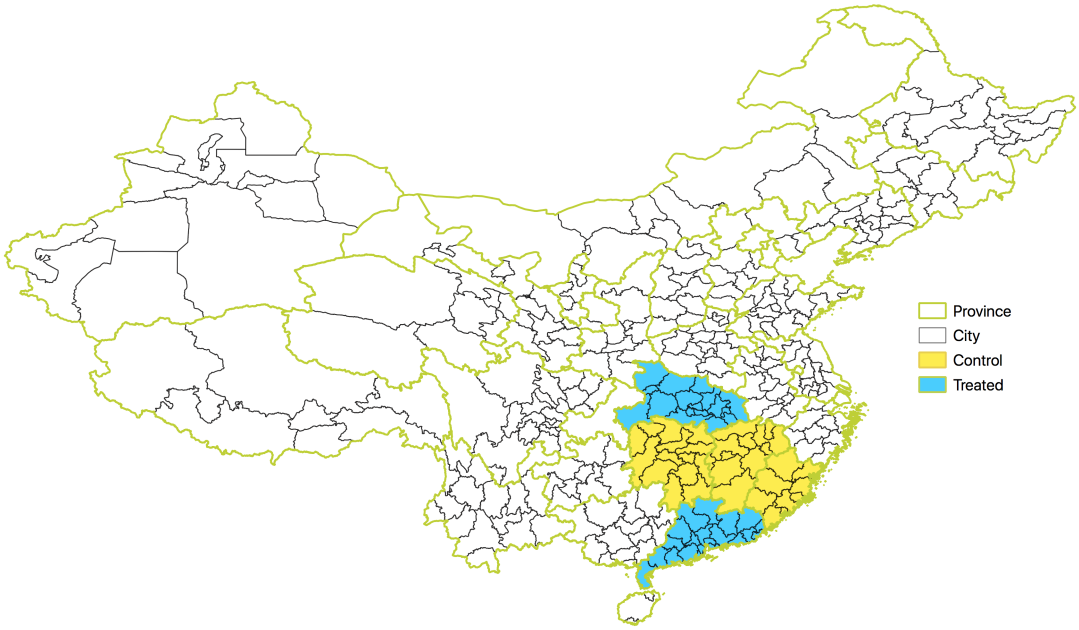

Figure 2.6: Treated and Control Cities

2.4.1 Static Two-Way Fixed Effects Model

In a static TWFE model, shown as equation 2.4, the Average Treatment effect on the Treated group (ATT) is assumed to be constant across pilots and time.

$$PM2.5_{it} = \alpha_{\mathbb{i}} + \lambda_{\mathbb{t}} + \delta ETS_{it} + \boldsymbol{X'\gamma} + \epsilon_{it} \tag{2.4}$$

$PM2.5_{it}$ is the annual average of $PM2.5$ level of city i in year t. ETS_{it}, is a binary indicator of ETS operation and equals 1 if city i has ETS in operation in year t; otherwise, 0. $\boldsymbol{X}$ denotes a matrix of control variables, and $\boldsymbol{\gamma}$ is the associated coefficient estimate vector. δ is a weighted average of $ATTs$ of all possible two-period two-group canonical DD from the dataset. The static TWFE model assigns negative weights to individual canonical DD estimates, and therefore leads

to a misleading[27] estimate of δ that does not necessarily summarize a meaningful ATT of interest [36, 46, 76]. Unobservables are allowed to be correlated within a province, and therefore I cluster the standard errors at the province level.

2.4.2 Dynamic Two-Way Fixed Effects Model (Event Study)

The dynamic Two-Way Fixed Effects (TWFE) model, sometimes referred as the event-study model, is adopted to allow the ATT to vary across pilots and time. A dynamic TWFE model where some units remain untreated through all time periods is specified as equation 2.5:

$$PM2.5_{it} = \alpha_i + \lambda_t + \left(\sum_{e=-L+1}^{-2} \delta_e \cdot \mathbb{1}\{t - G_i = e\} + \sum_{e=0}^{K} \delta_e \cdot \mathbb{1}\{t - G_i = e\} \right) \cdot Pilot_i + \boldsymbol{X'\gamma} + \epsilon_{it} \tag{2.5}$$

where G_i denotes the year city i enters ETS, $\mathbb{1}\{t - G_i = e\}$ is the binary indicator of whether calendar year t is e years away from the G_i, and $Pilot_i$ is the binary indicator for whether a city falls in the ETS pilot area. L and K are positive integers, and denotes the largest lags and leads from the dataset. In this study, I trim the data to make sure the panel data is balanced in L and K. To avoid collinearity, two lags need to be dropped, and in the equation 2.5 the lag $e = -1$ and $e = -L$ are dropped. It is a common practice to use insignificant $\delta_{e<-1}$ to support the parallel trend assumption [40]. However, it's been recognized that pre-trend tests are often underpowered, and are not sufficient to eliminate concerns related to pre-trends [32, 65, 66]. By only including observations in one pilot province and selected controlled cities, the province-specific time-variant treatment effect is obtained. If including all treated and selected control observations, then the average time-variant treatment effect is generated.

[27] For example, consider a setting with two treated groups that receive the treatments in different time periods and one control group that never receives the treatment. If individual DD estimates for both treated groups are positive, however, the weight assigned by the static TWFE to the later treated group is negative, then the resulting static TWFE estimate, a weighted average of the DD estimates, could be negative. In this case, the static TWFE estimate is misleading.

2.5 Data

Relevant data are obtained from various resources. Monitored air quality data of mainland China is publicly available after 2014[28] which does not cover the pre-ETS period. In addition, [34] has demonstrated that China's official daily air pollution data does not behave well, which suggests there is potential data manipulation. In this research I use the dataset by van Donkelaar et al. [84], which provides China's air quality data back to 2000 using interannual changes between ground-measured and satellite derived data. Though this dataset has a resolution of 0.1° by 0.1° ($\sim$ 10 km by 10 km). van Donkelaar et al. [84] suggest that this dataset is intended to aid in large-scale studies due to influences from the coarser resolution of information sources. In this research, I calculate the city annual mean PM 2.5 based on the annual grid-level PM 2.5 data. Figure 2.7 shows that annual PM 2.5 levels across China in 2006, 2011, 2016 and 2018. Lighter shaded areas are associated with lower PM 2.5 levels. On average, southeastern China are associated with lighter colors in 2018 compared with 2016, and in 2016 compared with 2011. This indicates a decreasing trend of PM 2.5 in China. The National Statistic Bureau of China provides city-level annual GDP and population.

The MERRA2 system provides annual weather data, including relative humidity indicator, temperature and wind with a spatial resolution[29] of 0.5° by 0.625° ($\sim$ 55 km by 60 km). City-level annual average values of weather variables are calculated based on the annual grid-level raster data.

As to other related air quality policy, China adopted a new National Ambient Air Quality Standard (NAAQS) which set stringent standards for various air pollutants, including PM 2.5. The NAAQS was implemented in different phases. The first phase of implementation was finished by December of 2012 in 66 cities including provincial capitals, municipalities, cities in Jing-Jin-Ji (JJJ), Yangzi River Delta (YRD) and Pearl River Delta (PRD) economic area. The second phase of

[28]Data can be found at http://beijingair.sinaapp.com/ over mainland China. These data are captured by individuals from instantaneous data records on the website of the Chinese EPA.

[29]The corresponding area of the spatial unit varies across the location. Distance due to a latitude change $\Delta y = 2\pi R_e \frac{\Delta latitude}{360^\circ}$, and distance due to a longitude change $\Delta x = 2\pi R_e cos(latitude) \frac{\Delta longitude}{360^\circ}$, where R_e is the radius of the earth. In the very south of China, a spatial unit of 0.5° by 0.625° approximately covers $55km$ by $66km$, and in the very north of China, the coverage is around $55km$ by $42km$.

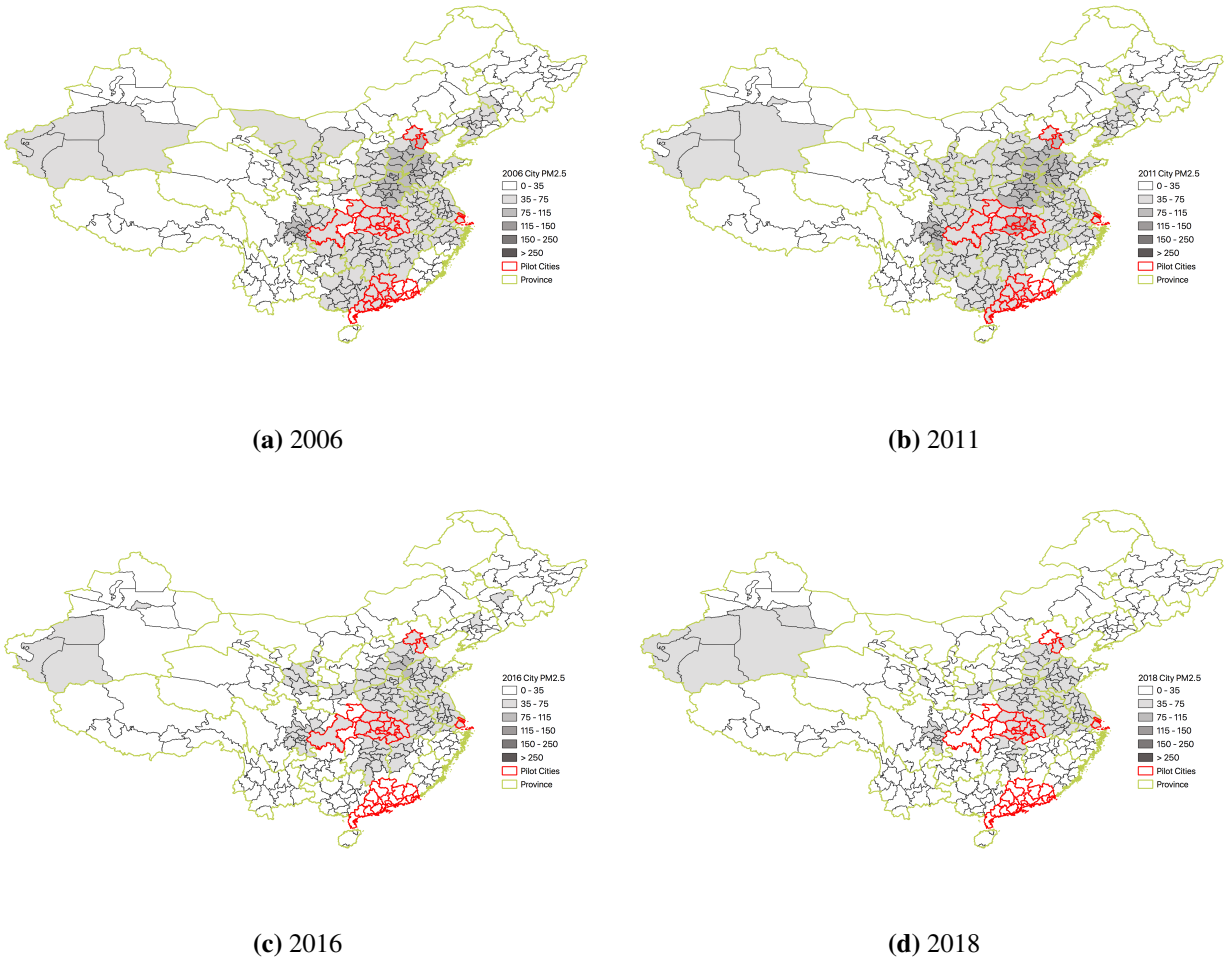

(a) 2006 **(b)** 2011

(c) 2016 **(d)** 2018

Figure 2.7: City-Level Annul PM 2.5 in 2006, 2011, 2016 and 2018

implementation was completed by December of 2013 in an additional 116 cities. The third phase added another 177 cities before 2015. After 2015, all prefecture cities were required to comply with the NAAQS.

China releases Five-Year Plans every five years to provide fundamental guidelines for social and economic development, and the Eleventh (2006-2010) for the first time explicitly list greenhouse gas control in the plan. Therefore, the study period is 2006 and afterwards. Due to data availability, I trim the study period to end in 2018. Table 2.4 summarizes the variables used in the analysis.

Table 2.4: Summary Statistics

Guangdong: 17 cities	N	Mean	St. Dev.	Min	Max
Year	221	2012	3.8	2006	2018
PM2.5	221	33.6	7.4	19.2	52.3
Temperature (C)	221	21.2	1.4	17.5	24.5
Wind (m/s)	221	5.0	0.4	4.1	6.1
Humidity	221	13.1	0.9	11.1	15.2
AAQS	221	0.0	0.0	0	0
Industrial Electricity (BKWh)	210	10.3	14.2	1.1	58.0
Hubei: 15 cities	**N**	**Mean**	**St. Dev.**	**Min**	**Max**
Year	195	2012	3.8	2006	2018
PM2.5	195	53.9	17.4	8.7	85.4
Temperature (C)	195	16.0	1.9	10.3	18.4
Wind (m/s)	195	4.3	0.7	2.8	5.4
Humidity	195	9.1	0.8	7.2	10.7
AAQS	195	0.0	0.0	0	0
Industrial Electricity (BKWh)	156	4.7	5.5	1.1	28.0
Control Area: 33 cities	**N**	**Mean**	**St. Dev.**	**Min**	**Max**
Year	429	2012	3.7	2006	2018
PM2.5	429	40.7	13.1	17.7	74.8
Temperature (C)	429	17.5	1.1	14.5	21.0
Wind (m/s)	429	4.5	0.6	3.1	6.8
Humidity	429	10.8	0.8	8.8	13.6
AAQS	429	0.0	0.0	0	0
Industrial Electricity (BKWh)	415	3.7	4.1	0.05	34.0

2.6 Results and Discussion

This section summarizes results from different model specification and further exploration of presented outcomes. Figures 2.8a and 2.8b compares the estimates from two similar static TWFE models (equation 2.4) where one controls for industrial electricity consumption and the other does not. Both figures show insignificant treatment effects when two provinces' data are combined.

Table 2.5 summarizes the results for the individual static TWFE models (equation 2.4) of Guangdong and Hubei. While ETS operations in Guangdong does not have a significant effect on air quality in Guangdong, having ETS operations is found to reduce PM2.5 levels by 4.31

$\mu g/m^3$, which represents an 8% reduction in Hubei on average. As the pooled static ETS estimate is a weighted average from the individual static TWFE, I observe generally no significant effects in Figure 2.8.

Table 2.5: Results for Individual Static TWFE Methods

	City-Level PM2.5 ($\mu g/m^3$)	
	Guangdong	Hubei
ETS	1.69	-4.31^{**}
	(2.09)	(2.02)
Industrial Electricity (BKWh)	0.13	0.37^{***}
	(0.18)	(0.09)
AAQS	-2.12^{**}	-2.13^{**}
	(0.87)	(0.89)
Temperature (C)	-0.46	-0.43
	(1.15)	(1.98)
Wind (m/s)	-4.02^{*}	-3.95^{*}
	(2.37)	(2.39)
Humidity	-4.16^{***}	0.50
	(0.57)	(1.60)
Constant	125.41^{***}	85.80^{***}
	(15.79)	(15.54)
Observations	625	571
R^2	0.95	0.96
Adjusted R^2	0.95	0.95
Residual Std. Error	2.72	3.38
F Statistic	177.17^{***}	177.64^{***}
Note:	*p<0.1; **p<0.05; ***p<0.01	

As Guangdong and Hubei started ETS operations in different years, dynamic TWFE results are presented next. Figures 2.9 and 2.10 plot the estimates of a dynamic TWFE following Sun and Abraham [76], where time-specific average treatment effect across groups are estimated and two periods indicators are dropped to avoid multicollinearity. The common practice is to drop the closest lead and a far lag. Estimates in Figure 2.9b are from a model in which lead1 and lag4 are dropped, while estimates Figure 2.10b are from a model in which lag0 and lag4 are dropped. Figure

2.9b suggests a possible anticipation effect within two years before the treatment. In general, the ETS treatment doesn't show a significant impact on PM 2.5 levels after the ETS operation, and the estimates are not significantly different across specifications and are therefore robust to the choices of dropping periods.

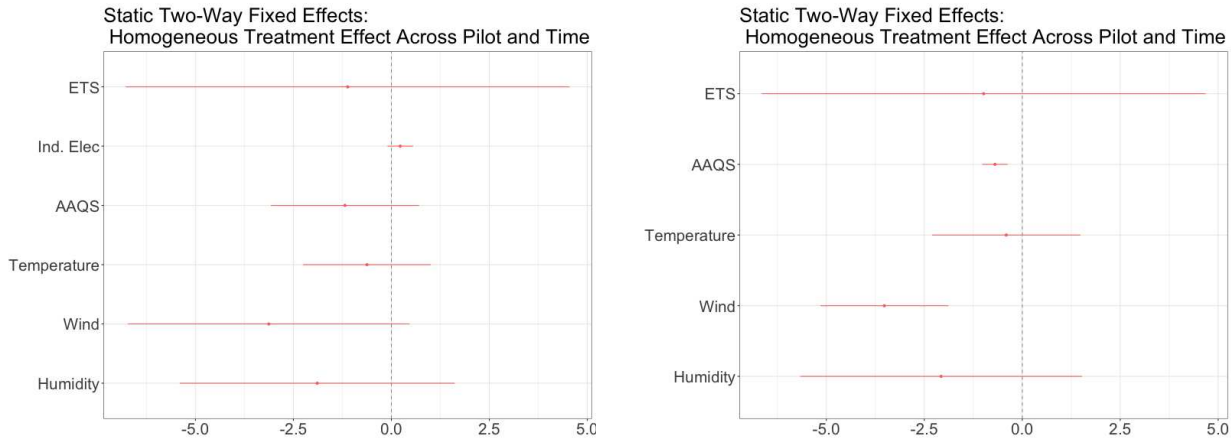

(a) Control for Industrial Electricity

(b) No Control for Industrial Electricity

Figure 2.8: Estimates from Static TWFE Models

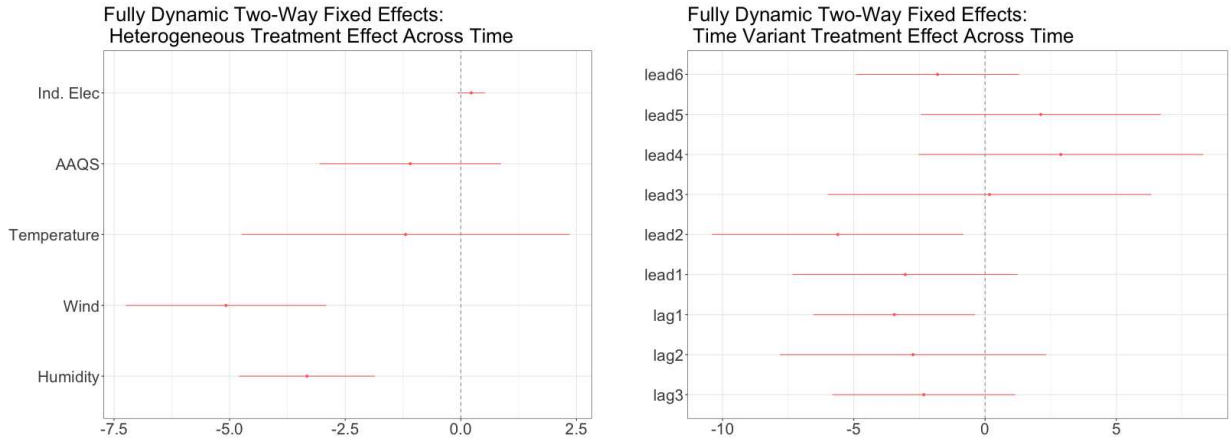

(a) Control Variables

(b) Treatment Effects

Figure 2.9: Estimates from Dynamic TWFE Models: Drop Lead1 and Lag4

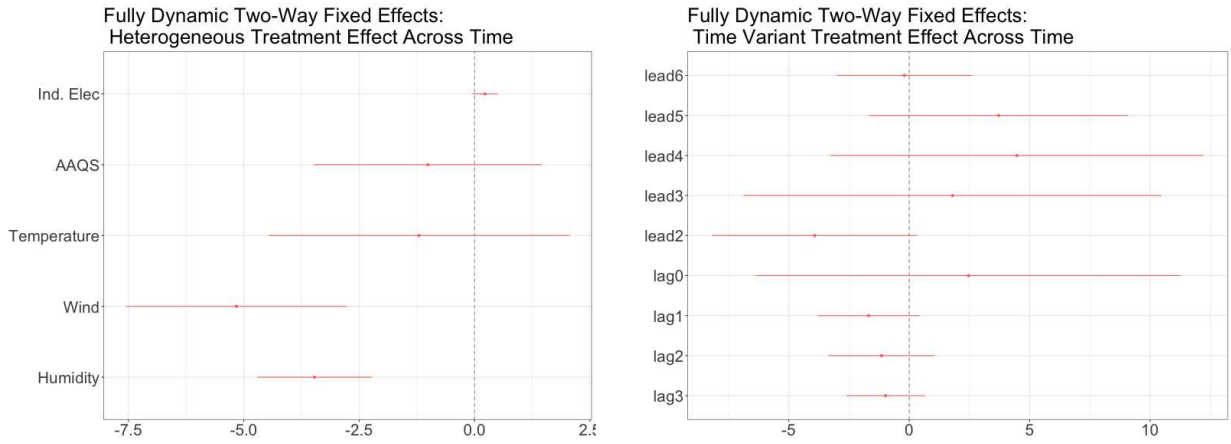

(a) Control Variables **(b)** Treatment Effects

Figure 2.10: Estimates from Dynamic TWFE Models: Drop Lag0 and Lag4

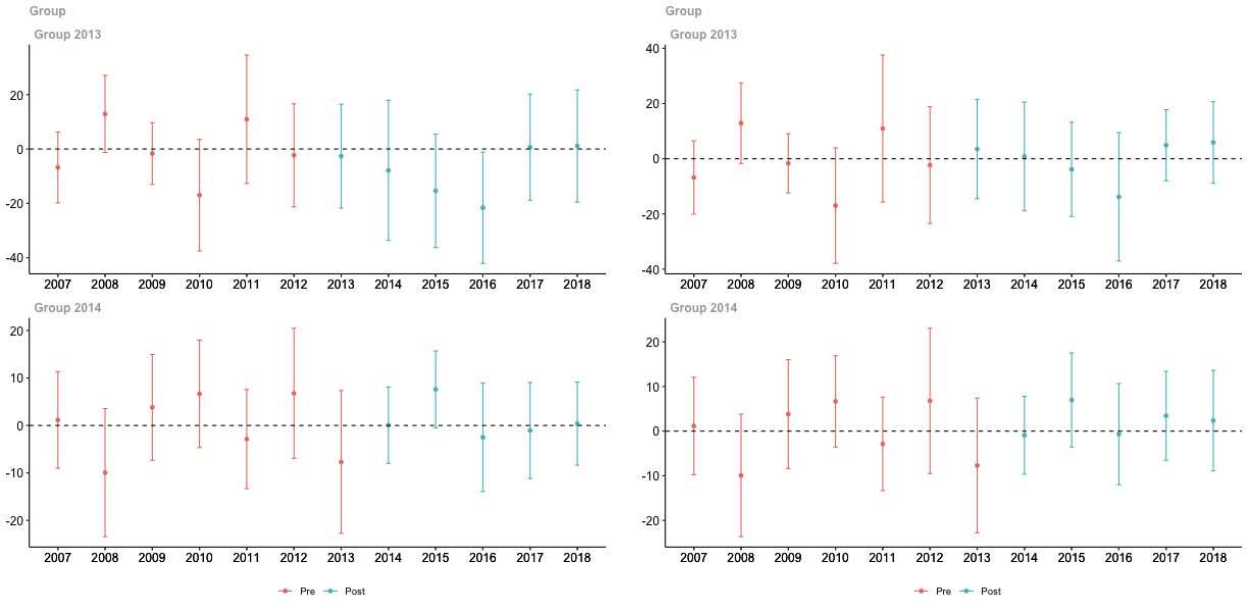

(a) No Anticipation **(b)** Two-year Anticipation

Figure 2.11: Group-Time Specific Treatment Effects: Never Treated Units as Control

Note: Group 2013 denotes Guangdong; Group 2014 denotes Hubei

Figure 2.11 plots the estimates of ETS treatment effect following Callaway and Sant'Anna [12] in which group-time specific treatment effects are estimated. Group 2013 represents Guangdong and Group 2014 represents Hubei. Figure 2.11b plots estimates with a same ETS treatment timing but allow a two-year anticipation, in which case regulated facilities are assumed to be able to take actions two years before ETS operations due to anticipation. While allowing two-year anticipation does affect the treatment effect estimates, the group-time specific estimates are not significantly different from zero.

In general, the estimated ETS treatment effects from a dynamic TWFE specification is not significantly different from 0. The insignificant estimates might be due to (1) limited statistical power with a relative small sample size; (2) a carbon-intensity targeted ETS program with output-based allowance assignment mechanisms (A2 and A3) has limited impact on production levels and the air quality.

2.6.1 Allowance Allocation Mechanism

As discussed in section 3.1, the allocation mechanism based on sector-standards provides the least incentive, on average, for regulated facilities to reduce output. Therefore, it is reasonable to assume that air quality in cities with more facilities that receive emission allowances based on sector-standards mechanism have smaller or even positive responses to the ETS program. The Guangdong and Hubei local governments release annual allowance allocation plans as well as the name of regulated facilities for each sector and cities. I use this information to calculate the number of regulated facilities ($Number$) and percentage of facilities that are associated with the sector-standards mechanism ($Ratio$) in each city and year.

$$PM2.5_{it} = \alpha_{\mathbb{i}} + \lambda_{\mathbb{t}} + \phi ETS_{it} + \lambda Number_{it} + \delta Ratio_{it} + \boldsymbol{X'\gamma} + \epsilon_{it} \tag{2.6}$$

Table 2.6 shows how PM 2.5 responses to different ETS designs. In column (1), the coefficient of ETS covers all different designs across locations and time, and does not show a significant impact on PM 2.5 level. Significantly negative estimate of Number in the column (2) indicates

Table 2.6: PM 2.5 Response to ETS Design

	Dependent variable:			
	PM2.5			
	(1)	(2)	(3)	(4)
ETS	−1.11	0.93	−5.39***	−6.52***
	(0.93)	(1.03)	(1.64)	(1.41)
Ind. Elec	0.23***	0.26***	0.21***	0.21**
	(0.08)	(0.08)	(0.08)	(0.08)
Number		−0.14***	−0.03	
		(0.04)	(0.04)	
Ratio			7.64***	9.74***
			(1.49)	(1.24)
Power				−0.41**
				(0.18)
Steel				−0.07
				(0.11)
Petro				0.27
				(0.47)
Cement				0.03
				(0.09)
Paper				0.44***
				(0.09)
Temperature	−0.62	−0.70	−1.22**	−1.38**
	(0.55)	(0.54)	(0.54)	(0.56)
Wind	−3.13**	−2.57*	−2.99**	−3.03**
	(1.54)	(1.53)	(1.47)	(1.43)
Humidity	−1.89**	−1.63*	−2.04**	−1.66**
	(0.79)	(0.85)	(0.85)	(0.78)
AAQS	−1.18	−1.10	−1.86**	−2.09***
	(0.85)	(0.84)	(0.79)	(0.79)
Constant	109.52***	105.52***	121.52***	120.96***
	(11.32)	(11.96)	(10.65)	(10.00)
Observations	781	781	780	780
R^2	0.95	0.95	0.95	0.96
Adjusted R^2	0.95	0.95	0.95	0.95
Residual Std. Error	3.37	3.32	3.24	3.22
F Statistic	173.26***	176.45***	183.52***	177.62***
Note:				*p<0.1; **p<0.05; ***p<0.01

that when more facilities are regulated under ETS, better air quality is achieved. The estimate of ETS remains insignificant as the allowance allocations are not distinguished. Ratio is included in column (3), and as expected, a positive coefficient on Ratio and a negative estimate on ETS are observed, which indicates that ETS implementation in general reduces the PM 2.5 level, but adoptions of A3 allowance allocation mechanism would offset this reduction. The results in column (4) include the numbers of regulated facilities from 5 common regulated sectors in Hubei and Guangdong. The significantly negative estimate of the coefficient for the Power variable indicates that the regulation on the Power sector tends to reduce the PM 2.5 level. The positive estimate on the Paper sector might due to the late Paper sector coverage in Guangdong. The Paper sector in Guangdong started to be regulated by ETS from 2017 which leads to higher Paper value after 2017. Therefore, the positive estimate of Paper could pick up the PM 2.5 difference before and after 2017. Generally, the larger the number of enrolled facilities, the more PM 2.5 reduction can be achieved. Positive estimates of the Ratio variable implies that adopting A3 in an ETS program can increase city-level PM 2.5. After different ETS designs are controlled, ETS operations are found to reduce city-level PM 2.5 by 6.52 $\mu g/m^3$ on average.

In Section 2.3.1, I hypothesize the sector-standard ETS design encourages industrial output, I further regress the industrial electricity consumption on the ETS and control variables to empirically investigate production responses to different ETS designs. Table 2.7 summarizes the outcomes. Column (1) shows an insignificant impact from the ETS on industrial electricity consumption, which aligns with previous treatment effect estimates when different designs of ETS are not considered. The positive coefficient on Ratio indicates that the sector-standard ETS design motivates regulated facilities to expand their production on average. When number and sector-standard regulated percentage of enrolled facilities are controlled, ETS implementations reduce industrial production.

Table 2.7: Industrial Electricity Consumption Response to ETS Design

	Dependent variable:			
	Industrial Electricity Consumption			
	(1)	(2)	(3)	(4)
ETS	0.57	−0.45	−3.25***	−3.45***
	(0.73)	(0.73)	(0.98)	(0.77)
Number		0.07***	0.11***	
		(0.03)	(0.03)	
Ratio			3.34**	2.42**
			(1.33)	(1.08)
Power				0.64***
				(0.13)
Steel				0.02
				(0.17)
Petro				0.67
				(0.69)
Cement				0.02
				(0.14)
Paper				0.25**
				(0.12)
Temperature	0.94**	0.97**	0.72**	0.69**
	(0.39)	(0.38)	(0.35)	(0.34)
Wind	−1.72	−1.97**	−2.10**	−1.74*
	(1.05)	(0.99)	(1.00)	(1.01)
Humidity	−0.79	−0.91	−1.03	−0.83
	(0.64)	(0.64)	(0.64)	(0.61)
AAQS	2.14***	2.06***	1.70***	1.30**
	(0.68)	(0.68)	(0.65)	(0.61)
Constant	1.09	3.06	9.43	6.65
	(7.91)	(7.74)	(6.90)	(6.22)
Observations	781	781	780	780
R^2	0.94	0.94	0.94	0.95
Adjusted R^2	0.93	0.94	0.94	0.94
Residual Std. Error	2.26	2.24	2.22	2.11
F Statistic	144.59***	145.17***	146.20***	154.58***
Note:				*p<0.1; **p<0.05; ***p<0.01

2.6.2 ETS and Public Health

Literature has shown how PM 2.5 impacts mortality around the world [24, 9, 42, 68]. Therefore, when ETS reduces PM 2.5, the co-benefit of ETS is not only to improve air quality, but also to improve public health. According to Shang et al. [73], every 10 $\mu g/m^3$ increase in PM 2.5 introduces an increase of 0.38% in total mortality in China, while Li et al. [50] suggest a hazard ratio of 1.08 which indicates an increase of 8% in total mortality per 10 $\mu g/m^3$ increase in PM 2.5. Hammitt et al. [39] report the Value of Statistical Life (VSL) in China from 22,000 USD in 2005 to 550,000 USD in 2016. Taking the estimates for Hubei in Table 2.5, where ETS implementation reduces city-level PM 2.5 by 4.31 $\mu g/m^3$, and combining estimates from Shang et al. [73] and Li et al. [50], then the mortality reduction ranges from 0.164% to 3.448% in Hubei.

Based on reported annual death rates from 2006 to 2018, the average annual death rate in Hubei is 0.0634%. After ETS operations, the average death rate falls between 0.0612% to 0.0633% in Hubei. The reported average annual population in Hubei is 57.89 million. Hence, the implementation of the ETS is estimated to reduce premature mortality by 57 to 1,273 lives in Hubei, which generates annual social welfare increases ranging from 3.135×10^7 to 7.002×10^8 USD per year.

2.7 Conclusions

This research is designed to assess the treatment effect of China's ETS pilot on local air quality. The designs as well as various allowance allocation mechanisms adopted by ETS pilots in Hubei and Guangdong provinces are described. Due to the flexibility of the ETS designs across pilot areas, heterogeneous treatment effects are expected. I compare estimates from static and dynamic two-way fixed effects models, and provide evidence for heterogeneous effects. I further investigate how the ETS designs contributes to the heterogeneous effects.

The empirical analysis shows that the ETS pilot program on average does not have a significant impact on local air quality, which is mainly due to the ETS design. The current ETS is carbon-intensity targeted rather than targeted on total carbon emissions. Carbon intensity programs do not necessarily provide sufficient incentives for output reductions. Especially with a sector-standards

mechanism (A3), the ETS can grant total emission allowances more than the total emission from a sector and provide incentives for more efficient facilities to expand their output. China's ETS can help to reduce carbon intensity, but it is not necessarily as beneficial in terms of improving local air quality. As reductions in PM 2.5 can improve public health, future ETS designs might consider constraining the adoption of A3 in the emission allowance allocation process.

China announced a nation-wide ETS for the electricity sector in 2017 and started the operations to July 16th 2021 due to the pandemic. The nation-wide ETS grants emission allowances using a sector standard mechanism[30] (A3) which implies that the nation-wide ETS is also carbon intensity targeted. Though the nation-wide ETS and ETS pilot programs are both carbon intensity targeted, estimates from this research have limited external validity in predicting the performance of the national ETS for several reasons: (1) during the ETS pilot period, the ETS design within each pilot changed over time, which made it hard for the regulated facilities to make long-term decisions; (2) the analysis includes only Hubei and Guangdong as the treated group, though these two provinces have a good representation of the southeastern China, they are quite different from the northwestern provinces in China; (3) the nation-wide ETS is targeted at the electricity sector while the ETS pilots cover many other sectors.

With the nation-wide ETS in the electricity sector, future studies can take advantage of relative more available electricity output data to empirically test whether China's ETS results in output reductions. In addition, future studies might want to include other environmental policies related to carbon emission control to see how the ETS in combination with other policies jointly affect local air quality. When better city-level economic indicator data is available, more detailed matching methods could potentially improve the precision of the estimates.

[30]https://www.mee.gov.cn/xxgk2018/xxgk/xxgk03/202012/t20201230_815546.html

Chapter 3

The Market Value of Water in the High Plains Aquifer: An Update

3.1 Introduction

The High Plains Aquifer (HPA), the largest groundwater resource of the United States, supports about 27% of the US irrigated lands [56]. Groundwater irrigated acreage in the High Plains increased from 2.1 million acres in 1950 to 13.9 million acres in 1997 and reached 15.5 million acres in 2005 [57]. Intensive irrigation demand raises overexploitation concerns for the HPA. McGuire [58] summarizes the water-level and recoverable water in storage changes from predevelopment to 2015. The HPA on average has experienced a 15.8 foot decrease in water-levels from 1950 to 2015. Scanlon et al. [69] point it out that depletion of the HPA is highly localized and the current depletion and recharge rates would result in groundwater shortage for 35% of the southern High Plains within the next two decades. Besides threatening future crop productions, low groundwater stock also has negative impacts on aquatic ecosystems [64]. In addition, under climate change, the High Plains are expected to face more competing water demands among residential, industrial and agricultural uses. Therefore, it is critical to maintain sustainable use of the HPA.

To develop efficient policy that achieves groundwater resource sustainability while maintaining sufficient food and energy production, reliable estimates of groundwater resource value is necessary. Higher groundwater resource values underpin groundwater conservation actions and encourage irrigation technology innovations. Due to the lack of competitive market, it is difficult to directly observe groundwater's value. Common approaches used to estimate the value of natural resources include optimization based approaches, stated-preference methods and hedonic analyses. An optimization based approach identifies the marginal value of the natural resource

through a profit-maximizing or cost-minimizing model given varying levels of resource availability [54]. When survey data is available, the stated-preference method can be adopted to evaluate total economic value of groundwater stock increase, including non-market values of the resource [77].

This paper aims to estimate the marginal values of HPA groundwater resources with a hedonic analysis. Specifically, we analyze repeated transactions of groundwater irrigated land in Colorado and Nebraska to estimate the responses in real land values to the changes in groundwater saturated thickness levels. The contribution of this paper is threefold: (1) to utilize the ZTRAX data products from Zillow to obtain transactions involving agricultural land across multiple states over a long time period; (2) to provide more accurate hedonic estimates by estimating econometric models that include parcel level fixed effects with repeated transactions; (3) while most previous studies focus on a single state, our paper takes the advantage of rich temporal and spatial variations in groundwater availability to update the value of water for Colorado and Nebraska since [79]. Results suggest positive marginal effects of groundwater availability on irrigated land value when groundwater stocks are sufficiently low. In general, additional units of groundwater are more valuable in Colorado than in Nebraska. The marginal effect of groundwater resources are also found to be responsive to drought pattern. Taken as a whole, the results also imply losses in economic value associated with current depletion behaviors.

3.2 Literature Review

Though hedonic methods were initially used to reveal consumer's marginal willingness to pay (MWTP) for residential property amenities, it has also been widely used to address the value of various environmental attributes of agricultural land, including scenic views [5], wildlife recreation [43], erosion control and drainage use [62]. Due to data availability, earlier studies tend to adopt pooled cross-sectional data and control for as many covariates as possible to reduce omitted-variable bias. Torell et al. [79] collect farm sales data from Farm Credit Services and control for different farm attributes for irrigated land and dryland. They estimate the value of groundwater

stock existence by comparing price differentials between irrigated and dryland farm sales, and estimate the marginal value ($/acre-foot) of additional saturated thickness by dividing the price differentials ($/acre) by the state average saturated thickness (feet). They find that irrigated land on average has higher land value, and impacts of saturated thickness on land value vary from $1.09/foot in Oklahoma in 1986 to $9.5/foot in New Mexico in 1986.

When omitted-variable bias is of big concern, simple functional forms such as linear and log-log are shown to outperform more flexible nonlinear models Cropper et al. [21]. With increasing data availability, it has become a standard practice to add spatial fixed effects and to utilize quasi-experiments to account for unobservable time-invariant heterogeneity. Kuminoff et al. [49] demonstrate, using Monte Carlo methods, that flexible functional forms, such as the quadratic Box-Cox model, with spatial fixed effects provide more accurate estimates than traditional linear models that previously dominate hedonic studies.

To obtain robust estimates through a hedonic model, the Law of One Price needs to hold, which means that identical properties are sold for the same price through the market. The definition of market consists of two dimensions: time and location. It's common for hedonic analyses to define a market as a single metropolitan area over a few years. As data availability expands, the spatial and temporal extent of the analysis can also increase, which challenges the assumption of one market in hedonic analyses. In this case, allowing for an evolving hedonic price is necessary. Adding interactions between time and spatial dummies with the price function parameters can help to mitigate this challenge [6]. Von Graevenitz [86] also addresses this issue by adopting a piecewise linear function, which allows marginal effects of road noise exposure on property value vary across noise ranges.

Theoretically, including fine scale spatial fixed effects in hedonic analyses can help to control for the unobservables and mitigate omitted variables bias. With increasing data availability, it is possible to include finer scale spatial fixed effects. However, only a few empirical studies have utilized repeated parcel sales data to estimate the value of water resources. Buck et al. [10] collect land transactions in eight California counties between 2001 and 2008 to recover the marginal

value of surface water. After filtering out high turnover parcels, non-crop parcels, parcels with bedrooms, a sample with 292 observations for 140 parcels are used for the hedonic analysis. Their results present an average capitalization value of $3723 for an additional acre-foot of surface water. However, due to the limited sample size, their results have limited relevance outside of the study area. Sampson et al. [67] applied hedonic models to repeated sales datasets and estimate the value of groundwater in Kansas. The authors allow for different value functions for irrigated and non-irrigated parcels. They collect arms-length transactions for parcels grater than 40 acres in Kansas from 1988 to 2015. The long time period provides them 2,269 parcels with repeated sales. They find that irrigated land on average has 53% higher land value than non-irrigated land, and that groundwater is capitalized in the land value with average marginal values ranging from 3.41$/acre to 15.86 $/acre with an additional foot increase in saturated thickness. Buck et al. [10] focuses on surface water, and Sampson et al. [67] address the value difference between irrigated and non-irrigated land. We focus on irrigated land value only and explore the heterogeneous impact of groundwater availability on land values across various groundwater endowments. Including parcel-level fixed effects helps to avoid bias from omitting parcel attributes that are correlated with the groundwater availability at a cost of losing some statistical power due to a smaller dataset. We compare results from various specifications to explore how groundwater availability impacts the value of irrigated land.

3.3 Method

Lack of competitive markets makes it difficult to observe the value of groundwater resources, and assessing agricultural land value's marginal response to groundwater availability is a common alternative to evaluate the shadow value of groundwater. To measure the marginal value of groundwater resources, we focus on groundwater irrigated parcel transactions only. The land value of a particular parcel represents the current value of expected rent flows:

$$P_{irr} = \int_{t=0}^{\infty} e^{-rt}(R_{irr}(t, X) + v(t))dt$$

where P_{irr} denotes the observed irrigated land price per acre with a discount rate r. $R_{irr}(t)$ is the rental rate for groundwater irrigated land, and $v(t)$ captures value due to other influences, such as price shocks and urbanization. $R_{irr}(t)$ is a function of aquifer characteristics X such as saturated thickness, hydraulic conductivity and specific yield, as well as soil attributes and climate characteristics. We begin by estimating a simple linear model without parcel-level fixed effects, as equation 3.1.

$$P_{it} = \alpha ST_{it} + \beta ST_{it}^2 + \gamma ST_{it}^3 + \tau Z_i + \delta_j + \lambda_t + \epsilon_{it} \tag{3.1}$$

where P_{it} denotes the real price [31] of per acre of parcel i at time t. ST_{it} denotes the saturated thickness, and we allow the marginal effect of ST on land value to vary by including the quadratic and cubic form of ST. Z_i denotes other observable attributes of a parcel, such as distance from bedrock to land surface, soil type[32], specific yield and conductivity and climate attributes. The climate attributes consist of 30-year normals of annual precipitation, mean temperature, max temperature and min temperature. δ_j is a spatial fixed effect that controls for unobserved time invariant attributes at a spatial scale larger than the parcel, for example, a county or a state. λ_t denotes the year fixed effect.

We also estimate a model with parcel-level fixed effects as in equation 3.2 :

$$P_{it} = \alpha ST_{it} + \beta ST_{it}^2 + \gamma ST_{it}^3 + \delta_i + \lambda_t + \epsilon_{it} \tag{3.2}$$

where δ_i denotes the parcel-level fixed effect, and the rest of the notation is defined the same as in equation 3.1 .

As hedonic analyses can be sensitive to functional forms, we also adopt a piece-wise linear function to allow for the estimation of more flexible, heterogeneous marginal effects of ST as equation 3.3:

$$P_{it} = \alpha ST_{it} + \eta(ST_{it} - M)B_{it} + \delta_i + \lambda_t + \epsilon_{it} \tag{3.3}$$

[31] The real price is in 2015 US dollars

[32] Table **??** describes soil types included in the analysis

where $B_{it} = 1$ if ST_{it} is larger than the threshold M meters, otherwise, $B_{it} = 0$. The choices of M are based on the mean ST in Colorado and Nebraska.

We expect to estimate α, β and γ that yield a positive first derivative and negative second derivative of land value with respect to ST, due to the diminishing returns of groundwater to agricultural production. Similarly, we also expect negative η for a positive but decreasing marginal effect of ST in areas where groundwater resources are constrained. The empirical analysis is conducted with combined data including both Colorado and Nebraska.

Since we hope to take advantage of wide coverage of time and space in the ZTRAX data, we might violate the Law of One Price which is the fundamental assumption for hedonic analysis. To obtain valid estimates from hedonic analysis, properties with the same attributes should sell for the same price, and therefore a well-defined market is required to maintain a unique hedonic price function. When the analysis involves large variation in time and space, allowing an evolving hedonic price function is appropriate. Therefore, we propose the specification as equation 3.4:

$$P_{it} = \alpha ST_{it} + \beta ST_{it}^2 + \gamma ST_{it}^3 + \alpha_D ST_{it} D_t + \beta_D ST_{it}^2 D_t + \gamma_D ST_{it}^3 D_t + \delta_i + \lambda_t + \epsilon_{it} \qquad (3.4)$$

where $D_t = \mathbb{1}(t > D)$. The choice of drought inflection point D is driven by the historical drought data in Colorado and Nebraska. Our assumption is that severe and continuous droughts would shift the demand of groundwater and eventually shift the implicit function of groundwater. As shown in Figures 3.1 and 3.2, both Colorado and Nebraska started to experience severe and frequent droughts since 2000, we estimate equation 3.4 with D ranging from 2000 to 2005 to check the robustness. We expect higher marginal effects of groundwater on real land value after D.

3.4 Data

To conduct a hedonic analysis evaluating how land value responds to groundwater stock, land transactions and groundwater availability data are required. The ZTRAX dataset from Zillow provides property transaction information. The ZTRAX data product consists of separate assessment

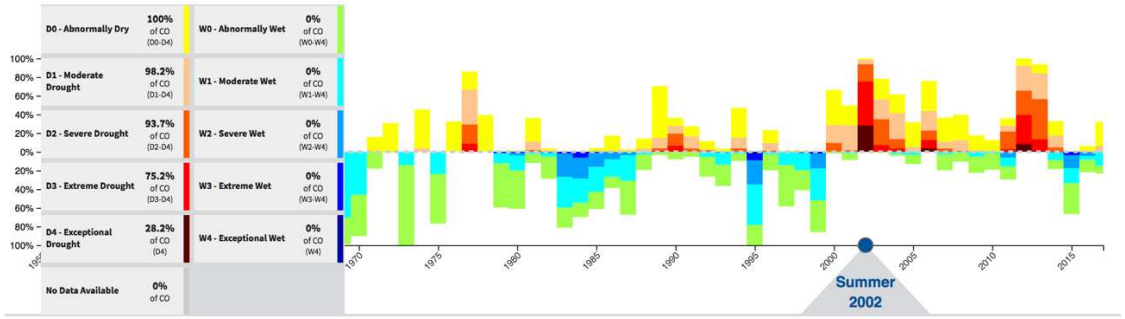

Note: Figure from NOAA NIDIS: Drought.gov

Figure 3.1: Drought Index in Colorado from 1970 to 2017

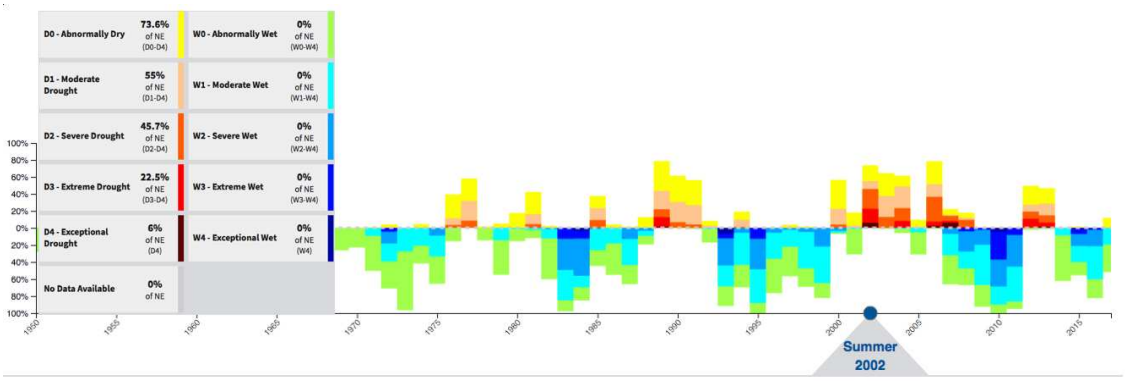

Note: Figure from NOAA NIDIS: Drought.gov

Figure 3.2: Drought Index in Nebraska from 1970 to 2017

(ASMT) data and transaction (TRANS) data. ASMT provides comprehensive parcel attributes. The following attributes are useful for our study: property full address, geographic coordinates, building area, transaction date, lot size, sale price, land use and property use. Data processing details can be found in the Appendix.

For the empirical analysis, ASMT and TRANS data are combined to generate a comprehensive land transaction data set. When a parcel exists in both ASMT and TRANS, the sale price amount and the parcel coordinates are obtained from TRANS, while attributes related to the building area and number of rooms are from ASMT. Land use from ASMT and TRANS are used to identify agricultural parcels. To expand the sample size, parcels with lot size greater than or equal to 30 acres and without specified land use are also included as agricultural parcels.

We use documentation type and intra-family transfer flag to rule out non arms-length transactions[33], and exclude transactions with nominal sale price amount lower than $100. As our study area is the Ogallala aquifer, we also drop parcels outside of the aquifer boundary. We further trim our data based on irrigation practice. Colorado's Decision Support Systems (CDSS) provide irrigated land GIS data for multiple years, and the Nebraska Department of Natural Resources (NDNR) provides Pivot Irrigation GIS data for 2005. We take advantage of these GIS data sources to identify groundwater irrigated parcels in Colorado and Nebraska. Due to these GIS data only being available in specific years, it is acknowledged that we might miss some groundwater irrigated parcels. Some parcel coordinates are derived based on the property address, and the derived coordinates describing the street may not necessary lie within the parcel. Therefore, rather than checking if the parcel coordinates fall into the groundwater irrigated polygons, we create artificial square-shape parcel boundaries based on the ZTRAX parcel coordinates and lot size. When a parcel's artificial boundary intersects with any CDSS/NDNR groundwater irrigated land parcel, the ZTRAX parcel is considered as a groundwater irrigated parcel. Figure 3.3 presents the study area of this essay. Due to the data availability of ZTRAX land transactions data, we limit our analysis to Colorado and Nebraska groundwater irrigated land.

Haacker et al. [38] provides annual saturated thickness (ST) data for the entire Ogallala aquifer from 1970 to 2016. We extract point values of ST as a parcel's ST based on the parcel's coordinates, rather than calculating the average ST for the artificial boundary. The assumption here is that the saturated thickness does not vary much within a parcel. To include more recent property transactions, we use 2016 ST to approximate ST from 2017 to 2019. The assumption here is that the ST does not vary much through a short time period. This approximation could bias the estimates if many repeated transactions happen between 2016 and 2019. Fortunately, less than 1% of the repeated transactions happens after 2016, which reduces concerns about the approximation. Schloss and Buddemeier [71] argue that ST level greater than 30 feet[34] is required for high-volume

[33]Details of data cleaning process can be found in the appendix.

[34]30 feet equal 9.144 meter.

pumping. Therefore, to reduce the risk of violating the Law of One Price, we drop the observations with ST levels smaller than 9 meters.

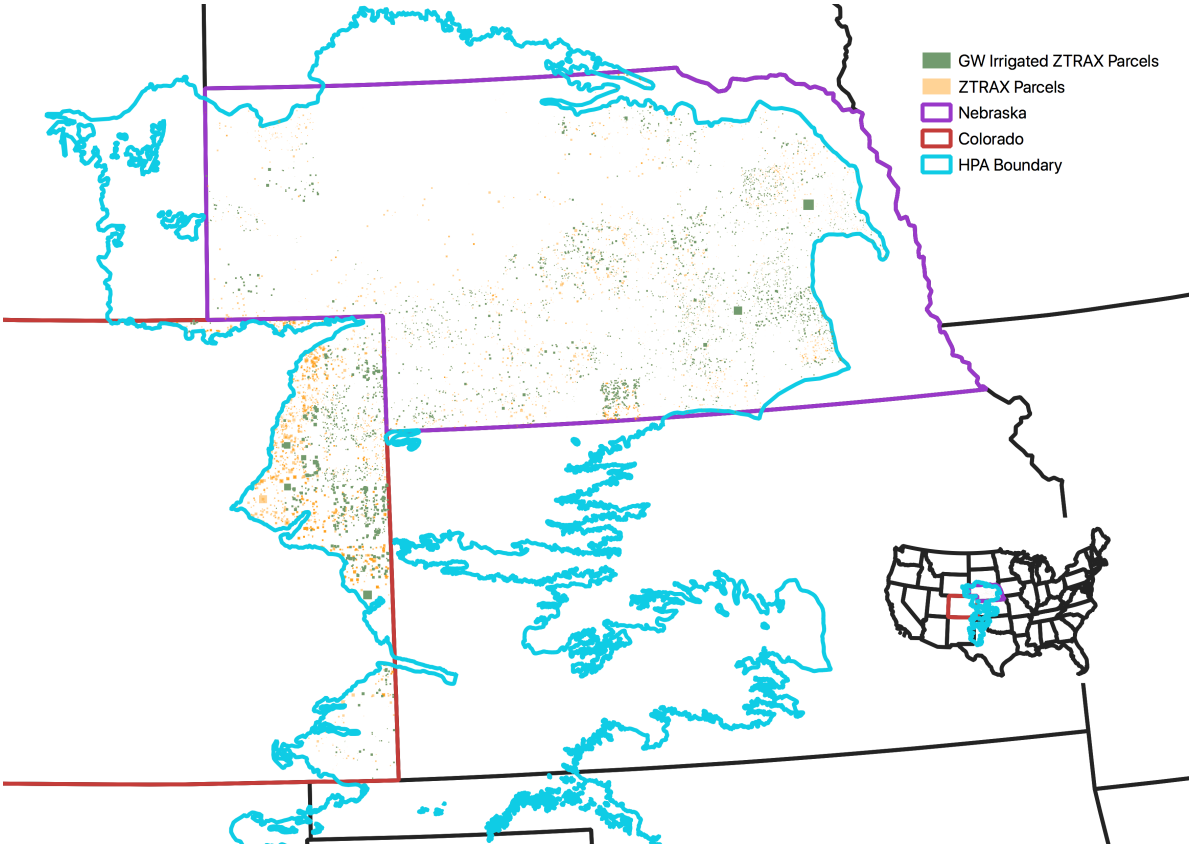

Figure 3.3: Study Area

The final data used in the analyses are further trimmed by excluding observations with real land value ($/acre) lower than the 12.5% percentile value or larger than the 87.5% percentile value in each state. We obtain a raster data of soil type for the study area from Global Soil Regions Map [81], then we extract the soil type information to each ZTRAX parcel of interest. We obtain long-term climate information from the PRISM 30-Year Normals data product [60], including precipitation, mean temperature, max temperature and min temperature. Tables 3.1, 3.2 and 3.3 present the summary statistics of parcel related variables for combined data of two states, as well as individual data for Nebraska and Colorado.

Table 3.1: Summary Statistics for All Transactions: CO & NE

All Transactions	N	Mean	St. Dev.	Min	Max
Year	4,336	2,008.70	6.74	1,976	2,019
Saturated Thickness (ST) (m)	4,336	61.07	45.84	9.00	223.48
ST $>$ 30m	4,336	0.70	0.46	0	1
ST $>$ 70m	4,336	0.31	0.46	0	1
Nominal Land Value ($/acre)	4,336	2,798.63	2,156.09	498.88	9,638.45
Real Land Value ($/acre)	4,336	2,954.33	2,249.88	462.21	18,747.73
Argids	4,331	0.001	0.03	0.00	1.00
Xerolls	4,331	0.01	0.10	0.00	1.00
Ustolls	4,331	0.75	0.43	0.00	1.00
Udolls	4,331	0.10	0.30	0.00	1.00
Orthents	4,331	0.14	0.34	0.00	1.00
Conductivity	4,336	116.34	82.64	25	550
Specific Yield	4,336	26.34	4.99	5.00	42.50
Mean Bedrock to Surface (m)	4,336	101.03	71.15	12.16	1,114.14
Precipitation (mm)	4,336	597.82	116.56	369.31	824.51
Average Temperature (C)	4,336	10.11	0.59	8.45	12.43
Max Temperature (C)	4,336	17.24	0.97	15.26	20.81
Min Temperature (C)	4,336	2.97	0.82	0.62	4.91
Repeated Transactions	**N**	**Mean**	**St. Dev.**	**Min**	**Max**
Year	753	2,009.34	6.20	1,985	2,019
Saturated Thickness (ST) (m)	753	68.13	50.65	9.90	220.59
ST $>$ 30m	753	0.74	0.44	0	1
ST $>$ 70m	753	0.36	0.48	0	1
Nominal Land Value ($/acre)	753	2,851.55	2,138.03	500.00	9,606.99
Real Land Value ($/acre)	753	2,959.68	2,161.88	506.51	11,346.81
Argids	753	0.003	0.05	0	1
Xerolls	753	0.01	0.09	0	1
Ustolls	753	0.77	0.42	0	1
Udolls	753	0.06	0.24	0	1
Orthents	753	0.16	0.37	0	1
Conductivity	753	106.76	75.73	25.00	550.00
Specific Yield	753	26.16	4.68	12	35
Mean Bedrock to Surface (m)	753	104.63	64.02	15.06	681.14
Precipitation (mm)	753	595.67	111.28	412.90	789.24
Average Temperature (C)	753	10.03	0.62	8.77	12.40
Max Temperature (C)	753	17.20	1.05	15.48	20.80
Min Temperature (C)	753	2.87	0.76	1.04	4.73

Table 3.2: Summary Statistics for All Transactions: NE

All Transactions	N	Mean	St. Dev.	Min	Max
Year	3,059	2,008.83	6.51	1,976	2,019
Saturated Thickness (ST) (m)	3,059	73.66	48.25	9.00	223.48
ST $>$ 30m	3,059	0.84	0.36	0	1
ST $>$ 70m	3,059	0.41	0.49	0	1
Nominal Land Value ($/acre)	3,059	3,021.17	2,168.20	498.88	9,638.45
Real Land Value ($/acre)	3,059	3,174.02	2,235.34	462.21	18,747.73
Argids	3,057	0.00	0.00	0.00	0.00
Xerolls	3,057	0.01	0.12	0.00	1.00
Ustolls	3,057	0.73	0.44	0.00	1.00
Udolls	3,057	0.14	0.35	0.00	1.00
Orthents	3,057	0.11	0.32	0.00	1.00
Conductivity	3,059	108.85	91.74	25	550
Specific Yield	3,059	25.95	5.28	5.00	42.50
Mean Bedrock to Surface (m)	3,059	108.52	82.55	12.16	1,114.14
Precipitation (mm)	3,059	660.00	77.58	369.31	824.51
Average Temperature (C)	3,059	10.01	0.64	8.45	11.30
Max Temperature (C)	3,059	16.82	0.80	15.26	19.17
Min Temperature (C)	3,059	3.21	0.84	0.62	4.91
Repeated Transactions	**N**	**Mean**	**St. Dev.**	**Min**	**Max**
Year	561	2,010.03	5.83	1,987	2,018
Saturated Thickness (ST) (m)	561	80.90	52.12	10.58	220.59
ST $>$ 30m	561	0.87	0.33	0	1
ST $>$ 70m	561	0.47	0.50	0	1
Nominal Land Value ($/acre)	561	3,108.22	2,148.50	500.00	9,606.99
Real Land Value ($/acre)	561	3,186.58	2,153.64	506.51	11,346.81
Argids	561	0.00	0.00	0	0
Xerolls	561	0.01	0.10	0	1
Ustolls	561	0.77	0.42	0	1
Udolls	561	0.09	0.28	0	1
Orthents	561	0.14	0.34	0	1
Conductivity	561	96.39	80.29	25.00	550.00
Specific Yield	561	25.66	4.80	12	35
Mean Bedrock to Surface (m)	561	111.74	71.89	15.06	681.14
Precipitation (mm)	561	646.57	79.57	415.28	789.24
Average Temperature (C)	561	9.91	0.64	8.77	11.03
Max Temperature (C)	561	16.80	0.88	15.48	19.10
Min Temperature (C)	561	3.02	0.80	1.04	4.73

Table 3.3: Summary Statistics for All Transactions: CO

All Transactions	N	Mean	St. Dev.	Min	Max
Year	1,277	2,008.41	7.26	1,982	2,019
Saturated Thickness (ST) (m)	1,277	30.92	16.45	9.01	95.29
ST $>$ 30m	1,277	0.37	0.48	0	1
ST $>$ 70m	1,277	0.05	0.22	0	1
Nominal Land Value ($/acre)	1,277	2,265.54	2,030.70	499.36	9,629.72
Real Land Value ($/acre)	1,277	2,428.07	2,197.57	469.31	12,794.09
Argids	1,274	0.004	0.06	0.00	1.00
Xerolls	1,274	0.00	0.00	0.00	0.00
Ustolls	1,274	0.81	0.40	0.00	1.00
Udolls	1,274	0.00	0.00	0.00	0.00
Orthents	1,274	0.19	0.39	0.00	1.00
Conductivity	1,277	134.27	50.77	62	250
Specific Yield	1,277	27.27	4.06	12.50	35.00
Mean Bedrock to Surface (m)	1,277	83.09	20.18	14.71	124.00
Precipitation (mm)	1,277	448.87	16.23	403.62	487.78
Average Temperature (C)	1,277	10.33	0.35	9.53	12.43
Max Temperature (C)	1,277	18.26	0.44	17.49	20.81
Min Temperature (C)	1,277	2.40	0.35	1.24	4.08
Repeated Transactions	**N**	**Mean**	**St. Dev.**	**Min**	**Max**
Year	192	2,007.33	6.78	1,985	2,019
Saturated Thickness (ST) (m)	192	30.83	16.14	9.90	82.44
ST $>$ 30m	192	0.36	0.48	0	1
ST $>$ 70m	192	0.05	0.21	0	1
Nominal Land Value ($/acre)	192	2,101.61	1,924.74	500.00	9,555.56
Real Land Value ($/acre)	192	2,296.69	2,051.68	601.46	10,037.00
Argids	192	0.01	0.10	0	1
Xerolls	192	0.00	0.00	0	0
Ustolls	192	0.77	0.42	0	1
Udolls	192	0.00	0.00	0	0
Orthents	192	0.22	0.41	0	1
Conductivity	192	137.04	49.41	62	250
Specific Yield	192	27.62	3.97	20	35
Mean Bedrock to Surface (m)	192	83.83	19.95	25.37	117.32
Precipitation (mm)	192	446.95	18.72	412.90	486.19
Average Temperature (C)	192	10.39	0.39	9.72	12.40
Max Temperature (C)	192	18.35	0.54	17.51	20.80
Min Temperature (C)	192	2.43	0.34	2	4

We observe no significant differences between all transactions and repeated transactions for any variable in either table, which implies that, on average, parcels sold only once are similar to parcels sold more than once. Based on the mean ST in Colorado and Nebraska, we choose 30 and 70 meters of saturated thickness as the break points of piece-wise function in equation 3.3.

Table 3.4 summarizes the year gap and ST changes across parcel transactions. For the repeated sales, the year gap and ST changes between transactions of a given parcel are larger in Colorado compared with Nebraska on average.

Table 3.4: Year Gap and ST Changes for Repeated Transactions

Repeated sales	CO	NE
Min year gap between transactions	1	1
Min ST changes between transactions (m)	0	0
Max year gap between transactions	20	26
Max ST changes between transactions (m)	9.762	8.255
Mean year gap between transactions	6.45	4.59
Mean ST changes between transactions (m)	1.714	1.279

3.5 Results and Discussion

This section summarizes the regression results for different datasets with various specifications. Tables summarizing the estimates across different specifications can be found in the Appendix. Figures 3.4c, 3.5c and 3.6c plots estimates from columns 3, 5 and 6 in Table C.2, respectively. Figures 3.4a, 3.5a and 3.6a present estimates from columns 3, 5 and 6 in Table C.3, respectively. Figures 3.4b, 3.5b and 3.6b are based on columns 3, 5 and 6 in Table C.4.

Figures 3.4a and 3.4b present point estimates of the marginal effect of saturated thickness (ST) from equation 3.1 for all transactions and repeated transactions, respectively; while Figure 3.4c plots marginal effects of ST from equation 3.2. The red and blue dashed lines denote the mean ST for Colorado and Nebraska, respectively. When ST levels are lower than the mean ST of Nebraska, all figures show a decreasing marginal effect of ST as ST level increases. Marginal effect of ST

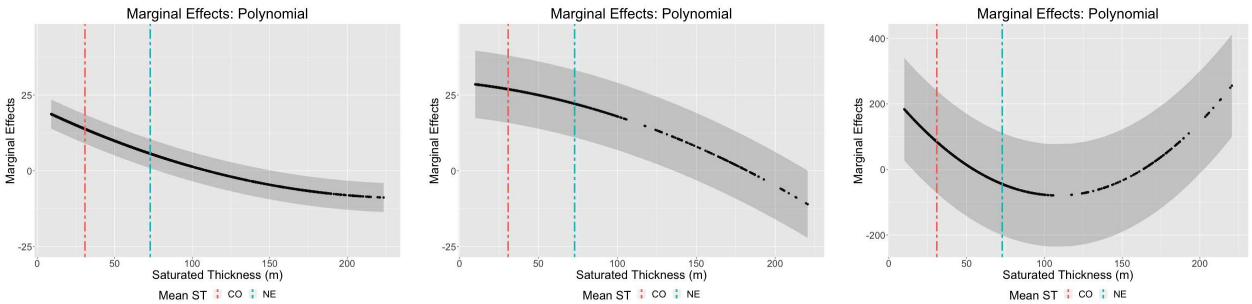

(a) Pooled OLS: All **(b)** Pooled OLS: Repeated **(c)** TWFE

Figure 3.4: Marginal Effect Estimates of Models with Polynomial Specification

is positive when ST level is sufficiently low. Table 3.5 summarizes the marginal effect of ST at the mean ST for Colorado and Nebraska. Pooled OLS estimates of ST at mean ST levels are significantly positive and an additional meter in saturated thickness could introduce $13.81/acre in Colorado and $5.66/acre in Nebraska on average. Pooled OLS with repeated transactions yields higher marginal effect estimates than that with all transactions, where an additional one meter increase in saturated thickness raises the land value by $26.94/acre in Colorado and $22.14/acre in Nebraska, which implies that values of parcels transacted more than once are more responsive to the ST levels. Though TWFE estimates show similar higher marginal effects with lower ST levels, estimates are not significantly different from 0 at mean ST levels. Our estimates of of the marginal effects are per meter increase in saturated thickness. To compare our results with estimates from Torell et al. [79], we transfer our estimates to land value change per foot increase in saturated thickness in Table 3.6. Our estimates from the pooled OLS with repeated transactions are similar to those from Torell et al. [79] whereas the estimates from the pooled OLS with all transactions are smaller than those in Torell et al. [79].

Figures 3.5a and 3.5b present point estimates of ST marginal effects from a piece-wise linear function similar to that in equation 3.3 that controls for soil types and climate attributes with county fixed effects for all transactions and repeated transactions, respectively; while Figure 3.5c plots marginal effects of ST from a TWFE model identical to that provided in equation 3.3. The estimated marginal effects of ST at Nebraska's mean ST level in Figure 3.5 are similar to those

Table 3.5: Marginal Effects of ST at Mean ST Levels with the Polynomial Specification

	CO Mean ST 30.8 m	NE Mean ST 72.9 m
Pooled OLS All Transactions	13.8053***	5.6621*
	(3.5172)	(3.1482)
Pooled OLS Repeated Transactions	26.9373***	22.144**
	(7.2861)	(9.8535)
TWFE	84.2023	-44.7245
	(170.4008)	(62.8313)
Note:	*p<0.1; **p<0.05; ***p<0.01	

Table 3.6: Marginal Value of Saturated Thickness Comparison

$/acre Increase in Land Value per Foot of ST Increase	CO Mean	NE Mean
Pooled OLS All Transactions	4.21	1.73
Pooled OLS Repeated Transactions	8.21	6.75
TWFE	25.66	-13.63
Torell et al. (1990)	5.45 (North CO) 2.99 (South CO)	2.89
Torell et al. (1990) in 2015 $	11.44 (North CO) 6.51 (South CO)	5.97

in Figure 3.4. Though estimates show different patterns across the three figures, the estimates of different ST ranges are not significantly different from each other. Therefore, we don't observe evidence for different land value responses to different ST range groups based on the piece-wise linear functions. We notice in Figure 3.5b that the marginal effect of ST is significantly larger than 0 when ST is greater than 70 meters, while it is not significantly different from 0 in Figure 3.5a. This reiterates that values of parcels transacted more than once are more responsive to ST levels.

Figure 3.6 plots estimates with drought reflection specification. Here we show results with a drought reflection point choice of D = 2004. Red dots are marginal effects of ST after 2004, and green dots are marginal effects of ST before 2004. Blue and purple dashed lines denote the

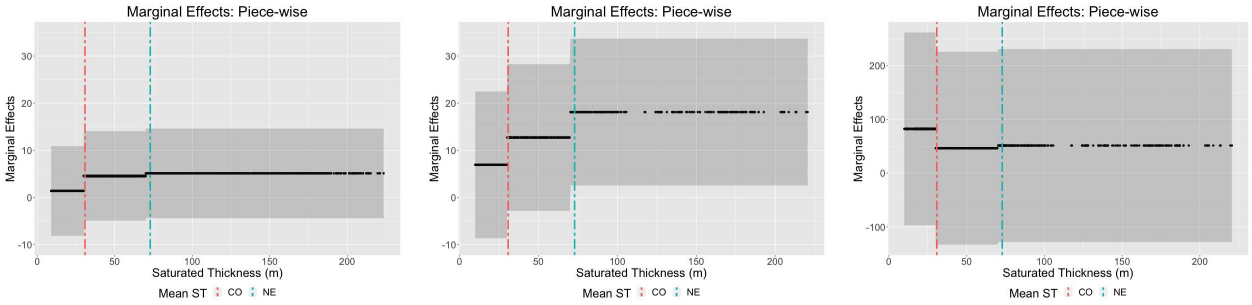

(a) Pooled OLS: All **(b)** Pooled OLS: Repeated **(c)** TWFE

Figure 3.5: Marginal Effect Estimates of Models with Piece-wise Specification

mean ST of Colorado and Nebraska, respectively. While all three subfigures show higher average marginal effect of ST after 2004 when frequent and severe droughts started to hit the study area, the functional form of the marginal effect of ST in Figure 3.6c looks different from those in Figures 3.6a and 3.6b. Differences in the estimated functional form of marginal effect could due to omitted parcel attributes correlated with ST level in the pooled OLS specification. Table 3.7 summarizes the marginal effects of ST at mean ST levels across states. Marginal effects of ST at mean ST levels from pooled OLS show that land values are more responsive to the ST levels after 2004 when drought frequency increases. Again, estimates from the TWFE model are not significantly different from 0 due to limited degree of freedom.

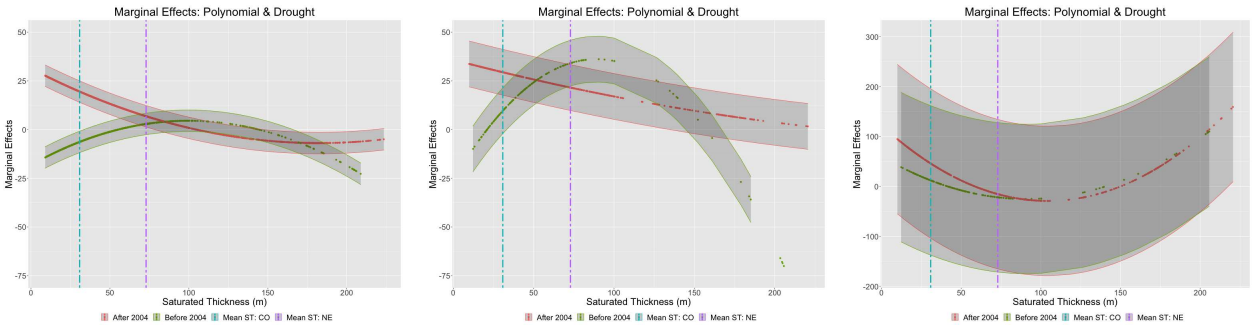

(a) Pooled OLS: All **(b)** Pooled OLS: Repeated **(c)** TWFE

Figure 3.6: Marginal Effect Estimates of Models with Drought Reflection Specification

Table 3.7: Marginal Effects of ST at Mean ST Levels with the Drought Reflection Specification

		CO Mean ST 30.8 m	NE Mean ST 72.9 m
Pooled OLS All Transactions	Before 2004	-6.3289	2.8999*
		(6.6007)	(6.1683)
	After 2004	19.5268***	6.8722***
		(4.4197)	(3.5944)
Pooled OLS Repeated Transactions	Before 2004	9.6538	34.1281**
		(24.546)	(9.8401)
	After 2004	29.4495***	21.5735*
		(8.2374)	(9.6616)
TWFE	Before 2004	12.2042	-21.7194
		(135.3913)	(52.8578)
	After 2004	46.0987	-15.2692
		(157.6412)	(53.0938)
Note:		*p<0.1; **p<0.05; ***p<0.01	

For a robustness check, we also use different drought reflection point D choices from 2000 to 2005. Figure 3.7 summarizes the marginal effect of ST at mean ST levels with different D choices. In the pooled OLS models, the marginal effect at the mean is not sensitive to the choice of D. In the TWFE models, while the marginal effect at mean varies with respect to D, it's not significantly different from 0. Therefore, the results are robust to different choices of D.

Hrozencik et al. [44] demonstrated that land profitability in the Republican River Basin of Colorado increases as well capacity increases, till well capacity reaches approximately 600 gallons per min (gpm). The profitability of land does not change significantly with well capacity greater than 600 gpm across land types. To justify why the marginal effect of ST drops as ST level increases, we use reported well capacity in Colorado [19] to estimate the relationship between ST and well capacity[35]. Applying the estimated relationship between ST and well capacity to the observations in Colorado shows that observations with ST greater than 25.17 meters have well capacity larger than 600 gmp, while the median ST level in our Colorado sample is 26.17 meters.

[35]The estimated well capacity is a function of ST, ST^2 and ST^3. The estimates for ST, ST^2 and ST^3 are -4.591, 0.3576 and – 0.002626, respectively. All estimates are statistically significant at a significant level of 0.05

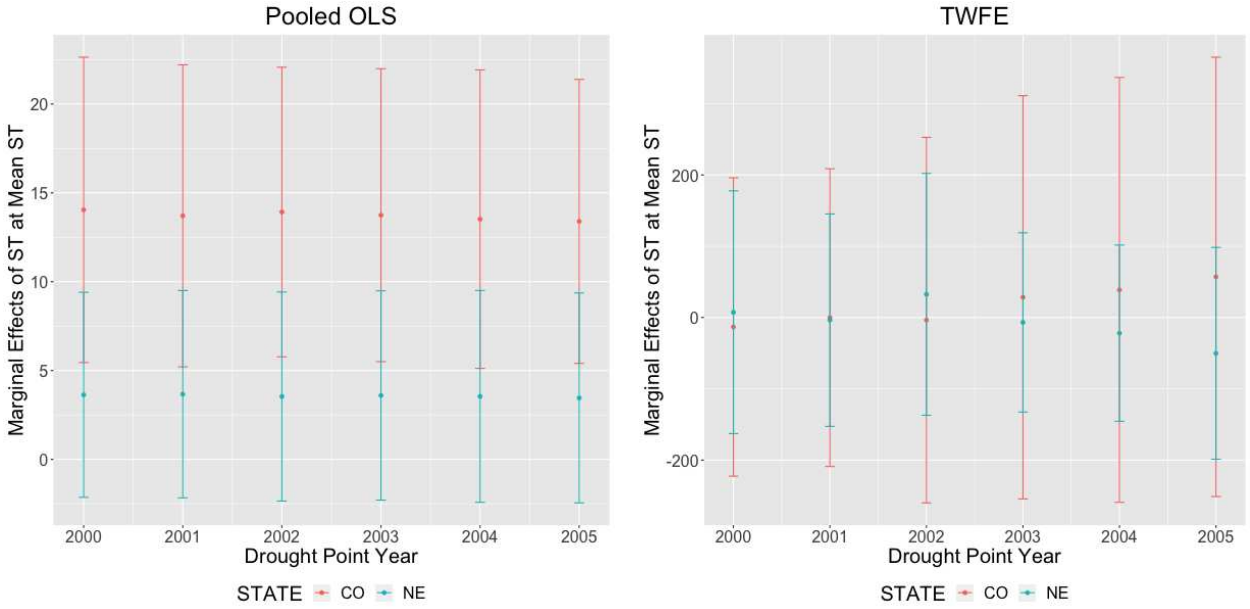

(a) Pooled OLS: All **(b)** TWFE

Figure 3.7: Marginal Effect Estimates at Mean ST across Different D Choices

Therefore, higher ST levels are not contributing to the land profitability to at least half of the parcels in our Colorado sample, which underpins the insignificant marginal effect of ST when ST levels are high in our results.

According to McGuire et al. [59], saturated thickness in Colorado and Nebraska declined 5.1[36] feet and 2.4 feet[37] from 2000 to 2009, respectively. Assuming the depletion behaviors in both states remain the same, and the estimated real land value losses every 10 years due to groundwater level loss in Colorado and Nebraska are 159.17 $/acre and 30.10 $/acre on average, which accounts for 6.6% and 0.95% of the mean real land values for Colorado and Nebraska, respectively[38]. In our dataset, the HPA irrigated land area is 494,819 acres in Colorado and 636,569 acres in Nebraska,

[36] 5.1 feet = 1.55448 meters

[37] 2.4 feet = 0.73152 meter

[38] Estimates from equation 3.2 are used for this calculation. Based on the column (3) in Table C.2, $Price = 238.79ST - 2.92ST^2 + 0.01ST^3$. Therefore, marginal effect (ME) of ST on land price = $238.79 - 5.84ST + 0.03ST^2$. We use parcel-level ST in 2016 to calculate the parcel-level ME of ST and then combined with estimated 10-year ST decline in Colorado and Nebraska from McGuire et al. [59] to calculate the parcel-level land value decreases from 2016 to 2025 with the current depletion pattern. The average land value reductions in Colorado and Nebraska are 159.17 $/acre and 30.10 $/acre.

and these HPA irrigated areas collectively lose an estimated $97,921,127 in land value every 10 years based on our estimates. Therefore, conservation programs and land use management practices that can improve groundwater use efficiency and maintain groundwater availability in HPA could be welfare increasing if the total social cost is smaller than the estimated land value loss.

3.6 Conclusions

The High Plains aquifer plays a vital role in U.S. crop production and local aquatic ecosystems. To achieve sustainable exploitation of the largest groundwater resource in the U.S., water conservation is necessary. Reliable estimates of groundwater value contribute to efficient water conservation design. Due to the lack of competitive market, it is difficult to observe the value of groundwater directly, and therefore we adopt the hedonic method to reveal its value through the groundwater irrigated land market.

With modern ZTRAX data products from the Zillow corporation, we are able to obtain repeated agricultural land transactions to control for parcel-level, time-constant unobservables. The regression outcomes reveal that (1) including parcel-level fixed effects to control for parcel-level time-constant attributes does not necessarily provide different outcome from pooled OLS models with county fixed effects; (2) groundwater irrigated land value is higher on average in areas with higher groundwater stock; (3) when the groundwater resource is constrained, the marginal value of ST decreases with high ST levels; (4) when the groundwater stock is abundant, the marginal value of ST on land value is not different from zero. Our estimates from pooled OLS with repeated transactions are comparable to Torell et al. [79], while estimates from a TWFE model are not.

The estimates of groundwater value from this research can contribute to cost-benefit analysis of facilities and policies aiming to conserve the groundwater resource. Higher values of groundwater imply greater benefits related to resource conservation and therefore can justify higher implementation costs of facilities and policies.

Identifying whether a parcel is groundwater irrigated and where the parcel is located are critical for this analysis. In this study, some parcel transactions do not provide clear land use descriptions

but are larger than 30 acres are classified as agricultural land. A larger minimum parcel size filter can be used in future studies. In addition, the to avoid mislocating a parcel, parcels without coordinates can be excluded from the future studies. Pooled OLS models in future studies can also account for soil type as well as climate characteristics. Interactions between ST and soil type might also be helpful. Though we hope to provide an update for the groundwater resource value for the entire HPA, we are constrained by the land transactions data across states. Since the south HPA is expected to be more constrained by groundwater stock declines, it would be beneficial for future studies to carry out a similar analysis of irrigated land transactions in Texas, Oklahoma, and New Mexico.

Bibliography

[1] Almond, D., Chen, Y., Greenstone, M., and Li, H. (2009). Winter heating or clean air? unintended impacts of china's huai river policy. *American Economic Review*, 99(2):184–90.

[2] Armsworth, P. R., Acs, S., Dallimer, M., Gaston, K. J., Hanley, N., and Wilson, P. (2012). The cost of policy simplification in conservation incentive programs. *Ecology letters*, 15(5):406–414.

[3] Arnold, J., Kiniry, J., Srinivasan, R., Williams, J., Haney, E., and Neitsch, S. (2013). Swat 2012 input/output documentation. Technical report, Texas Water Resources Institute.

[4] Auffhammer, M. and Kellogg, R. (2011). Clearing the air? the effects of gasoline content regulation on air quality. *American Economic Review*, 101(6):2687–2722.

[5] Bastian, C. T., McLeod, D. M., Germino, M. J., Reiners, W. A., and Blasko, B. J. (2002). Environmental amenities and agricultural land values: a hedonic model using geographic information systems data. *Ecological economics*, 40(3):337–349.

[6] Bishop, K. C., Kuminoff, N. V., Banzhaf, H. S., Boyle, K. J., von Gravenitz, K., Pope, J. C., Smith, V. K., and Timmins, C. D. (2020). Best practices for using hedonic property value models to measure willingness to pay for environmental quality. *Review of Environmental Economics and Policy*, 14(2):260–281.

[7] Blann, K. L., Anderson, J. L., Sands, G. R., and Vondracek, B. (2009). Effects of agricultural drainage on aquatic ecosystems: a review. *Critical reviews in environmental science and technology*, 39(11):909–1001.

[8] Börner, J., Baylis, K., Corbera, E., Ezzine-de Blas, D., Honey-Rosés, J., Persson, U. M., and Wunder, S. (2017). The effectiveness of payments for environmental services. *World Development*, 96:359–374.

[9] Brunekreef, B. and Holgate, S. T. (2002). Air pollution and health. *The lancet*, 360(9341):1233–1242.

[10] Buck, S., Auffhammer, M., and Sunding, D. (2014). Land markets and the value of water: Hedonic analysis using repeat sales of farmland. *American Journal of Agricultural Economics*, 96(4):953–969.

[11] Calel, R. and Dechezleprêtre, A. (2016). Environmental policy and directed technological change: evidence from the european carbon market. *Review of economics and statistics*, 98(1):173–191.

[12] Callaway, B. and Sant'Anna, P. H. (2020). Difference-in-differences with multiple time periods. *Journal of Econometrics*.

[13] Chan, H. S. R., Li, S., and Zhang, F. (2013). Firm competitiveness and the european union emissions trading scheme. *Energy Policy*, 63:1056–1064.

[14] Chan, N. W. and Morrow, J. W. (2019). Unintended consequences of cap-and-trade? evidence from the regional greenhouse gas initiative. *Energy Economics*, 80:411–422.

[15] Chang, T. Y., Graff Zivin, J., Gross, T., and Neidell, M. (2019). The effect of pollution on worker productivity: evidence from call center workers in china. *American Economic Journal: Applied Economics*, 11(1):151–72.

[16] Chen, Y., Ebenstein, A., Greenstone, M., and Li, H. (2013). Evidence on the impact of sustained exposure to air pollution on life expectancy from china's huai river policy. *Proceedings of the National Academy of Sciences*, 110(32):12936–12941.

[17] Chen, Y. and Whalley, A. (2012). Green infrastructure: The effects of urban rail transit on air quality. *American Economic Journal: Economic Policy*, 4(1):58–97.

[18] Cheng, B., Dai, H., Wang, P., Zhao, D., and Masui, T. (2015). Impacts of carbon trading scheme on air pollutant emissions in guangdong province of china. *Energy for sustainable development*, 27:174–185.

[19] Colorado Decision Support Systems (2022). Well applications.

[Colorado State University] Colorado State University. Enterprise budgets-crop.

[21] Cropper, M. L., Deck, L. B., and McConnell, K. E. (1988). On the choice of funtional form for hedonic price functions. *The review of economics and statistics*, pages 668–675.

[22] Currie, J., Hanushek, E. A., Kahn, E. M., Neidell, M., and Rivkin, S. G. (2009). Does pollution increase school absences? *The Review of Economics and Statistics*, 91(4):682–694.

[23] Davis, L. W. (2008). The effect of driving restrictions on air quality in mexico city. *Journal of Political Economy*, 116(1):38–81.

[24] Dockery, D. W., Pope, C. A., Xu, X., Spengler, J. D., Ware, J. H., Fay, M. E., Ferris Jr, B. G., and Speizer, F. E. (1993). An association between air pollution and mortality in six us cities. *New England journal of medicine*, 329(24):1753–1759.

[25] Dong, F., Yu, B., and Pan, Y. (2019). Examining the synergistic effect of co2 emissions on pm2. 5 emissions reduction: Evidence from china. *Journal of cleaner production*, 223:759–771.

[26] Ebenstein, A., Fan, M., Greenstone, M., He, G., and Zhou, M. (2017). New evidence on the impact of sustained exposure to air pollution on life expectancy from china's huai river policy. *Proceedings of the National Academy of Sciences*, 114(39):10384–10389.

[27] Engel, S. (2016). The devil in the detail: a practical guide on designing payments for environmental services. *International Review of Environmental and Resource Economics*, 9(1–2):131–177.

[28] Ezzine-de Blas, D., Wunder, S., Ruiz-Pérez, M., and del Pilar Moreno-Sanchez, R. (2016). Global patterns in the implementation of payments for environmental services. *PloS one*, 11(3):e0149847.

[29] Fan, M. and Grainger, C. (2019). The impact of air pollution on labor supply in china. Technical report, Working Paper.

[30] Ferraro, P. J. (2008). Asymmetric information and contract design for payments for environmental services. *Ecological economics*, 65(4):810–821.

[31] Ferraro, P. J. and Miranda, J. J. (2017). Panel data designs and estimators as substitutes for randomized controlled trials in the evaluation of public programs. *Journal of the Association of Environmental and Resource Economists*, 4(1):281–317.

[32] Freyaldenhoven, S., Hansen, C., and Shapiro, J. M. (2019). Pre-event trends in the panel event-study design. *American Economic Review*, 109(9):3307–38.

[33] Gallego, F., Montero, J.-P., and Salas, C. (2013). The effect of transport policies on car use: Evidence from latin american cities. *Journal of Public Economics*, 107:47–62.

[34] Ghanem, D. and Zhang, J. (2014). 'effortless perfection:'do chinese cities manipulate air pollution data? *Journal of Environmental Economics and Management*, 68(2):203–225.

[35] Gilliam, J., Baker, J., and Reddy, K. (1999). Water quality effects of drainage in humid regions. *Agricultural drainage*, 38:801–830.

[36] Goodman-Bacon, A. (2018). Difference-in-differences with variation in treatment timing. Technical report, National Bureau of Economic Research.

[37] Greenstone, M. and Fan, C. (2018). Introducing the air quality life index-twelve facts about particulate air pollution, human health, and global policy. *Energy Policy Institute at the University of Chicago*.

[38] Haacker, E. M., Kendall, A. D., and Hyndman, D. W. (2016). Water level declines in the high plains aquifer: Predevelopment to resource senescence. *Groundwater*, 54(2):231–242.

[39] Hammitt, J. K., Geng, F., Guo, X., and Nielsen, C. P. (2019). Valuing mortality risk in china: Comparing stated-preference estimates from 2005 and 2016. *Journal of Risk and Uncertainty*, 58(2):167–186.

[40] He, G. and Wang, S. (2017). Do college graduates serving as village officials help rural china? *American Economic Journal: Applied Economics*, 9(4):186–215.

[41] He, J., Liu, H., and Salvo, A. (2019). Severe air pollution and labor productivity: Evidence from industrial towns in china. *American Economic Journal: Applied Economics*, 11(1):173–201.

[42] Heft-Neal, S., Burney, J., Bendavid, E., and Burke, M. (2018). Robust relationship between air quality and infant mortality in africa. *Nature*, 559(7713):254–258.

[43] Henderson, J. R. and Moore, S. (2006). The capitalization of wildlife recreation income into farmland values. *Journal of agricultural and applied economics*, 38(1379-2016-112862):597–610.

[44] Hrozencik, R. A., Manning, D. T., Suter, J. F., Goemans, C., and Bailey, R. T. (2017). The heterogeneous impacts of groundwater management policies in the republican river basin of colorado. *Water Resources Research*, 53(12):10757–10778.

[45] Huang, J., Shen, J., Miao, L., and Zhang, W. (2021). The effects of emission trading scheme on industrial output and air pollution emissions under city heterogeneity in china. *Journal of Cleaner Production*, 315:128260.

[46] Imai, K. and Kim, I. S. (2020). On the use of two-way fixed effects regression models for causal inference with panel data. *Political Analysis*, pages 1–11.

[Iowa State University] Iowa State University. Historical costs of crop production.

[48] Kahn-Lang, A. and Lang, K. (2020). The promise and pitfalls of differences-in-differences: Reflections on 16 and pregnant and other applications. *Journal of Business & Economic Statistics*, 38(3):613–620.

[49] Kuminoff, N. V., Parmeter, C. F., and Pope, J. C. (2010). Which hedonic models can we trust to recover the marginal willingness to pay for environmental amenities? *Journal of environmental economics and management*, 60(3):145–160.

[50] Li, T., Zhang, Y., Wang, J., Xu, D., Yin, Z., Chen, H., Lv, Y., Luo, J., Zeng, Y., Liu, Y., et al. (2018). All-cause mortality risk associated with long-term exposure to ambient pm2· 5 in china: a cohort study. *The Lancet Public Health*, 3(10):e470–e477.

[51] Lundberg, L., Persson, U. M., Alpizar, F., and Lindgren, K. (2018). Context matters: exploring the cost-effectiveness of fixed payments and procurement auctions for pes. *Ecological Economics*, 146:347–358.

[52] Manion, M., Zarakas, C., Wnuck, S., Haskell, J., Belova, A., Cooley, D., et al. (2017). Analysis of the public health impacts of the regional greenhouse gas initiative. *Abt Associates*, 11.

[53] Margolis, J., Dudek, D., and Hove, A. (2015). Rolling out a successful carbon trading system. *Paulson Institute*.

[54] Marques, G. F., Lund, J. R., and Howitt, R. E. (2005). Modeling irrigated agricultural production and water use decisions under water supply uncertainty. *Water resources research*, 41(8).

[55] Mason, C. F. and Plantinga, A. J. (2013). The additionality problem with offsets: Optimal contracts for carbon sequestration in forests. *Journal of Environmental Economics and Management*, 66(1):1–14.

[56] McGuire, V. L. (2012). Water-level and storage changes in the high plains aquifer, predevelopment to 2011 and 2009–11. Technical report, US Geological Survey.

[57] McGuire, V. L. (2014). Water-level changes and change in water in storage in the high plains aquifer, predevelopment to 2013 and 2011–13. Technical report, US Geological Survey.

[58] McGuire, V. L. (2017). Water-level and recoverable water in storage changes, high plains aquifer, predevelopment to 2015 and 2013–15. Technical report, US Geological Survey.

[59] McGuire, V. L., Lund, K. D., and Densmore, B. K. (2012). Saturated thickness and water in storage in the high plains aquifer, 2009, and water-level changes and changes in water in storage in the high plains aquifer, 1980 to 1995, 1995 to 2000, 2000 to 2005, and 2005 to 2009. *US Geological Survey Scientific Investigations Report*, 5177:28.

[60] Oregon State University (2014). Prism climate group. https://prism.oregonstate.edu. Online; accessed 10 July 2022.

[61] Palm-Forster, L. H., Swinton, S. M., Lupi, F., and Shupp, R. S. (2016). Too burdensome to bid: Transaction costs and pay-for-performance conservation. *American Journal of Agricultural Economics*, 98(5):1314–1333.

[62] Palmquist, R. B. and Danielson, L. E. (1989). A hedonic study of the effects of erosion control and drainage on farmland values. *American journal of agricultural economics*, 71(1):55–62.

[63] Perera, F., Cooley, D., Berberian, A., Mills, D., and Kinney, P. (2020). Co-benefits to children's health of the us regional greenhouse gas initiative. *Environmental Health Perspectives*, 128(7):077006.

[64] Perkin, J. S., Gido, K. B., Falke, J. A., Fausch, K. D., Crockett, H., Johnson, E. R., and Sanderson, J. (2017). Groundwater declines are linked to changes in great plains stream fish assemblages. *Proceedings of the National Academy of Sciences*, 114(28):7373–7378.

[65] Rambachan, A. and Roth, J. (2019). An honest approach to parallel trends. *Unpublished manuscript, Harvard University.[99]*.

[66] Roth, J. (2019). Pre-test with caution: Event-study estimates after testing for parallel trends. *Unpublished manuscript, Department of Economics, Harvard University*.

[67] Sampson, G. S., Hendricks, N. P., and Taylor, M. R. (2019). Land market valuation of groundwater. *Resource and Energy Economics*, 58:101120.

[68] Sarkodie, S. A., Strezov, V., Jiang, Y., and Evans, T. (2019). Proximate determinants of particulate matter (pm2. 5) emission, mortality and life expectancy in europe, central asia, australia, canada and the us. *Science of the Total Environment*, 683:489–497.

[69] Scanlon, B. R., Faunt, C. C., Longuevergne, L., Reedy, R. C., Alley, W. M., McGuire, V. L., and McMahon, P. B. (2012). Groundwater depletion and sustainability of irrigation in the us high plains and central valley. *Proceedings of the national academy of sciences*, 109(24):9320–9325.

[70] Schlenker, W. and Walker, W. R. (2016). Airports, air pollution, and contemporaneous health. *The Review of Economic Studies*, 83(2):768–809.

[71] Schloss, J. A. and Buddemeier, . R. (2000). An atlas of the kansas high plains aquifer. University of Kansas.

[72] Shan, Y., Guan, D., Zheng, H., Ou, J., Li, Y., Meng, J., Mi, Z., Liu, Z., and Zhang, Q. (2018). China co 2 emission accounts 1997–2015. *Scientific data*, 5:170201.

[73] Shang, Y., Sun, Z., Cao, J., Wang, X., Zhong, L., Bi, X., Li, H., Liu, W., Zhu, T., and Huang, W. (2013). Systematic review of chinese studies of short-term exposure to air pollution and daily mortality. *Environment international*, 54:100–111.

[74] Skaggs, R. W., Breve, M., and Gilliam, J. (1994). Hydrologic and water quality impacts of agricultural drainage. *Critical reviews in environmental science and technology*, 24(1):1–32.

[75] Steigerwald, D. G., Vazquez-Bare, G., and Maier, J. (2021). Measuring heterogeneous effects of environmental policies using panel data. *Journal of the Association of Environmental and Resource Economists*, 8(2):277–313.

[76] Sun, L. and Abraham, S. (2020). Estimating dynamic treatment effects in event studies with heterogeneous treatment effects. *Journal of Econometrics*.

[77] Suter, J. F., Rad, M. R., Manning, D. T., Goemans, C., and Sanderson, M. R. (2019). Depletion, climate, and the incremental value of groundwater. *Resource and Energy Economics*, page 101143.

[78] Thistlethwaite, D. L. and Campbell, D. T. (1960). Regression-discontinuity analysis: An alternative to the ex post facto experiment. *Journal of Educational psychology*, 51(6).

[79] Torell, L. A., Libbin, J. D., and Miller, M. D. (1990). The market value of water in the ogallala aquifer. *Land economics*, 66(2):163–175.

[80] Uchida, E., Xu, J., and Rozelle, S. (2005). Grain for green: Cost-effectiveness and sustainability of china's conservation set-aside program. *Land Economics*, 81(2):247–264.

[81] UDSA-NRCS (2005). Global soil regions map.

[82] USDA FSA (2015). Conservation reserve program, cp-22.

[83] USDA NASS (2015). National agricultural statistics services—quick stats.

[84] van Donkelaar, A., Hammer, M. S., Bindle, L., Brauer, M., Brook, J. R., Garay, M. J., Hsu, N. C., Kalashnikova, O. V., Kahn, R. A., Lee, C., et al. (2021). Monthly global estimates of fine particulate matter and their uncertainty. *Environmental Science & Technology*, 55(22):15287–15300.

[85] Verde, S. F. (2020). The impact of the eu emissions trading system on competitiveness and carbon leakage: the econometric evidence. *Journal of Economic Surveys*, 34(2):320–343.

[86] Von Graevenitz, K. (2018). The amenity cost of road noise. *Journal of Environmental Economics and Management*, 90:1–22.

[87] Wang, H., Chen, Z., Wu, X., and Nie, X. (2019). Can a carbon trading system promote the transformation of a low-carbon economy under the framework of the porter hypothesis?—empirical analysis based on the psm-did method. *Energy Policy*, 129:930–938.

[88] Wei, X., Bailey, R. T., and Tasdighi, A. (2018). Using the swat model in intensively managed irrigated watersheds: model modification and application. *Journal of Hydrologic Engineering*, 23(10):04018044.

[89] Wunder, S. and Albán, M. (2008). Decentralized payments for environmental services: the cases of pimampiro and profafor in ecuador. *Ecological Economics*, 65(4):685–698.

[90] Wunder, S., Brouwer, R., Engel, S., Ezzine-de Blas, D., Muradian, R., Pascual, U., and Pinto, R. (2018). From principles to practice in paying for nature's services. *Nature Sustainability*, 1(3):145–150.

[91] Wünscher, T. and Engel, S. (2012). International payments for biodiversity services: Review and evaluation of conservation targeting approaches. *Biological Conservation*, 152:222–230.

[92] Wünscher, T., Engel, S., and Wunder, S. (2008). Spatial targeting of payments for environmental services: a tool for boosting conservation benefits. *Ecological economics*, 65(4):822–833.

[93] Zhang, J. and Mu, Q. (2018). Air pollution and defensive expenditures: Evidence from particulate-filtering facemasks. *Journal of Environmental Economics and Management*, 92:517–536.

Appendix A

Chapter 1: Supplemental Material

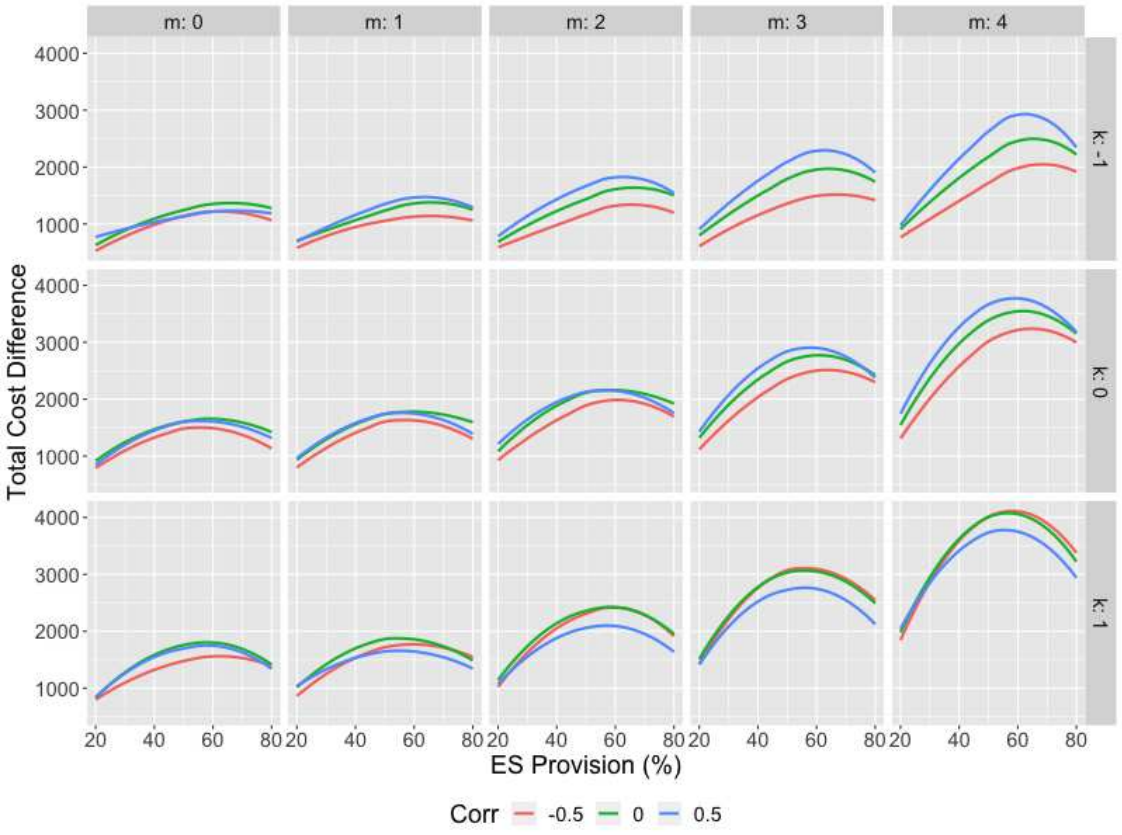

Figure A.1: Total Cost Difference between Uniform Payment and Efficient Payment

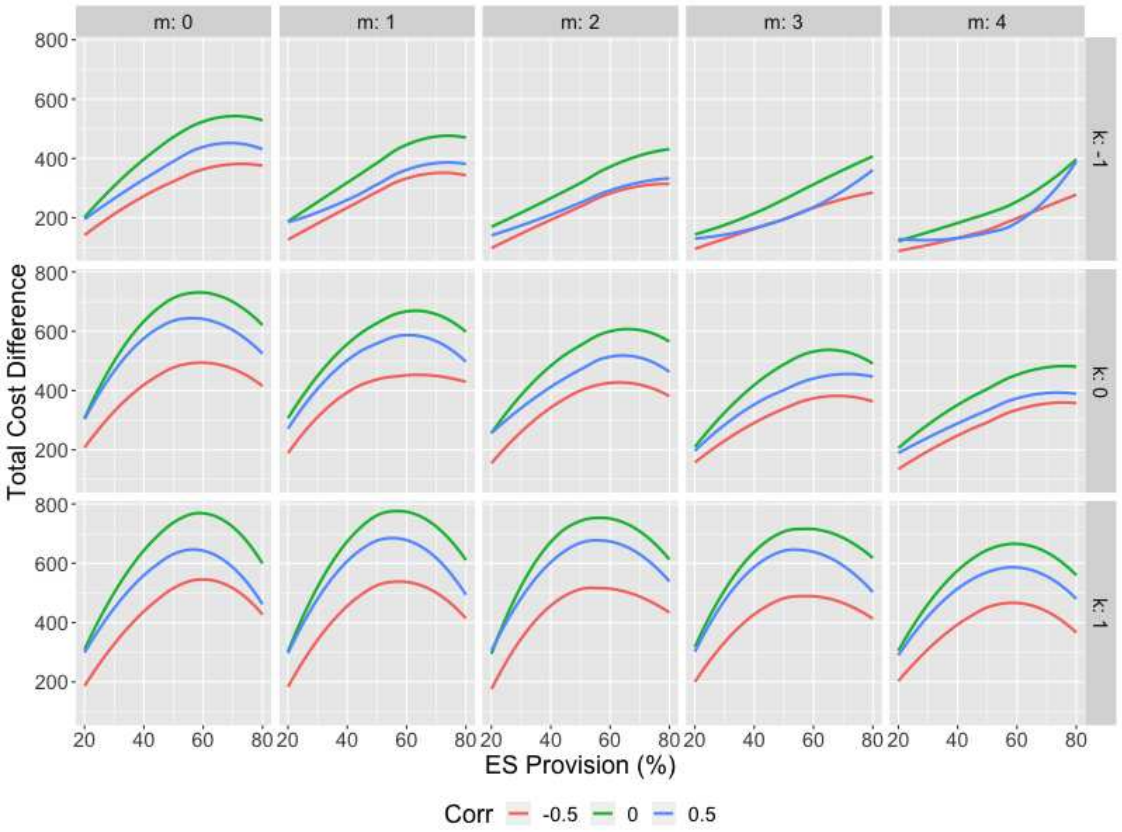

Figure A.2: Total Cost Difference between Differentiated Payments and Efficient Payment

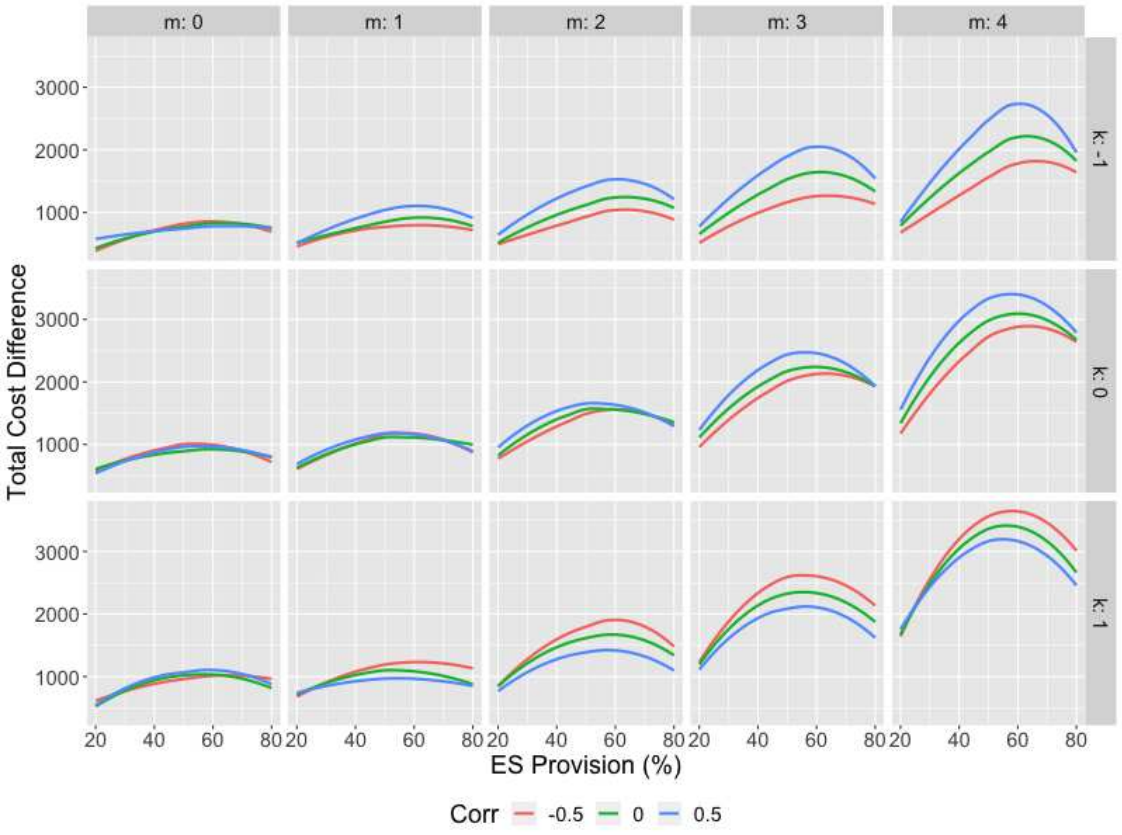

Figure A.3: Total Cost Difference between Uniform Payment and Differentiated Payments

Table A.1: Conceptual PES Program Comparison

Payment Design	Payment Rate	Enrollment Selection	ES Targeting
Uniform	Same across parcels	Enroll all parcels with ES provision cost smaller than or equal to the payment rate	No
Differentiated	Same within a parcel type, different across parcel types	Enroll all parcels with ES provision cost smaller than or equal to the payment rate	Target on land attributes
Efficient	No less than parcel's opportunity cost	Rank parcels based on ES provision benefit and cost ratio, and enroll until the ES provision target is fulfilled	Target on ES provision

92

Appendix B

Chapter 2: Supplemental Material

Table B.1: Coverage of Each ETS Pilots

	Emission reduction target (intensity-based)	Emission compliance threshold	Cap coverage	Baseline years
Beijing	18% over 2010 levels	+ 5,000 tonnes CO2 per year as the average from 2009 to 2011	50% of the city's total emissions: Around 1000 companies from heat supply, power generation, cement, petrochemical, car manufacturing, and public buildings	2009 to 2011

Continued on next page

Table B.1 – continued from previous page

	Emission reduction target (intensity-based)	Emission compliance threshold	Cap coverage	Baseline years
Shanghai	19% over 2010 levels	+ 20,000 tonnes CO2 per year for industrial sectors in 2010 or 2011, >10,000 tonnes per year for other sectors	57% of the city's total emissions: 191 entities are listed (steel, petrochemical, chemical, power, non-ferrous metal, building materials, textile, paper, rubber, and chemical fibre)	2009 to 2011
Guangdong	19% over 2010 levels	+ 20,000 tonnes CO2 per year from 2010 to 2012	42% of the province's total energy consumption: 242 firms are listed (power, cement, steel, ceramics, plastics, petrochemical, non-ferrous, and paper)	2011, 2012

Continued on next page

Table B.1 – continued from previous page

	Emission reduction target (intensity-based)	Emission compliance threshold	Cap coverage	Baseline years
Shenzhen	15% over 2010 levels	+ 3,000 tonnes CO2 per year and any building >20,000 m2	635 entities listed from 26 sectors which cover various forms of industry in addition to power, gas, and water supply. Participation is open to any financial institution, 197 public-use buildings	2009 to 2011
Tianjin	15% over 2010 levels, <0.169 CO2/GDP (kg/CNY)	+ 20,000 tonnes CO2 per year in any year since 2009	60% of the city's total emissions: 114 entities including iron and steel, chemicals, electricity, heat, petrochemical, oil and gas mining, and civil construction	2009 to 2013

Continued on next page

Table B.1 – continued from previous page

	Emission reduction target (intensity-based)	Emission compliance threshold	Cap coverage	Baseline years
Hubei	17% over 2010 levels	+ 60,000 tonnes coal consumption for major sectors in 2010 or 2011	35% of the province's total carbon emissions: 138 entities are listed (steel, chemical, cement, automobile manufacturing, power generation, glass, paper, non-ferrous metals)	2010, 2011
Chongqing	20% over 2010 levels	+ 20,000 tonnes CO2 per year from 2010 to 2014	125 million allowances were issued to 242 companies in the electricity, aluminum, iron and steel, cement, and other industrial sectors	2010 to 2014

Source: Margolis et al. [53]

Table B.2: Summary of China ETS Pilots Penalty Mechanism

Pilots	Penalty (Fine)	Penalty (Quota Debit)
Shenzhen	Shortfall $\times$ $3P_6$	Shortfall $\times$ 1
Beijing	Shortfall $\times$ 3 to $5P_a$	/
Shanghai	50,000 to 10,0000	/
Tianjin	/	/
Chongqing	/	/
Guangdong	50,000	Shortfall $\times$ 2
Hubei	Shortfall $\times$ $3P_a \leq$ 150,000	Shortfall $\times$ 2

Note: Type P_6 = Average allowance price over last 6 months; P_a = Average allowance price (no time period specified); Shortfall = Reported emissions $-$ surrendered allowance. The information presented in this table are from Margolis et al. [53] and official governmental documents.

Appendix C

Chapter 3: Supplemental Material

C.1 ZTRAX Data Processing Details

The original ZTRAX data are organized by the date. Each date folder includes individual zip file for each state. In each state zip file, two folders for ZAsmt and ZTrans are included. ZAsmt folder includes 22 data files, and 3 of them are used to generate our dataset: ZAsmtMain, ZAsmtSaleData, and ZAsmtBuidling. ZTrans folder consists of 20 table files, and 2 of them contribute to our final dataset: ZTransMain and ZTransPropertyInfo The following are detailed data process step, taking Colorado for example. RowID is the common identifier across all ZAsmt data products, and each RowID identifies a property within a parcel. Therefore, an ImportParcelID can be associated with multiple RowIDs. TransId is the common identifier across all ZTrans data products, and each TransId represent a transaction. As multiple parcels can be transacted within a transaction. Therefore, a TransId can be associated with multiple ImportParcelIDs. On the other hand, a parcel can be transacted multiple times across the years, and therefore one ImportParcelID can be associated with multiple TransIds.

C.1.1 ZAsmt Data Product

ZAsmtMain is first read in with 3,502,340 observations, and I keep 1,035,781 unique observations that (1) are within the aquifer boundary, (2) are with positive "LotSizeAcre" values, (3) at least have valid "PropertyFullStreetAddress" or coordinates input. To remove duplicated inputs, I change all string to lower case and remove extra blanks between strings. "PropertyFullStreetAddress" is "zzzz" or "null" are treated as no address input. Ideally, each of these 1,035,781 observations would have a unique RowID. However, this is not the case. Therefore, I group the data by RowID and rewrite the coordinates with the group mean coordinates, which reduces the data to 1,020,541 unique observations. By this point, there are still 1639 RowIDs are associated

with more than 1 observation and have different “LotSizeAcre”. To avoid linking wrong “LotSizeAcre” to transactions, I drop the observations with those 1639 RowIDs, and get 1017263 unique observations with 1,017,263 RowIDs.

Then ZAsmtBuilding is read in with 3,977,632 observations. I keep 696,450 observations with explicitly agricultural land use or with no land use specified. I further remove duplicated observations and get 213,715 unique observations with 213,715 RowIDs.

To select transactions for agricultural land, I merge ZAsmtMain and ZAsmtBuilding, and keep 141,441 observations with either agricultural land use (141170 observations) or “LotSizeAcre” greater than 30 acres with no land used specified (271 observations).

The last but not the least is the ZAsmtSaleData which provides transaction price and time information. The original data file reads in 17,965,663 observations. I keep 5,973,896 unique observations (1) with “SalesPriceAmount” $>$ 100, (2) with valid transaction year information since 1970, (3) not likely to be non arm-length transaction. Observations with a “DocumentTypeStndCode” in the list of “AFDT, BFDE, CVDE, DEDB, GFDE, GRDE, INTR", JTDE, PRDE, PTDE, QCDE, SVDE, TFDD, TRFC, RCDE, BSDE, COCA, DELU, EXDE, AFDV, FCDE" are treated as non arm-length transaction. Observations with “SalesPriceAmountStndCode” in the list of “NA, QU, ST, BL, RA" are also treated as non arm-length transactions. Ideally, each RowID and year combination is associated with only one “SalesPriceAmount” input. If a RowID and year combination consists of more than one transaction inputs, I drop the associated observations. After these filtering processes, I end up with 5,604,801 unique observations.

Then I merge the ZAsmtSaleData with selected agricultural parcels and get unique observations at RowID level. As the analysis is conducted at ImportParcelID level, I group the data by ImportParcelID and (1) rewrite the “LotSizeAcre” and “SalesPriceAmount” with the group sum, (2) rewrite the coordinates with group mean, (3) rewrite the “PropertyFullStreetAddress” with the longest input within the group.

While many observations come with coordinates of the transacted parcel, the rest of observations have full street address. To assign the saturated thickness value to each parcel, coordinates

for each parcel is required. To maintain a decent sample size, I adopt Google geocode service to transfer “PropertyFullStreetAddress” into coordinates, rather than dropping observations without coordinates. Robustness check can be conducted with different datasets.

C.1.2 ZTrans Data Product

ZTransMain is first read in 2,770,630 observations and I keep 426,412 unique observations, at TransId level, (1) within the aquifer boundary, (2) with positive “SalesPriceAmount”, (3) not likely to be non arm-length transaction, and (4) with valid transaction year information. Observations with a “DocumentTypeStndCode” in the list of “AFDT, BFDE, CVDE, DEDB, GFDE, GRDE, INTR", JTDE, PRDE, PTDE, QCDE, SVDE, TFDD, TRFC, RCDE, BSDE, COCA, DELU, EXDE, AFDV, FCDE" are treated as non arm-length transaction. Observations with a “SalesPriceAmountStndCode” in the list of “NA, QU, ST, BL, RA" are also treated as non arm-length transactions. In addition, ZTransMain provides “IntraFamilyTransferFlag”, I also drop observations with the flag.

Then ZTransPropertyInfo is read in 11,531,559 observations and I keep 319,975 unique observations (1) within the aquifer boundary, (2) with valid ImportParcelID and “LegalLotSize”, and (3) at least have valid “PropertyFullStreetAddress” or coordinates input. I drop observations with square feet as the unit of the“LegalLotSize” variable, as it is not likely for agricultural land measured in square feet.

I merge the ZTransMain and ZTransPropertyInfo by the TransId, then I keep unique observations with either agricultural land use or “LotSizeAcre” greater than 30 acres with no land used specified. I further aggregate the TransId level data to ImportParcel level. As some of the observations come with “PropertyFullStreetAddress” but no coordinates, I adopt the geocoding transformation again.

ZTRAX suggests to use ZTrans data product when available, I therefore only include ZAsmt inputs when the ImportParcelID does not exist in the ZTrans data product.

Table C.1

Soil order	Characteristics	Suborder	Discription
Mollisols	Soft, thick and dark, one of the most fertile soils on Earth.	Ustolls	subhumid climate
		Udolls	humid climate
		Xerolls	Mediterranean climate
Aridisols	Soils containing $CaCO_3$ in arid regions, irrigation is required for agricultural production, and productivity is generally low	Argids	Mostly used as rangeland or wildlife habitat. Some are used as irrigated cropland
Entisols	soils of unstable environments and productivity varies widely	Orthents	Commonly on recent erosional surfaces. Mostly used as rangeland, pasture, or wildlife habitat.

Table C.2: Estimates of TWFE: Repeated CO & NE

	Dependent variable: Deflated Land Price					
	(1)	(2)	(3)	(4)	(5)	(6)
Saturated Thickness (ST)	38.32***	75.01***	238.79***	89.73***	82.27***	60.12
	(6.87)	(10.18)	(19.96)	(12.95)	(14.88)	(53.86)
ST^2		−0.25***	−2.92***			−0.94*
		(0.03)	(0.26)			(0.56)
ST^3			0.01***			0.003**
			(0.001)			(0.002)
PieceWise(30)				−36.19***	−35.86***	
				(9.39)	(10.17)	
PieceWise(70)					4.90	
					(5.70)	
ST: After 2004						62.10
						(61.63)
ST^2: After 2004						−0.51
						(0.65)

Continued on next page

Table C.2 – continued from previous page

	Dependent variable: Deflated Land Price					
	(1)	(2)	(3)	(4)	(5)	(6)
ST^3: After 2004						0.001
						(0.002)
Constant	−2,482.21*	−2,986.61**	−4,576.63***	−3,059.80**	−2,925.17**	−1,473.60
	(1,337.45)	(1,437.60)	(1,415.57)	(1,317.13)	(1,349.27)	(2,285.17)
Parcel FE	Yes	Yes	Yes	Yes	Yes	Yes
Year FE	Yes	Yes	Yes	Yes	Yes	Yes
Observations	753	753	753	753	753	753
R^2	0.76	0.76	0.76	0.76	0.76	0.76
Adjusted R^2	0.48	0.48	0.48	0.48	0.48	0.48
Residual Std. Error	1,560.49	1,562.32	1,562.08	1,558.24	1,560.18	1,561.72
F Statistic	2.73***	2.72***	2.71***	2.73***	2.72***	2.70***

*p<0.1; **p<0.05; ***p<0.01

Table C.3: Estimates of Pooled OLS with Climate and Soil Factors: All Transactions CO & NE

	Dependent variable: Deflated Land Price					
	(1)	(2)	(3)	(4)	(5)	(6)
Saturated Thickness (ST)	5.60*	17.11***	20.90***	2.37	1.37	−18.22
	(2.94)	(3.70)	(7.72)	(9.12)	(8.87)	(15.85)
ST^2		−0.07***	−0.12			0.23
		(0.01)	(0.10)			(0.21)
ST^3			0.0002			−0.001
			(0.0003)			(0.001)
Conductivity	0.32	0.53	0.56	0.33	0.33	0.57
	(0.60)	(0.60)	(0.62)	(0.63)	(0.63)	(0.59)
Storability	−1.39	−0.51	−0.42	−1.52	−1.63	−0.30
	(11.77)	(11.63)	(11.50)	(12.02)	(11.91)	(11.66)
Bedrock to Surface	0.07	0.20	0.22	0.09	0.07	0.31
	(0.44)	(0.42)	(0.42)	(0.44)	(0.45)	(0.44)
PieceWise(30)				2.81	3.19	
				(6.65)	(6.37)	

Continued on next page

Table C.3 – continued from previous page

	Dependent variable: Deflated Land Price					
	(1)	(2)	(3)	(4)	(5)	(6)
PieceWise(70)					0.55	
					(1.49)	
ST:After 2004						49.59***
						(14.00)
ST^2: After 2004						−0.44**
						(0.18)
ST^3:After 2004						0.001*
						(0.001)
Soil (Xerolls)	1,827.35	1,418.49	1,384.85	1,796.35	1,778.51	1,248.72
	(1,379.64)	(1,284.38)	(1,304.53)	(1,409.98)	(1,404.16)	(1,343.31)
Soil (Ustolls)	1,923.62	1,510.17	1,484.32	1,895.10	1,875.11	1,296.24
	(1,308.80)	(1,229.20)	(1,240.93)	(1,335.25)	(1,331.42)	(1,285.54)
Soil (Udolls)	1,573.43	1,173.08	1,152.53	1,546.98	1,526.02	944.20
	(1,339.42)	(1,263.07)	(1,272.01)	(1,364.88)	(1,360.90)	(1,315.28)

Continued on next page

Table C.3 – continued from previous page

	Dependent variable: Deflated Land Price					
	(1)	(2)	(3)	(4)	(5)	(6)
Soil (Orthents)	1,770.29	1,388.14	1,364.94	1,745.27	1,722.70	1,190.06
	(1,293.84)	(1,207.90)	(1,218.26)	(1,312.76)	(1,307.48)	(1,263.71)
Precipitation	−3.98	−1.70	−1.31	−3.80	−3.88	−1.75
	(3.72)	(3.63)	(3.77)	(3.84)	(3.84)	(3.70)
Mean Temperature	16,657.96	17,198.95*	17,326.78*	16,754.04*	16,745.76*	17,017.35*
	(10,219.98)	(10,264.39)	(10,308.75)	(10,164.18)	(10,173.23)	(10,212.07)
Max Temperature	−8,617.03*	−8,786.35*	−8,826.34*	−8,645.13*	−8,650.69*	−8,745.57*
	(5,144.23)	(5,118.52)	(5,129.41)	(5,110.15)	(5,107.81)	(5,099.50)
Min Temperature	−7,519.49	−7,959.77	−8,049.04	−7,571.16	−7,558.79	−7,839.21
	(5,159.12)	(5,201.13)	(5,230.72)	(5,129.13)	(5,139.88)	(5,183.50)
Constant	6,006.26	3,292.53	2,676.06	5,622.11	5,849.43	5,469.03
	(4,655.52)	(4,311.97)	(4,200.98)	(4,346.64)	(4,421.39)	(4,769.23)
County FE	Yes	Yes	Yes	Yes	Yes	Yes
Year FE	Yes	Yes	Yes	Yes	Yes	Yes

Continued on next page

Table C.3 – continued from previous page

	Dependent variable: Deflated Land Price					
	(1)	(2)	(3)	(4)	(5)	(6)
Observations	4,329	4,329	4,329	4,329	4,329	4,329
R^2	0.16	0.16	0.16	0.16	0.16	0.17
Adjusted R^2	0.14	0.14	0.14	0.14	0.14	0.14
Residual Std. Error	2,092.71	2,089.84	2,090.02	2,092.87	2,093.10	2,085.36
F Statistic	6.18***	6.25***	6.20***	6.14***	6.09***	6.25***

*p<0.1; **p<0.05; ***p<0.01

Note:

Argids soil type is left out as the reference

5 observations are dropped due to missing soil type data

2 observations are dropped due to invalid soil type (water)

Table C.4: Estimates of Pooled OLS with Climate and Soil Factors: Repeated Transactions CO & NE

	Dependent variable: Deflated Land Price					
	(1)	(2)	(3)	(4)	(5)	(6)
Saturated Thickness (ST)	19.25***	33.82***	29.13*	16.67	6.93	−25.79
	(7.20)	(9.59)	(16.19)	(12.89)	(15.37)	(50.91)
ST^2		−0.09***	−0.03			0.70
		(0.03)	(0.23)			(0.53)
ST^3			−0.0002			−0.003*
			(0.001)			(0.002)
Conductivity	0.07	0.40	0.35	0.08	0.03	0.14
	(1.60)	(1.72)	(1.72)	(1.61)	(1.59)	(1.79)
Storability	−6.73	−5.40	−5.78	−6.60	−7.23	−4.78
	(25.76)	(25.93)	(25.51)	(25.98)	(25.59)	(25.78)
Bedrock to Surface	1.47	1.38	1.37	1.47	1.54	1.27
	(1.85)	(1.74)	(1.75)	(1.84)	(1.86)	(1.71)
PieceWise(30)				2.23	5.79	
				(9.72)	(10.94)	

Continued on next page

Table C.4 – continued from previous page

	Dependent variable: Deflated Land Price					
	(1)	(2)	(3)	(4)	(5)	(6)
PieceWise(70)					5.40	
					(5.73)	
ST: After 2004						61.62
						(58.89)
ST^2: After 2004						−0.80
						(0.62)
ST^3: After 2004						0.003
						(0.002)
Soil (Xerolls)	7,268.69***	6,908.72***	6,947.32***	7,229.25***	7,226.65***	6,966.91***
	(987.92)	(1,004.70)	(1,039.84)	(959.72)	(956.59)	(1,084.68)
Soil (Ustolls)	11,779.73***	11,404.67***	11,491.04***	11,734.57***	11,759.26***	11,468.58***
	(2,267.63)	(2,203.60)	(2,271.96)	(2,254.64)	(2,212.40)	(2,307.71)
Soil (Udolls)	10,930.34***	10,566.98***	10,648.78***	10,892.47***	10,882.93***	10,619.02***
	(2,310.53)	(2,257.96)	(2,324.09)	(2,295.22)	(2,262.11)	(2,372.31)

Continued on next page

Table C.4 – continued from previous page

	Dependent variable: Deflated Land Price					
	(1)	(2)	(3)	(4)	(5)	(6)
Soil (Orthents)	11,310.45***	10,917.91***	11,004.05***	11,263.65***	11,261.65***	10,984.76***
	(2,070.43)	(2,039.58)	(2,101.77)	(2,063.19)	(2,006.25)	(2,135.30)
Precipitation	−21.46***	−20.02***	−20.42***	−21.35***	−22.05***	−20.69***
	(3.16)	(3.41)	(3.85)	(3.25)	(3.27)	(3.86)
Mean Temperature	1,457.77	765.05	872.50	1,535.03	1,693.37	1,710.43
	(25,044.48)	(24,895.88)	(25,031.74)	(24,987.15)	(25,033.65)	(25,304.27)
Max Temperature	−140.96	246.46	183.71	−171.84	−297.33	−263.52
	(12,571.91)	(12,463.91)	(12,549.08)	(12,549.16)	(12,591.91)	(12,684.16)
Min Temperature	2.69	182.61	145.60	−42.09	−99.83	−212.70
	(12,606.51)	(12,497.55)	(12,541.04)	(12,568.92)	(12,576.08)	(12,661.09)
Constant	−6,408.06	−7,869.98	−7,431.48	−6,552.47	−4,986.77	−5,744.93
	(9,562.61)	(10,114.27)	(9,856.13)	(9,791.24)	(9,860.78)	(10,608.01)
County FE	Yes	Yes	Yes	Yes	Yes	Yes
Year FE	Yes	Yes	Yes	Yes	Yes	Yes

Continued on next page

Table C.4 – continued from previous page

	Dependent variable: Deflated Land Price					
	(1)	(2)	(3)	(4)	(5)	(6)
Observations	753	753	753	753	753	753
R^2	0.34	0.34	0.34	0.34	0.34	0.34
Adjusted R^2	0.25	0.26	0.26	0.25	0.25	0.26
Residual Std. Error	1,866.65	1,862.84	1,864.13	1,868.00	1,867.77	1,864.41
F Statistic	4.06***	4.07***	4.02***	4.00***	3.97***	3.91***

*p<0.1; **p<0.05; ***p<0.01

Note:

Argids soil type is left out as the reference